THE UNIVERSITY OF CALGARY

Morphology and Rheology of Binary Blends of Polypropylene and Linear Low Density Polyethylene

by

Priti Singh

A THESIS

SUBMITTED TO THE FACULTY OF GRADUATE STUDIES IN PARTIAL FULFILLMENT OF THE REQUIREMENTS FOR THE DEGREE OF

MASTER OF SCIENCE IN CHEMICAL ENGINEERING

Department of Chemical and Petroleum Engineering

Calgary, Alberta

February 2000

Abstract

Polymers are often blended to enhance the final product properties. This technology has proven to be both economical and environmental in recycling of polymers. While the addition of polyethylene to polypropylene is normally done to improve the resin toughness, in some cases it negatively impacts on other mechanical properties as well as on the processability of the resin. The objective of this work is to study the morphology evolution of polyethylene/polypropylene (PE/PP) blends in relation to the resins molecular characteristics and rheological properties. A better understanding of the relationship between the resins molecular characteristics, blends morphology and their rheological properties will facilitate the formulation of new resins and broaden their field of applications.

Six commercial linear low density polyethylene (LLDPE) of varying comonomer type (Butene, Hexene, and Octene) were used together with one homopolymer polypropylene and one ethylene-propylene copolymer. Using Gel Permeation Chromatography, it was found that all LLDPE resins used in this study have narrow molecular weight distribution. The comonomer distribution and content in all LLDPE resins used were determined from Temperature Rising Elution Fractionation. Based on rheological characterization, it was established that the PP homopolymer has a broad molecular weight distribution and higher elastic modulus than that of the PP copolymer.

PE/PP blends were prepared using a batch mixer with a composition of 5, 20, 50, 80, and 95 % PE in PP by volume, at a temperature of 190°C and a rotor speed of 50 rpm. Blends samples were cold fractured and their surface morphology was examined using Scanning Electron Microscopy. A two-phase morphology was observed for all PE and PP homopolymer blends with a drop-in matrix, beehive or lamella type depending on the volume fraction of each resins and related to the different fracture mechanisms. It was found that the minimum particle size of the dispersed phase occurred for a viscosity ratio around one (i.e. when the viscosity of the matrix and dispersed phase are equal). It was

also found that blends composed of Butene comonomer LLDPE and PP homopolymer resins had finer morphology, indicating low interfacial tension between the resins. Moreover for the PE/PP homopolymer blends the particle size diameter of the dispersed phase followed the trend: Butene<Hexene<Octene.

The crystallinity of the PP homopolymer and its blends were studied using Optical Microscopy. It was observed that the formation of the type of spherulite (i.e α-spherulites and β-spherulites) in the PP homopolymer and its blends depended mainly on the cooling rates and were not affected by the content of the dispersed phase. The size of the spherulites for the blends became quite small as the sample cooling rate increased and thus the effect of the molecular structure on the size of the spherulites could not be assessed.

The rheological characterization of the PP homopolymer blends showed an increase in the storage modulus and zero shear viscosity, as compared to the matrix. However, no significant effect of the molecular structure of the LLDPE resins could be observed in the rheological properties. An attempt was also made to determine the interfacial tension using Palierne model. Results show large variations and indicate that this model is not valid for the blends studied in this work. The study of PP copolymer blends also showed a dramatic increase in elasticity in comparison to its matrix. The morphology of these blends, however, could not be examined using scanning electron microscope, probably due to the formation of ternary blends.

Acknowledgement

I would like to acknowledge a few people whose contribution has been significant in completion of this work. First of all, I would like to thank my supervisor, Dr. Celine. T. Bellehumeur, for providing me an opportunity to work under her. I really appreciate, the constant support and guidance provided throughout the masters degree. I would also like to thank my committee members Dr. Guojun Liu, Dr. Robert A. Heidemann and Dr. Jalel Azaiez for taking out time to read my thesis.

I would like to thank Dr A. K. Mehrotra for allowing me to use the Differential Scanning Calorimeter for the experiments. I also wish to acknowledge Mr. Mingqian Zhang of University of Alberta for performing the GPC and TREF experiments, which are a vital part of my thesis.

I would like to thank NOVA Chemicals, Exxon and Equistar for providing the LLDPE and PP resins. I wish to express my gratitude towards the Natural Science Engineering and Research Council (NSERC) and the Department of Chemical and Petroleum Engineering and Engineering for the Environment for providing funding for the project.

I am very grateful to my husband for his support and help during my Master's thesis, especially during the last few days. I also appreciate the help and useful comments on my work by Mr. Jen Shueng Tiang and Ms. Francis Alvarez. Finally, I would like to thank all the fellow graduate students for their help during my studies at the university.

To,

My Guruji

Ability is what you are capable of doing
Motivation determines what you do
Attitude determines how well you do it
-Lou Holtz

TABLE OF CONTENTS

Chapter 3: Literature Review

Chapter 4: Experimental Work

Chapter 5: Results and Discussions

LIST OF TABLES

LIST OF FIGURES

ABBREVIATIONS

CoHo	Copolymer : Homopolymer ratio
DSC	Differential scanning calorimetry
FTIR	Fourier transform infrared spectrophotometry
GPC	Gel permeation chromatography
HDPE	High density polyethylene
IR	Infrared
LCB	Long chain branches
LDPE	Low density polyethylene
LLDPE	Linear low density polyethylene
MSL	Methylene sequence length
MW	Molecular weight
MWD	Molecular weight distribution
MFI	Melt flow index
PA6	Polyamide
PC	Polycarbonate
PE	Polyethylene
PET	Polyethylene terephthalate
PI	Polydispersity index
PP	Polypropylene
PS	Polystyrene

PUR	Polyurethane
PVC	Poly vinyl chloride
SANS	Small angle neutron scattering
SEM	Scanning electron microscopy
SCB	Short chain branches
TEM	Transmission electron microscopy
TREF	Temperature rising elution fractionation
WAXD	Wide angle X-ray diffraction

NOMENCLATURE

c	Calibration parameter
Ca	Capillary number
D	Dispersed drop diameter, μm
D_v	Volume average diameter, μm
D_n	Number average diameter, μm
G_c	Crossover modulus, Pa
$G'(\omega)$	Storage modulus, Pa
$G''(\omega)$	Loss modulus, Pa
$G^*(\omega)$	Complex modulus, Pa
ΔH_f^{comp}	Heat of fusion of the components, J/g
ΔH_f^o	Heat of fusion of the 100% crystalline polymer, J/g
M_n	Number average molecular weight
M_w	Weight average molecular weight
M_z	z average molecular weight
$N_{1\alpha}$	First normal stress of the dispersed phase, Pa.
$N_{1\beta}$	First normal stress of the matrix phase, Pa.
p	Viscosity ratio
R	Drop radius, m
T_{el}	Elution temperature, °C
T_o	Calibration parameter

T_i	Torque of component *i*, mgf

Greek Letters

$\beta'(\omega), \beta''(\omega)$	Interfacial parameters
$\sigma_{\alpha\beta}$	Dynamic interfacial tension, mN/m
$\sigma^0_{\alpha\beta}$	Interfacial tension at rest, mN/m
$\eta^*(\omega)$	Complex viscosity, Pa.s
$\eta(\dot{\gamma})$	Shear viscosity, Pa.s
η_{65}	Shear viscosity at a shear rate of 65 s^{-1}, Pa.s
η_0	Zero shear viscosity, Pa.s
ω	Frequency, rad/s
ω_c	Crossover frequency, rad/s
$\dot{\gamma}$	Shear rate, s^{-1}
Γ	Interfacial tension, mN/m
δ	Mechanical loss angle
ϕ_i	Volume fraction of component *i*
λ	Terminal relaxation time, s

Subscript

d	dispersed phase
m	matrix
b	blend

Introduction

Chapter 1

1.1 General Description

Over the years, polymers have found their applications in different areas such as packaging, electrical industry/electronics, automobile industry, building industry and agriculture. Various polymers and fiber-reinforced composites have been developed, which exhibit high performance and longer service life. Some of these resins find extensive use in Aircraft/Aerospace industry replacing high performance metals. Recent use of polymers in the household construction industry, replacing wood, makes them an environment friendly alternative.

Polymer properties such as light weight, corrosion resistance, decay resistance, thermal resistance, electrical insulation and the ability to be shaped into complex geometries have helped the plastic industry to broaden its application and achieve its growth. The production of polymer was around 120 million tons in 1997 and is estimated to reach over 210 million tons in 2007 and 400 million tons in 2020 (Pardos, 1999). A recent study indicates the breakdown of the different polymeric resins being used as follows- Polyethylene (PE) - 47%, Polystyrene (PS) - 16%, Polypropylene (PP) - 16%, Polyethylene Terephthalate (PET) - 5%, Poly Vinyl Chloride (PVC) - 7%, Polyurethane (PUR) - 5% and other materials such as Polycarbonates (PC) - 4%. It is estimated that

83% of all plastics produced and almost 100% of the plastics used in packaging are thermoplastic materials, i.e. which can be remelted or reformed. Research is being continuously done to make tailor made resins with enhanced properties to meet the demands of the upcoming requirements. Besides synthesis of new resins that are expensive, mix formulations are also being used to produce material of optimal cost and performance.

One of the negative aspect of growth of the polymer industry is the increase in solid waste. Most of the wastes enter the municipal solid waste stream through the converters, wholesalers/retailers, households, restaurants, hospitals, schools and other institutions. The composition of municipal solid waste by volume is estimated as 34% paper, 20% plastics, 12% metal, 10% yard waste, 2% glass, 3% food, and 19% of all other (Udipi and Zolotor, 1993). Solid waste disposal has been a major concern for our society, due to its adverse impacts on the environment such as air and water pollution and declining landfills. Since plastics are lightweight materials, they occupy a great deal of volume, which significantly contributes to the problem of disappearing landfill space.

A global awareness towards the protection of the environment has led to integrated waste management practices, where all the various methods of solid waste reduction such as source reduction of packaging material, reuse, recycling, off-landfill composting of biodegradable wastes, barring of toxics and incineration are gaining equal importance (Baumann, 1998). Efforts are also being made to market the various products in smaller overall package and also in improving the barrier properties and the strength of the packaging material in order to reduce the quantity used. Extensive work is being done on reprocessing, as it is the most economic and ecologically advantageous process to recycle plastic wastes. However, the current recovery rates, for all materials in the solid waste stream, with the exception of food wastes, exceeds that of plastics (Ehring, 1992). The recovery rates have been estimated as 26% for paper, 32% for aluminum and around 12% for glass, while plastics is only 2%. The low rate may be attributed to poor

economical, technological and material performance factors, including problems associated with material handling.

Recycling of polymers, in general, involves different steps such as collection, separation, cleaning, processing and remanufacture. Each step is associated with its own challenges. One of the significant problems associated with recycling is the deterioration of the material properties, which occurs due to the degradation of the polymer either during the lifetime time of the product or due to the presence of additives/impurities. Efforts are therefore being made to enhance the properties of the recycled polymers by a wide variety of techniques and may involve compounding the recycled resin with materials like wood fibers (Yam *et al.*, 1990), rubber particles (Li and Liu, 1997) or blend it with other polymers (Khait and Carr, 1997; Rueda *et al.*, 1994). These methods can markedly change mechanical as well as the rheological properties. Thus blending has been found to not only improve the properties of the polymer but also as an efficient way to fill new requirements for material properties.

1.2 Motivation

The study of polyethylene and polypropylene blends has been a subject of interest for quite a long time. Generally, in these studies, PE was added to PP to improve the strength and toughness of PP (Schurmann *et al.*, 1998; Kukaleva *et al.*, 1998). PE/PP blends are also of great relevance to their recycling. This is mainly because polyolefins (PE, PP) are amongst the major constituents of plastics waste and are difficult to separate due to similar densities. Different grades of polyolefins thus end up as a contaminant to one another.

Polyethylenes, besides being used for blending, are used for a variety of applications such as packaging, molding, coating, etc. depending on the different grades. In general, they have been classified according to the density and the process of

polymerization. Linear low density polyethylene (LLDPE) is one of them and is produced by copolymerization of ethylene and a comonomer such as hexene, butene or octene. In the recent years, LLDPE is capturing an increasing share of the PE market due to its characteristic properties, which are imparted due to the absence of long chain branches and the presence of only short chain branches. There has been around 6.9% increase in the production of LLDPE in 1999 and around 13% increase has been estimated for year 2000 (Kulkhe, 1999). It is generally observed that even though the processability of the LLDPE is relatively difficult as compared to low density polyethylene (LDPE), it has largely replaced LDPE in the production of blown film for packaging. This is because LLDPE is tougher than LDPE at the same melt flow index, as a result thinner films of LLDPE can be produced, which have the same mechanical properties to that of the thicker LDPE films (Bailey *et al.*, 1994). The properties of LLDPE are being further improved by having a superior control over the branching distribution using the various recent innovations in polymer synthesis.

In general, blends of PE and PP are immiscible and incompatible, which may result in poor mechanical properties. To enhance their properties, compatibilizers may be required, which are expensive. So to put these blends to more efficient use, both in terms of recycling and improvement of strength of PP, it becomes imperative to have a better understanding of their structure, properties and processing behavior.

1.3 Research Objectives and Thesis Outline

The present study therefore aims at determining which properties influence the strength of LLDPE/PP blends. Particularly, one of the main objectives of the work, is to study the effect of the molecular characteristics of the blend components on the morphology and rheology of blends. As the morphology and rheology of the blends are closely related to the mechanical properties, their study would be able to give valuable

insight on the consequences of the molecular structure of the components on the mechanical properties of the blend.

In this study, LLDPE resins of varying comonomer type (butene, hexene and octene), comonomer content and distribution manufactured using Ziegler Natta catalyst are used. LLDPE/PP blends of various compositions are prepared using a batch mixer and their morphology and rheology are studied. The morphology of the blends is examined using scanning electron microscopy (SEM) and optical microscopy, while the rheological properties are measured using a rotational rheometer.

The thesis is comprised of six chapters including this introduction. To familiarize the reader with the various polymeric properties and the different aspects of polymer blending, background information is presented in Chapter 2. Chapter 3 presents a detailed literature review on the PE/PP blends. The experimental setup and procedures for polymer blending and measurement of various properties are described in the Chapter 4. This chapter also includes the description and measurement techniques used to characterize the various virgin resins. Experimental results are presented and thoroughly analyzed in chapter 5. The last chapter contains conclusions and recommendations for future work on the subject.

Background

Chapter 2

This chapter presents a brief description of the rheological properties of the polymers and also reviews the effects of different molecular architectures of the resins on their rheological characteristics. Polymer blends are also discussed. A review of the relevant literature about the effects of various parameters on the morphological and rheological properties of the blends is included.

2.1 Rheological Properties of Polymers

The response of a pure elastic solid to applied stress is expressed by Hooke's law, which states that the strain is proportional to the applied stress. Similarly, pure Newtonian fluids have been shown to follow a simple relation, which states that the rate of strain is proportional to the stress applied on the fluid. Polymers in general, exhibit an intermediate behavior and are termed as viscoelastic. The rheological properties of the polymers are strongly dependent on temperature, shear rate and time scale of deformation.

The simplest type of viscoelastic behavior is linear viscoelasticity. This type of behavior, is observed when both the deformation and deformation rate are sufficiently small, such that the molecules are disturbed from their equilibrium configuration and

entanglement state to a negligible extent. Though this kind of deformation is normally not encountered in polymer processing, linear viscoelasticity is normally used for characterizing the molecules, for resin quality control (Covas *et al.*, 1995; Dealy and Wissburn, 1995). Since the rheological properties are closely related to the molecular structure, rheological measurements are an important tool for building an understanding of the molecular structure of the polymers.

2.1.1 Effect of molecular weight and molecular weight distribution

The molecular weight (MW) of polymers is usually characterized as number average molecular weight (M_n), weight average molecular weight (M_w) and z average molecular weight (M_z). Polymer molecular weight distribution (MWD) is typically a skewed Gaussian distribution and is generally quantified by polydispersity index (PI). PI is the ratio of M_w/M_n and is an indication of the molar mass distribution.

It is well known that the molecular weight affects the viscosity of the resins. The zero shear viscosity is observed to increase with approximately 3.4 power of the weight average molecular weight (M_w) (Minoshima *et al.*, 1980) and the intrinsic viscosity is observed to vary almost linearly with the weight average molecular weight (M_w) (Tzoganakis *et al.*, 1990). The shear rate dependent viscosities, in general, are used to study the effect of the differences in MWD for systems of similar MW and molecular architecture. This analysis is based on the concept that the viscosity measured at low shear rate reveals the relaxation processes of larger molecules, whereas viscosity measured at high shear rate reveals the relaxation processes of smaller molecules and segments of larger molecules (Harrell and Nakajima, 1984). Tuminello (1990) reported that for polymers with narrow MWD, the shear rate at which the shear thinning behavior begins (viscosity decreases with shear rate) was more clearly defined and occurred at a higher shear rate.

The MW and MWD also influence properties such as melt recovery, melt strength and extrudate swell that are related to the elasticity of the polymer. In general it is observed that an increase in the molecular weight results in the increase of melt elasticity. Tzoganakis *et al.* (1990) observed that resins with high molecular weight show high extrudate swelling and Goyal *et al.* (1995) observed an increase in the melt strength, with the increase in molecular weight. Further, it has been observed that the melt elasticity also increases with the increase in the PI (i.e. broad MWD) (Guillet *et al.*, 1965; Minoshima *et al.*, 1980; Tuminello, 1990). Guillet *et al.* (1965) observed an increase in the melt strength with broad MWD while Minoshima *et al.* (1980) observed an increase in the first normal stress with broad MWD. Tuminello (1990) reported that extrudate swell remains constant until a critical shear stress after which the swell rapidly increases. The critical shear stress was shown to vary inversely with increasing polydispersity. However, there have been some contradicting results, which show that the die swell and the compliance decrease with the increase in MW and MWD (Shroff and Shida, 1977). This anomalous behavior has been explained by considering the die swell and compliance to be affected not only by elasticity but also by viscosity. The effect of increasing MW (increases viscosity) is opposite to the broadening of MWD (decreases viscosity), and therefore depending on the predominating effect of the MW or MWD there may be an increase or decrease in the die swell and compliance. Further, Goyal (1995) reported no significant changes in the melt strength with the change in MWD, but observed a change in melt strength with the modality of MWD. The anomalous behaviors indicate that elucidation of the effects of the MWD is very complex. This is due to difficulty in separating the effect of MWD from that of branching. In some commercial elastomers, the increase in the long chain branches has been reported to result in broadening of the MWD (Harrell and Nakajima, 1984).

2.1.2 Effect of level of branching and branching distribution

Polymers generally have either linear or branched or star shaped molecular structure. Branching in polymers may further be classified as long chain branches (LCB)

and short chain branches (SCB). SCB are generally considered to be between one to five carbons in length. The length of LCB, on the other hand, is often comparable to that of the main polymer chain. It has been reported that SCB normally originate from intramolecular hydrogen atom abstractions and LCB, on the other hand, are the products of intermolecular hydrogen atom abstractions (Bugada and Rudin, 1987). The different manufacturing technologies, conditions of the process, kind of catalyst used are the different variables, responsible in the formation of quite different types, amounts and distribution of short and long branches (Goyal *et al.*, 1998).

Alteration in the number/size of the chain branches in polyethylene manifests itself in terms of differences in density and crystallinity and also influences rheological properties. Polyethylenes, in general, have been categorized as High density polyethylene (HDPE), Low density polyethylene (LDPE) and Linear low density polyethylene (LLDPE) according to the density and type of branching. HDPE is a homopolymer of ethylene with a linear molecular structure and high density. LDPE is also a homopolymer of ethylene but the molecules have a branched structure with both LCB and SCB. It has a lower density as compared to HDPE, mainly due to the presence of SCB. LLDPE is a copolymer produced by polymerizing ethylene with an α olefin comonomer. It has a linear molecular structure, due to the absence of LCB, but has a lower density as compared to HDPE, due to the presence of SCB. In general, it has been found that SCB control the density but have little effect on the rheological properties (Kim *et al.*, 1996). Goyal (1995) observed that the comonomer content had no significant effect on the melt strength, however, the type of comonomer had a significant effect on the melt strength. He showed that polymer with a longer comonomer resulted in higher melt strength. Further, it has been observed that the length of the SCB is also instrumental in controlling the density, with a longer side chain resulting in lower density (Daane *et al.*, 1977, Kim *et al.*, 1996).

It has been reported (Kim *et al.*, 1996) that while LCB have little effect on the density and thermodynamics, they have a profound influence on melt rheology. Daane *et al.* (1977) observed that polymers with LCB, exhibited higher melt strength and flow activation energy. An increase in extrudate swell and first normal stress for polymers with higher LCB was reported by Vega *et al.* (1998). Harrell and Nakajima (1984) studied the effect of the LCB on linear viscoelastic properties and reported an increase of the storage modulus with the increase in long chain branching. They attributed this observation to the increase in the relaxation mechanism. Vega *et al.* (1998), further stated that the polyethylene with low LCB shows lower zero shear viscosities and also cause a decrease in the severity of the pseudoplasticity, whereas medium and high degrees of LCB exhibit opposite trend.

Beside the number and size of branching, the distribution also seems to affect properties such as the melt strength. Goyal *et al.* (1998) observed that uniform branching distribution was more effective in reducing the density and also helped in improving the melt strength. However, they found properties like shear viscosity and extrudate swell behavior that are influenced by M_w, MWD and the amount of branching, were not affected by the branching distribution.

2.2 Polymer Blends

Polymer blends, by definition, are physical mixtures of different polymer/copolymer components. The blend components may be either miscible or immiscible depending on the level of thermodynamic interactions between themselves. The usual qualitative criteria to predict miscibility is that the Gibbs free energy of mixing (ΔG_m) must be negative and its second derivative with respect to the volume fraction of the dispersed phase ($\delta^2 \Delta G_m / \delta \phi_i^2$), be positive for the system to be thermodynamically stable. The other criteria usually are, observation of a single glass transition temperature, optical clarity and homogeneity in the scale of 50-100 A^0 (Utracki, 1989). In general, miscibility is defined as the adequate level of molecular mixing yielding macroscopic

properties of one single phase material. Miscible blends are therefore mechanically compatible and exhibit properties that are a compromise to that of the blend constituents. Miscibility should not be confused with compatibility, which generally signifies a good interfacial adhesion amongst the components in a multiphase system (Favis, 1991).

The technology of polymer blends is dominated by immiscible polymers (Utracki, 1989), and this is normally attributed to the small entropy of mixing, which is caused due to the large molecules of the polymers. One of the major issues with these blends is the component's incompatibility, which generally results in poor mechanical properties. A lack of adhesion between immiscible phases and a coarse morphology are considered to be responsible for inferior properties. Immiscible systems are generally characterized by distinct transition temperatures and opacity. Despite these drawbacks, many of the immiscible blends are gaining commercial importance. This has been made possible by compatibilizing either by addition of a compatibilizer or cosolvent, or mechanically using a high shear blender. This results in the formation of fine dispersed morphology and good adhesion, which not only improves the mechanical properties but also affects the rheological properties, which are interrelated. Though the various properties are interrelated in a complex manner, an attempt has been made through this simple flow diagram to relate the various parameters affecting the mechanical properties.

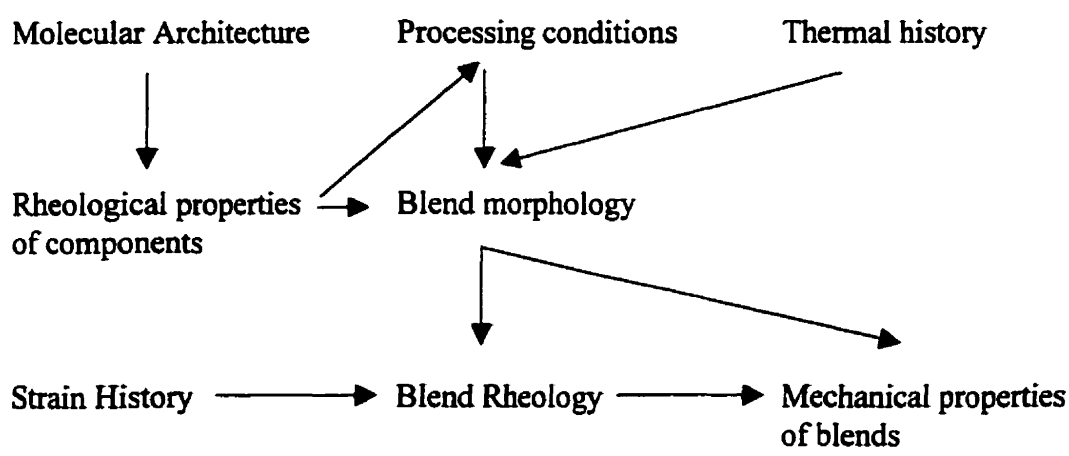

2.2.1 Blend morphology

2.2.1.1 Morphology formation during mixing

The development of the phase morphology in polymer blends generally occurs during the macroscopic mixing process. The mixing processes usually involve size reduction and its spatial redistribution, which are known as dispersive and distributive mixing (Radusch, 1998). The dispersive mixing may be defined as a process of breaking up the dispersed phase by stresses acting at the interface. The stresses are transmitted through the matrix from a moving surface (e.g.: roller blades) and act against the interfacial forces of the dispersed phase. Distributive mixing on the other hand is defined as the distribution of the phases by convection and diffusion. This would be affected by mixer dead spaces, flow patterns and initial phase distribution.

Mixing of one component inside the other proceeds through various transient stages of morphology (Sundararaj *et al.*, 1992; Scott and Macosko, 1995). In mixing process, the major reduction in phase domain occurs in conjunction with the melting or softening of the components. According to them, initially there is the formation of sheets or ribbons of the dispersed phase, which then due to effects of flow and interfacial tension, become unstable resulting in the formation of holes. These holes subsequently grow in size and concentration until a fragile lace-like structure is formed. The lace-like structure then finally breaks and forms the dispersed phase particles. These dispersed drops may further break or coalesce to obtain stable droplets and thus a stable morphology. The morphology evolution depends on many factors, and the various parameters that have been reported to be important for the development of morphology during melt mixing of polymer blends, are described in the following section.

2.2.1.2 Factors affecting the final morphology

The theoretical and experimental studies have shown that the processing conditions (composition, shear rate, time, type of blending equipment, temperature) and the material

properties (interfacial tension, viscosity ratio and elasticity) are important in the development of the phase morphology during the melt mixing of polymer blends.

- *Composition*

The blend's composition has a profound influence on the particle size. The particle size and the particle size distribution both increase with the increase in the percentage of dispersed phase and this phenomenon is attributed to the increased coalescence of the dispersed particles (Sundararaj and Macosko, 1995). It is generally shown that a continuous phase is formed by the components of larger volume fraction. At higher concentrations, however, phase inversion may occur and around this point, there is a range of compositions in which both phases are continuous (Melkhilef and Verhoogt, 1996). Semi-empirical models have been proposed to predict the composition when the phase inversion occurs. Avgeropoulos *et al.* (1976) based their formula on the peak torque ratios and is given as

$$T_1/T_2 = \phi_1/\phi_2 \qquad (2.1)$$

where, T_i is the torque at the blending shear rate for component i and ϕ_i is the volume fraction of the polymer i. Jordhamo *et al.* (1986) further proposed a semi-empirical equation, which was later generalized by Miles and Zurek (1988) and is based on the viscosity ratios and is given as

$$\eta(\dot{\gamma})_1/\eta(\dot{\gamma})_2 = \phi_1/\phi_2 \qquad (2.2)$$

where $\eta(\dot{\gamma})_i$ is the viscosity of polymer i at the shear rate imposed on the blend and ϕ_i is the volume fraction of polymer i.

- *Shear Rate*

Early studies showed that the scale of phase morphology becomes much finer with the increase in the shear rate (Min *et al.*, 1984; Wu, 1987). However, Favis (1990)

observed no appreciable difference in the dispersed drop diameter by changing the shear rate for a system of PP/PC of 7% composition. He explained this deviation due to the non-continuity of the shear rate/shear stress at the interface of the two components of the immiscible blend. Furthermore, for some polymer blends, the drop diameter was found to increase with shear rate (Sundararaj and Macosko, 1995). The increase in the drop diameter with the shear rate was attributed to the increased approach velocities at higher shear rates, leading to increased coalescence probability. The other explanation offered was the lowering of the matrix viscosity at high shear rates, which would enhance the resistance of the drop to greater deformation. Ghodgaonkar *et al.* (1996) also observed, for the various systems studied, that the drop diameter initially decreases with increasing the shear rate, up to a critical shear rate beyond which the drop diameter increases with shear rate. However, the minimum was not observed for high concentration (20%), probably due to the effect of coalescence becoming more significant at low shear rates.

- *Blending Equipment*

The type of blending equipment affects the properties of the blend based on how efficiently it provides momentum and heat transfer to the polymer melts. Han and Kim (1975) studied the effect of mixing on PS/PP blends using single screw extruder combined with static mixer and a twin screw extruder. They found that the different mixing devices had a profound influence on the state of dispersion of one polymer in another. Favis and Therrien (1991) also reported that the phase size of 5% PC in PP was four times higher in an internal mixer than in a twin screw extruder at a viscosity ratio of 17.3. They found, however, that at low viscosity ratios the difference between the morphologies obtained using different mixing devices is insignificant. Sundararaj *et al.* (1992), on the other hand, observed no difference between the morphology obtained from a batch mixer and extruder, even for high viscosity ratio blends. These authors further concluded that the batch mixers could be used to simulate extrusion processes, in which the different times in the mixer, represent the different lengths of the extruder.

- *Mixing Time*

It has been shown that most of the deformation or disintegration process occurs in the first few minutes of mixing. Plochocki *et al.* (1990) saw no differences in the blend morphology after 5 min of mixing. They postulated that an abrasion mechanism was responsible for the quick morphology development. Favis (1990) also found that extending the time of mixing from 2 to 20 min has little or no influence on the morphology. He concluded that the major portion of the morphology development occurred during the melting of the pellets. This was also confirmed by Sundararaj *et al.* (1992) and Scott and Macosko (1995) in their recent work on blend morphology.

- *Temperature and Pressure*

The temperature, though an important processing parameter, may not significantly affect the viscosity ratio and is therefore not expected to have a major effect on drop size. Other temperature dependent variables, such as interfacial tension, also show a weak dependence on temperature. The effect of pressure on blend morphology has not been widely studied in the literature mainly due to the fact that polymers show viscoelastic behavior. This is because on removal of the stress the polymer relaxes. Thus any pressure applied during processing can reduce the dimensional accuracy of the molded part made out of the blend (Rao, 1999).

- *Interfacial Tension*

Interfacial tension between the two phases plays an important role in determining the blend morphology. In fact, it is considered to be the dominant parameter in controlling the dispersed phase. A decrease in the interfacial tension results in a decrease of the dispersed particle size (Wu, 1987). Chemical compatibility of the materials is generally manifested in low interfacial tension. Hence, many compatibilizers are normally added to decrease the interfacial tension in order to obtain a fine dispersed morphology. They may also work by forming a sufficient interfacial layer around the particles resulting in decreased coalescence (Wallheinke *et al.*, 1997).

- *Viscosity Ratio*

The viscosity ratio of the blend has been shown to be one of the most critical variables in controlling the blend morphology. Taylor (1932) performed the pioneering work on the breakup of a single Newtonian drop in a simple shear field. He modeled drop size defining viscosity ratio $p = \eta_d/\eta_m$ and the capillary number $Ca = D\dot{\gamma}\eta_m/2\Gamma$, where Γ is the interfacial tension, η_m is the viscosity of the matrix at the blending shear rate, η_d is the viscosity of dispersed phase at the blending shear rate, D is the drop diameter and $\dot{\gamma}$ is the shear rate. He obtained the diameter of the stable drop by balancing the shear forces to the interfacial forces and is given as

$$D = \frac{4\Gamma(p+1)}{\dot{\gamma}\eta_m\left[\frac{19}{4}p+4\right]} \qquad p < 2.5 \tag{2.3}$$

He predicted that for a viscosity ratio greater than 2.5, no droplet break up would occur. Experimental observations by Karam and Bellinger (1968) also showed that in the simple shear flow, the droplet breakup only occurred at viscosity ratios ranging from 0.005 to 4. A similar range of values was observed by other researchers (Tavagac, 1972; Torza *et al.*, 1972). Further, Grace (1982) studied the droplet breakup in extensional flow and found that the droplet breakup was possible at all viscosity ratios unlike in simple shear flow.

Wu (1987) studied droplet breakup experimentally, when both the droplet and matrix are viscoelastic liquids. He reported that drops can breakup at high viscosity ratios, even at $p > 4$. He obtained a correlation relating capillary number to viscosity ratio and obtained the following empirical expression for the final particle diameter.

$$D = \frac{4\Gamma p^{\pm 0.84}}{\dot{\gamma}\eta_m} \tag{2.4}$$

where the exponent is equal to +0.84 when $p>1$ and -0.84 when $p<1$. He reported that the smallest particles were obtained at a viscosity ratio equal to 1. Since the blends used by him had a dispersed phase concentration of 15 wt%, it could not be related to the Taylor limit (single drop breakup). Also the complex nature of deformation during the flow that consists of both extensional and shear field, makes it difficult to understand the breaking phenomenon of the viscoelastic drop. The complexity in predicting the final morphology is further enhanced by the counteracting mechanism of droplet coalescence. Coalescence effects have been observed for dispersed phase concentration as low as 0.5% (Sundararaj and Macosko, 1995). Since Wu's (1987) equation does not have a term to represent coalescence, Serpe *et al.* (1990) further developed the equation by substituting the matrix viscosity with blend viscosity and added another term for composition, which accounts for coalescence.

$$D = \frac{4\Gamma p^{\pm 0.84}}{\gamma \eta_b (1 - 4(\phi_d \phi_m)^{0.8})} \tag{2.5}$$

Where, η_b is the blend viscosity, ϕ_d is the volume fraction of the dispersed phase and ϕ_m is the volume fraction of the matrix phase. Serpe *et al.* (1990) confirmed validity of equation 2.5 for a blend system of PE/PA6.

Besides the above studies, a large body of work has been presented in the literature where the effect of the viscosity of the components on the blend morphology has been studied. However, many conflicting results have been reported. A brief review of these studies has been done by Pötschke *et al.* (1997) and the discrepancies are attributed to the differences in the dispersed phase content, mixing technologies, particle size measurement methods and shear rates used for the calculation of viscosity ratios by different investigators.

- *Material Elasticity*

In case of polymer-polymer systems, the droplets experience not only dissipative (viscous) forces but also the deformation resisting forces arising from the material elasticity (Utracki and Shi, 1992). Van Oene (1972) studied the mixture of viscoelastic fluids and pointed out the importance of elasticity in addition to viscosity ratio and interfacial tension in the deformation of droplets. Based on thermodynamic reasoning, he developed a model for the dynamic interfacial tension coefficient which is given as

$$\sigma_{\alpha\beta} = \sigma^{0}_{\alpha\beta} + (\frac{D}{12})(N_{1\alpha} - N_{1\beta}) \qquad (2.6)$$

Where, $\sigma_{\alpha\beta}$ is the dynamic interfacial tension and $\sigma^{0}_{\alpha\beta}$ is the interfacial tension at rest, D is the diameter of the droplet and $N_{1\alpha}$ and $N_{1\beta}$ are the first normal stress of the dispersed and matrix phase respectively. This model predicts that higher elasticity of the dispersed phase than the matrix phase results in more stable drops. On the other hand if $N_{1\beta} > N_{1\alpha}$, then equation 2.6 predicts $\sigma_{\alpha\beta} < \sigma^{0}_{\alpha\beta}$, thus the flow tends to enhance the dispersing process. However, if there is a large normal stress difference and for large drop diameter this would result in stratified morphology, as $\sigma_{\alpha\beta}$ cannot be negative.

2.2.2 Rheological properties

Rheological characterization of blends is used as a tool to understand the phenomena encountered during processing of the material. Rheological models are extensively used to generate data for process and equipment design. The rheological properties of the blends depend in a complex manner on the composition, properties of the components, morphology, interaction between phases, interfacial tension and the strain history during processing. At present, the processing/morphology/property relationship in immiscible blend remains poorly understood and for a given composition we may obtain a wide range of properties. Better processing strategies, may result in

consistent and high value-added products, if the understanding of these relationships became clearer.

Rheological measurements on blends, however, are usually done in the linear viscoelastic domain, such as small amplitude oscillatory shear experiments to obtain useful information on blends. Further, rheological models have been developed using linear viscoelastic data to relate microscopic and macroscopic quantities. These models are assessed based on the assumption that for small strain the morphology of the blends would not change and thus properties such as storage modulus and loss modulus would give us an idea about the blend characteristics.

Palierne (1990) has proposed a model that relates the complex moduli of the blend to that of the complex moduli of both the matrix and the dispersed phase. The Palierne model is valid for an emulsion type blend and its main assumption is that the droplet deformation remains small. This indicates that this theory is only valid for linear viscoelastic behavior. In this model he has taken into account several important features of the multiphase system such as the viscoelastic properties of both phases, the morphological characteristics (dispersed drop size and droplet size distribution) and the interfacial tension. The general Palierne model formulation also contains parameters $[(\beta'(\omega), \beta''(\omega)]$ which are related to the interface and are due to the change in the interfacial area and local shear. However, since it is nearly impossible to determine these parameters experimentally, they are normally set equal to zero (Bousmina and Muller, 1993; Lacroix *et al.*, 1996). Based on these assumptions, the simplified expression for the complex shear modulus of the emulsion is given as

$$G_b^*(\omega) = \frac{1+3\sum_i \phi_i H_i^*(\omega)}{1-2\sum_i \phi_i H_i^*(\omega)} G_m^*(\omega) \qquad (2.7)$$

where

$$H_i^*(\omega) = \frac{4\left(\frac{\Gamma}{R_i}\right)\left[2G_m^*(\omega)+5G_d^*(\omega)\right]+\left[G_d^*(\omega)-G_m^*(\omega)\right]\left[16G_m^*(\omega)+19G_d^*(\omega)\right]}{40\left(\frac{\Gamma}{R_i}\right)\left[G_m^*(\omega)+G_d^*(\omega)\right]+\left[2G_d^*(\omega)+3G_m^*(\omega)\right]\left[16G_m^*(\omega)+19G_d^*(\omega)\right]}$$

where, Γ is the interfacial tension, R_i is the radius of the droplet, ϕ_i is the volume fraction of the droplets with the radius R_i, G^*_m is the complex modulus of the matrix, G^*_d is the complex modulus of the inclusions and G^*_b is the complex modulus of the blends.

It has also been shown that for a polydispersity of the droplet size D_v/D_n (ratio of the volume average diameter to the number average diameter) less than 2, the model predictions can be calculated assuming monodispersed droplets (i.e i=1) and using the volume average diameter (Graebling *et al.*, 1993). This assumption simplifies the equation 2.7 and the storage and loss modulus of the blend can be thus expressed as

$$G_b' = \frac{1}{C}\left[G_m'(A_1A_2 + A_3A_4) - G_m''(A_4A_1 - A_2A_3)\right] \tag{2.8}$$

$$G_b'' = \frac{1}{C}\left[G_m'(A_1A_4 - A_2A_3) + G_m''(A_1A_2 + A_3A_4)\right] \tag{2.9}$$

where the constants are

$$A_1 = B_1 - 2\phi B_3$$
$$A_2 = B_1 + 3\phi B_3$$
$$A_3 = B_2 - 2\phi B_4$$
$$A_4 = B_2 + 3\phi B_4$$
$$C = (B_2 - 2\phi B_4)^2 + (B_1 + 2\phi B_3)^2$$

with

$$B_1 = 40\frac{\alpha}{R}(G_m' + G_d') + 38(G_d'^2 - G_d''^2) + 48(G_m'^2 - G_m''^2) + 89(G_m'G_d' - G_m''G_d'')$$

$$B_2 = 40\frac{\alpha}{R}(G_m'' + G_d'') + 96G_m'G_m'' + 76G_d'G_d'' + 89(G_m''G_d' - G_m'G_d'')$$

$$B_3 = 4\frac{\alpha}{R}\left(2G_m^{'} + 5G_d^{'}\right) + 19\left(G_d^{'2} - G_d^{''2}\right) - 16\left(G_m^{'2} - G_m^{''2}\right) - 3\left(G_m^{'}G_d^{'} - G_m^{''}G_d^{''}\right)$$

$$B_4 = 4\frac{\alpha}{R}\left(2G_m^{''} + 5G_d^{''}\right) - 32G_m^{'}G_m^{''} + 38G_d^{'}G_d^{''} - 3\left(G_m^{''}G_d^{'} + G_m^{'}G_d^{''}\right)$$

In the case of small amplitude oscillatory flow the predictions of rheological behavior of the immiscible blends using Palierne model has been found to be in good agreement with the experimental results (Bousmina and Muller, 1993; Graebling *et al.*, 1993). The Palierne model has been successfully used to fit the rheological and morphological data and determine the interfacial tension (Lacroix *et al.*, 1996; Graebling *et al.*, 1994) and also in determination of particle size distribution (Friedrich *et al.*, 1995). This model however, fails for systems that have a high concentration of the dispersed phase or cases where there is strong particle interactions or agglomerated particles (Graebling *et al.*, 1993).

Lee and Park (1994) further developed a model for multiphase systems based on Doi and Ohta theory (1991), which is not restricted to dilute or semidilute concentrations of the dispersed phase. In this model they accounted for coalescence and breakup phenomena and thus it can be used to describe the rheological behavior of polymer blends for any type of flow. This model assumed that the Cox-Merz rule is valid for the blends. However, it has been reported that the Cox-Merz rule is not always valid for blends mainly because of the morphology evolution during shear flow (Han *et al.*, 1995) and also because of the nonlinearity of the contribution of bulk properties and interfacial effect (Lacroix *et al.*, 1997). It is quite useful in describing the blend morphology under large deformation and was found to fit quite well at low frequencies but discrepancies were observed at high frequencies (Lacroix *et al.*, 1997). Besides predicting the morphological and rheological changes occurring in the simple shear flow, efforts are also being made to model the changes occurring in the elongational flow (Lacroix *et al.*, 1999).

2.2.3 Interfacial tension

Interfacial tension may be defined as the excess free energy per unit area, due to the formation of the interface between two immiscible polymers. The excess energy is due to the unbalanced molecular forces at the interface. Interfacial tension has been found to have a profound impact on the dispersed drop diameter in the blends of two immiscible polymers. Interfacial tension may depend on various parameters such as MW of the components, type of branching, branching content, and temperature. Control of the interfacial tension is critical to develop blend morphologies that yield systems with consistent and acceptable mechanical properties. Determination of the interfacial tension is therefore important in developing a predictive understanding, of the effects of processing conditions, on the morphology and the physical properties of multicomponent systems.

Wu (1974) and Luciani (1996a) have reviewed various experimental techniques for the measurement of interfacial tension. The experimental techniques can be mainly divided into two categories: equilibrium methods (static) and dynamic methods. Some of the static methods are the pendant drop, sessile drop and rotating drop. Some of the dynamic methods are the breaking thread and the imbedded fiber retraction. Most of these techniques, however, have been reported to be quite cumbersome and extremely sensitive.

Several theoretical models have been developed for predicting polymer interfacial tension and are primarily based on two approaches: the lattice theories and the semi-empirical correlation's based on the surface tension. On one hand, the models based on lattice theories are of difficult use in that they require determining the lattice and binary interaction parameters. The semi-empirical relationships, on the other hand, need experimental values of the surface tension or the solubility parameters. Luciani *et al.* (1996b) has done a good review on the various theoretical models and concluded that they are not advanced enough to replace the experimental measurement of the interfacial

tension coefficient. Besides these methods, rheological data that is the storage and loss moduli, measured using oscillatory sweep experiments have also been correlated with the interfacial tension using Palierne and Lee and Park models. These models as discussed earlier have their limitations. They are however, convenient to use and have been reported to give a fair estimate of the range of interfacial tension.

Literature Review

Chapter 3

This chapter focuses on the study of the relevant literature on PE/PP blends in terms of their mechanical properties, flow properties and morphology. Mechanical properties of the blends are extremely important in determining the blend's end use. They depend in a complex manner on various factors such as crystallinity, morphology, interfacial bonding between the components, composition, additives and processing conditions. As these properties (mechanical, flow and morphological) are interrelated, different researchers have performed studies from various perspectives, with a common objective to improve the mechanical properties of these blends.

3.1 Immiscibility / Incompatibilty

Polyethylene and Polypropylene both are semicrystalline in nature and are capable of crystallizing with lamellar and spherulitic morphology. Generally PE crystallizes in an orthorhombic form while PP crystallizes into a α-monoclinic form and/or β-hexagonal form. Polyethylenes exhibit melting points of 110-140°C, whereas PP's α form melts at 160-170°C and β form melts at 140–150°C (Teh *et al.*, 1994). This distinct difference in the spherulitic morphology and their melting temperatures has been reasoned by some authors as the prime cause for incompatibility and immiscibility in the solid state (Shanks *et al.*, 1998; Teh *et al.*, 1994). Immiscibility of these components in

the liquid state has been attributed to the small differences in the shape of the molecules which overcome the weak intermolecular forces (Shanks *et al.*, 1998). Various techniques such as Differential Scanning Calorimetery (DSC), X-ray Diffraction, Small Angle Neutron Scattering (SANS) have been used to study the miscibility and compatibility of PE/PP blends. DSC and Wide Angle Xray diffraction (WAXD) techniques were used by Teh (1983) for LDPE/PP system. The DSC results showed two distinct melting peaks for the blends, which almost coincided with the melting point of the homopolymers, suggesting no interaction between the components. Furthermore this was confirmed with WAXD results, in which he observed no detectable change in the interplanar spacing and no new diffraction pattern. In certain specific cases, however, a partial miscibility and compatibility has been reported. Crystallization kinetics studied using optical microscopy was done by Shanks *et al.* (1998) to examine the miscibility of PE/PP blends. They reasoned that the crystalline structure formed from the melt of a miscible blend would be different than that formed from an immiscible blend. The miscible blends exhibited a co-continuous morphology whereas the immiscible blends showed a two phase crystalline structure on cooling of these blends. They used crystallization half time to show that LLDPE and PP used in their study were either miscible or partially miscible. Further, Alle and Lyngaee-Jorgensen (1980) studied the capillary flow behavior of PP/HDPE blends for different compositions and temperature. They reported a good superposition of steady state viscosity data onto master curves indicating "that all the blends of PP and HDPE are either compatible in the molten state under shear flow conditions or have a morphology which is independent of temperature".

3.2 Mechanical Properties

Blend compatibility is also assessed by comparing the measured mechanical properties of the blend to the value of the weighted average property of the pure components. In general, it has been found that for PE/PP blends, the mechanical properties such as impact strength, tensile strength and yield stress, show either positive deviation, negative deviation or may follow the rule of mixture. Extensive studies have

been done on HDPE/PP blends to understand how the processing and material properties affect the mechanical properties of these blends. Early studies by Noel and Carley (1975) showed a maximum in both the tensile modulus and the tensile strength at a composition of 90% PP. They also found that 90% PP blends exhibit considerably more elongation than the others. Based on these observations, they suggested that at the low-PE end because of high crystallinity, the PE acts as a stiffener for the PP while, at the other end PP plasticizes the PE, making it more ductile. Lovinger and Williams (1980) further studied these blends and attributed the increase in the tensile modulus to the combined effect of (i) the reduction of the size of the spherulite on addition of PE, and (ii) the increase in the overall crystallinity and the formation of intercrystalline links. Bartlett *et al.* (1982), on the other hand found that the strength and the modulus followed a simple additive relationship with no synergism in case of injection molded sample of the PP/HDPE blends. They observed, however, a synergistic effect when the samples where compression molded and quenched. Bartlett and his coworkers concluded that the changes in the processing and thermal conditions significantly affects the crystallization kinetics and phase orientation, which in turn affect the mechanical properties. In a recent study, Schurmann *et al.* (1998) observed that the tensile modulus, somewhat followed the mixing rule. They observed, however, a pronounced positive deviation in the impact strength for all PP/HDPE blends. They attributed this deviation to the decrease in spherulite size as previously observed by Lovinger and Williams (1980). Additionally, they postulated that the increase in the impact strength was due to the excellent distribution of the nucleation centres, which result in the increase of the total interphasial volume. The synergistic effect in the HDPE/PP blends has also been attributed to the closeness of the melting points of HDPE and PP, which enables simultaneous crystallization of the PP and PE under rapid cooling conditions (Teh *et al.*, 1994).

While a lot of work has been done on HDPE/PP blends to get a better understanding of these blends and put them to better use, studies on mechanical properties of LLDPE/PP blends are limited, as LLDPE is relatively a newer polymer.

These blends in general, have shown positive deviations and/or follow the additivity rule thus leading to the conclusion that these blends are compatible. Dumoulin *et al.* (1984a) studied for 50% composition and observed positive deviation for tensile modulus, maximum elongation and yield stress at both ambient (23°C) and low temperature (-40°C). They attributed the deviation to the strong inter-phase interaction. Dumoulin *et al.* (1984b) further studied these blends using compatibilizers of different molecular weight. They found that addition of the compatibilizer further enhanced the properties both at ambient and low temperatures, independent of the molecular weight of the compatibilizer. Further studies led them to the conclusion that the low strain mechanical properties of these blends are nearly additive and are independent of the viscosity of the components (Dumoulin *et al.*, 1987). They also observed that the blend composition containing 5% LLDPE showed a particularly attractive behavior, and was attributed to the decrease in the crystallinity. Utracki *et al.* (1987) on the other hand reported a systematic decrease in the modulus for blends containing 5% PE. This unusual behavior was unexplained by them. Flaris and Stachursky (1992) also observed a reduction in the impact properties upon 20% addition of LLDPE to PP. They attributed it to the small particle sizes of the dispersed LLDPE phase, which were unable to control the craze growth in PP.

Muller *et al.* (1994) further studied PE/PP blends to reconcile the discrepancies observed in the literature. They found that the izod impact properties were highly sensitive to temperature and notch behaviour. Their results showed that the impact properties improved only at room temperature. Bain *et al.* (1994) found that while matching the viscosities of the components greatly improved the modulus of the blends at all compositions, the izod impact properties only improved for a range of compositions. Kukaleva *et al.* (1998) in a recent study also observed an increase in the tensile modulus, yield stress and impact strength for 40% or more PP content and attributed to some interaction between the two components. It should be further noted that, though some encouraging results were obtained at low strains, a drastic deterioration in properties like

elongation at break was normally reported. The elongation at break is higher in the homopolymers due to the ability of the semicrystalline polymers to be cold drawn through an orientation process where the lamella are rotated towards the draw direction and broken up into microlamella and submicroscopic units. In the blends, however, the weak interspherulite boundaries rupture before the orientation or the cold drawing process (Teh *et al.*, 1994).

3.3 Morphology, Rheology and Interfacial Tension

The mechanical properties of polymer blends are not just dependent on the composition and crystallinity of the components, but also on the morphology and the interfacial bonding of the components. The blend properties are therefore dependent upon the processing conditions such as the degree of mixing, rate of cooling, orientation and annealing history that affect the phase distribution and thus the final morphology of the blends. Morphology of crystalline polymer blends is complexly controlled by various parameters such as the crystallization conditions, composition, temperature of crystallization, rate of cooling, stress or strain orientation and annealing. Generally, when the melt blend is solidified, PP spherulites are encountered by domains of PE melt. The resulting morphology depends on whether the PE domains are expelled by the PP growing spherulite front, or whether the PE domains are engulfed and remain within the PP spherulite as inclusions (Teh *et al.*, 1994). Marteuscelli (1984) observed that when the blends were cooled from melting point above that of PP, to a crystallization temperature well above that of melting point of PE, polyethylene melt drops were incorporated in the intraspherulitic regions during the growth of the PP. The number of crystallites, their dimension and the their shape were dependent on the composition and the thermal history. Further Teh *et al.* (1994) explained that if the blends are cooled at slow rate from temperature well above the melt point of PP to much below that of the PE, it would result in the initial crystallization of PP followed by that of PE, and would result in larger spherulite size. On the contrary, fast cooling would result in the simultaneous crystallization of PE and PP, which would result in smaller sized spherulites

As PE/PP blends are generally immiscible and incompatible, the phase boundary also plays an important role in controlling and determining the material properties. This is especially true for mechanical performance where stresses have to be transmitted between the phases. In general, it has been shown (Kryszewski *et al.*, 1973) that interpenetration of PE and PP across the boundary takes place, thus forming an interphase. The thickness of the interphase, or the extent of interdiffusion, depends mostly on the melt temperature and the heating time. A further study by Bartczak and Galeski (1986) showed that during crystallization of PP the shape of the interface undergoes significant changes. The interface changes from flat to highly developed with many deep and branched influxes of the PE. This was attributed to the adhesion between melts, which acted as the driving force for the formation of these influxes. The presence of influxes was further reasoned to increase the interface strength mainly due to the increase in area. Dong *et al.* (1998) in a recent study observed that the nature of the interface between the PE and PP depends on which polymer crystallizes first. If polyethylene was first to crystallize, the two regions did not interpenetrate, but they interpenetrated when PP crystallizes first, thus strengthening the interface.

Phase morphology has been widely investigated with scanning electron microscopes. Lovinger and Williams (1980) studied the morphology of compression molded PE/PP blends by fracturing it in liquid nitrogen. They observed two distinct phases and found that the blends containing less than 50% PE, formed PE as the dispersed phase, while PP formed the dispersed phase at higher percentages of PE. The PE phase was characterized by short lamella, while the PP had broad and long lamella. They further observed that for 50/50 composition the blend was characterized by an interconnecting morphology. Galeski *et al.* (1984), also studied these blends and observed that the area occupied by the dispersed droplets and voids was much greater than the volume concentration. They attributed this to the fracture mechanism, which is probably directed towards the largest perimeters of embedded dispersed phase.

It has been observed that injection molded samples yielded a different fracture surface morphology as compared to compression molded ones. This is probably because in injection molded samples, the dispersed phase became elongated due to high shear rate and fast cooling while in compression molded samples remained spherical (Alle *et al.*, 1981). Liu and Truss (1996) studied the effect of remelting on the morphological stabilities of the LLDPE/PP blends. They found that the morphology of the blends was generally stable except for a 50/50 composition.

The rheological behavior of the blends is quite complex and extensive work has been done to relate them with composition, morphology and processing conditions. In an early study Alle and Lyngaae-Jorgensen (1980) observed that the viscosity curves of the blends follow closely the same behavior as that of the pure components at all temperatures. They also found that for homopolymers with large differences in their viscosities, the melt viscosities of their blends lie between those of the pure homopolymers. This was also observed by Valenza *et al.* (1984). However, in some cases the viscosity curves may be lower than both the pure homopolymers (Noel and Carley, 1975) or gradually changes its characteristic from the character of PP to PE with the increasing content of PE for viscosity curves in which crossover were observed (Fujiyama and Kawasaki, 1991). The melt viscosity at constant shear stress was further found to be dependent on viscosity ratio (Fujiyama and Kawaski, 1991). Linear, negative deviation, minimum behavior or sigmoidal behaviors have been observed depending on the type of PE and PP (Alle and Jergenson, 1980; Valenza *et al.*, 1984; Fujiyama and Kawaski, 1991).

Beside viscosity, extrudate swell has also been found to be dependent on the composition, shear rate and temperature (Valenza *et al.*, 1984; Fujiyama and Kawasaki, 1991). Some researchers claimed temperature dependency for certain range of compositions only (Alle *et al.*, 1981). A complex dependency of extrudate swell with

shear rate and composition was also observed and was found to be controlled by viscosity ratio (Fujiyama and Kawasaki, 1991). A good review on the rheological properties of these blends has been done by Teh *et al.* (1994). They concluded that rheological behavior cannot be described by a simple additivity law as the rheological behavior of the components may vary with shear and temperature and, in turn, would affect the morphological behavior.

Considerable efforts are being further devoted to study the relationships between rheology and morphology of immiscible polymers and many various models have been proposed. While a large amount of work has been carried out for small amplitude oscillatory flow, the Palierne model is the one most widely used to describe the linear properties of emulsion type polymer blends. This model has been used by quite a few researchers to successfully predict the dispersed phase size or interfacial tension (Graebling *et al.*, 1993). However, since the Palierne model is limited to low strains, models such as Lee and Park (1994) and Grmela and Ait-Kadi (1994) have been proposed which can be used for nonlinear viscoelasticity.

Measurement of interfacial tension is another field that has received a lot of attention in the past decade. Interfacial tension between the components is known to significantly affect the blend morphology and thus in turn the mechanical properties. Since the interfacial tension, morphology and mechanical properties are interrelated, measurements of the interfacial tension of the system can give us an insight on the mechanical properties of the blend. Carriere and Silvis (1997) studied the effect of the comonomer type on the interfacial tension of PP/LLDPE blends using imbedded fiber retraction method. It was observed that the interfacial tension decreased with an increase in the octene content. This was attributed to the enhancement in the chain ends per molecule and a lower average molecular weight between chain ends. Furthermore Yamaguchi (1998) studied the adhesion of LLDPE/PP and LDPE/PP and calculated interfacial tension using the Palierne model from the rheological data. He found that the

LLDPE/PP had better adhesive properties as compared to LDPE/PP and attributed it to the enhanced entanglements between PE and PP which was related to the interfacial thickness and also to the low interfacial tension. Rao (1999) used breaking thread method to quantify the interfacial tension of LLDPE and PP system. He observed the lowest interfacial tension with Butene comonomer. However, he did not observe any trend for the other resins used.

3.4 General Observations

The various studies on PE/PP blends indicate a complex relationship amongst the various properties and also show the interdependence on one another. It is also seen that contradictory observations have been made by different researchers. This is probably due to the differences in the molecular structure of the starting resins and also due to the differences in the processing. However, it can be inferred that in general, addition of PE to PP improves the mechanical properties such as tensile modulus and impact strength. These mechanical properties may be further improved with the addition of a compatibilizer.

Many attempts are still being made to further improve the impact property of PP, especially at low temperatures, where the mechanical properties are limited by the relatively high glass transition temperature of PP as compared to PE. The success of some of the PE to be used as impact modifiers has motivated the use of LLDPE in PP blend. Recycling of these resins, is another issue that has interested the researchers to study these blends and ultimately put them to better use. However, it is difficult to draw any conclusions from the literature on these blends, as usually the starting polymers are quite different in their molecular structure (type of copolymer, MW, MWD, comonomer content etc). The objective of the current study is therefore to relate the molecular structure (MW, MWD, type of comonomer, branch content and distribution) to the morphology and rheological properties.

Experimental Work

Chapter 4

Six Linear low density polyethylene (LLDPE) of varying comonomer types (1-butene, 1-Hexene and 1-Octene) and two types of polypropylene (homopolymer and propylene ethylene copolymer) were used in this study. These are all commercial resins and were procured in the form of pellets from different suppliers (NOVA Chemicals, Exxon and Equistar). The characterization of these resins was done, using Differential Scanning Calorimetry (DSC), Temperature Rising Elution Fractionation (TREF) and Gel Permeation Chromatography (GPC). These resins were used to prepare blends (LLDPE/PP). The morphology of the blends was observed using Scanning Electron Microscopy (SEM) and Optical Microscopy. Rheological measurements of both virgin resins and their blends were performed using a controlled stress rotational rheometer. The details of the various experimental measurements are given below.

4.1 Thermal Behavior

Differential Calorimetery is a thermal analysis technique in which the differential energy required to keep the sample and the reference at the same temperature, is measured by subjecting it to controlled heating procedure. It is one of the most widely used techniques to determine degree of crystallinity, melt temperature and glass transition temperatures of the polymer.

The melting and crystallization behavior of the homopolymers and blends were examined using a Mettler 12E Differential Scanning Calorimeter along with its TA89E software. Indium was used for the calibration of the melting peak temperature and enthalpy of fusion. The samples were scanned up to 190°C at a heating rate of 10°C/min and then cooled down to 60°C at 10°C/min (Rana *et al.*, 1998). The sample was then again rescanned at the same heating rate and temperature interval as mentioned above. The melting temperature, heat of fusion and the degree of crystallization were calculated from the second scan. The degree of crystallinity of the blends was determined using the areas under the two peaks and using the following relationship (Choudhary *et al.*, 1991).

$$\% \text{ crystallinity} = \frac{\Delta H_f^{comp}}{\Delta H_f^{o}} * 100 \qquad (4.1)$$

where ΔH_f^{comp} is the measured heat of fusion of the components and ΔH_f^{o} is the heat of fusion of the 100% crystalline polymer. The value of ΔH_f^{o} was taken as 285J/g for 100% crystalline PE and 188J/g for 100% crystalline PP (Progelhof and Throne, 1993). The details of the experimental procedure and data processing has been attached as Appendix A.

4.2 Gel Permeation Chromatography (GPC)

Molecular weight and the molecular weight distribution of the polymers is usually measured using Gel Permeation Chromatography (GPC) method. The measurements however, could not be performed in our lab due to the unavailability of the equipment to perform the GPC experiments and so were contracted out. These experiments in general are done by dissolving the resin in a solvent and then injecting this solution into the solvent flowing through the packed bed. The analysis is based on the concept that different size molecules would diffuse at different rates through a packed column of absorbing gel beads. Smaller molecules have a greater solubility in the gel beads and so diffuse through the bed at a slower rate than the larger molecules. Thus by monitoring

the polymer concentration of the eluting solution as function of time and comparing the result with the standard calibration curve for that type of polymer, the molecular weight distribution can be determined.

4.3 Temperature Rising Elution Fractionation (TREF)

The branching distribution and its content were analyzed using data obtained from TREF. This is a method to classify molecules based upon their crystallizability. The higher the degree of crystallinity the higher is the dissolution temperature of the sample. Based on the crystal dissolution temperature, the distribution of the short chains is inferred. Though this technique is relatively new, it is gaining a lot of popularity for characterization of the branching distributions in LLDPEs. A review on the TREF apparatus and its applications has been done by Glockner (1990). These experiments were performed at the University of Alberta and a general experimental procedure follows. The experimental procedure mainly requires two steps, i.e. crystallization and elution. The crystallization step involves dissolving of the polymer in the solvent at elevated temperature in order to disentangle the chains. The sample is then crystallized at controlled temperatures and this helps in the regular crystallization of the molecules based upon their ability to crystallize. The linear molecules crystallize at higher temperatures as compared to the branched molecules. The next step is the elution step and is the reverse of the crystallization step. Here the crystallized sample is dissolved in the solvent flowing through the column. The elution temperature is increased gradually leading to the fractionation of the material based on the solubility of its crystallized constituents. The eluting sample is then passed through infrared detector to measure the amount of material eluting at certain temperature. This analysis is termed as Analytical TREF (ATREF). The term Preparative TREF (PTREF) is used when fractions of the polymer eluted at different temperatures are collected for subsequent analysis by techniques such as Nuclear Magnetic Resonance (NMR), Differential Scanning

Calorimetry (DSC), Fourier Transform Infrared Spectrophotometry (FTIR) (Defoor, 1993). In our work, ATREF was used to characterize the resins studied.

4.4 Blending Procedure

A Haake Rheocord 40 torque rheometer equipped with a Haake 600 series internal batch mixer was used to prepare the PE/PP blends. The sectional view of the mixer is illustrated in Fig 4.1.

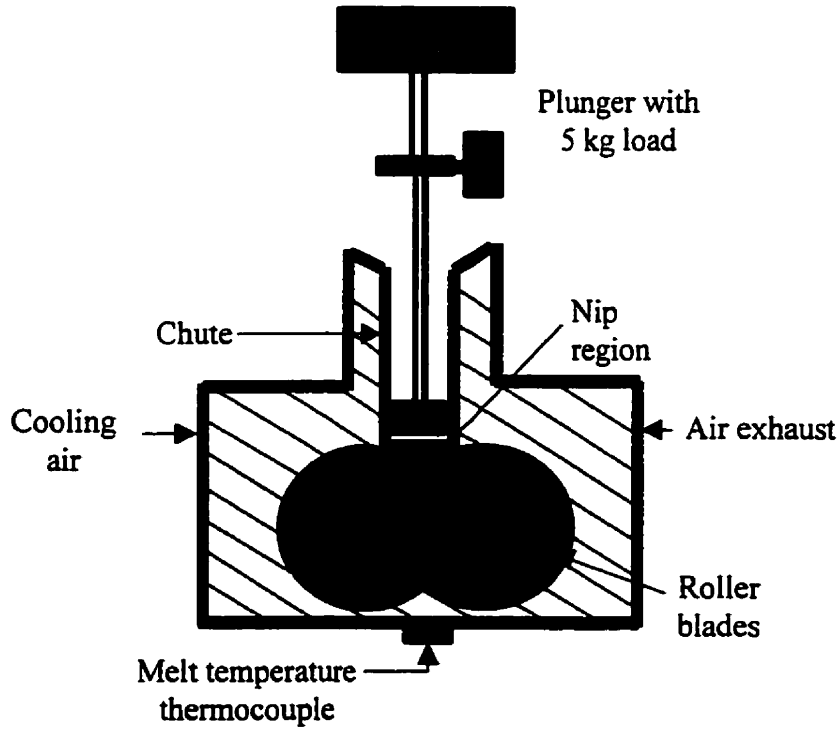

Fig 4.1: Sectional view of the internal batch mixer

The mixer has programmable temperature and speed and was air cooled. The mixer was preheated to the run temperature, 190°C, before adding the pellet mixture. The pellets were weighed using an Ohaus balance, which had an accuracy of 0.001g. To ensure a good dispersion, the mixing volume at the run temperature was set at 70% of the total mixer volume (69 cc). It has been advised by the manufactures that for this volume, there would be optimal material interchange between the mixer chambers. This would

minimize the stagnant areas in the mixer due to overloading and segregation of the phases around the mixer blades in the case of under loading. The weight of the individual components to obtain the 70% volume loading was then determined based on the pellet densities at ambient temperatures.

The weighed pellets were initially mixed in a container and then loaded into the chute of the mixer. A plunger, which is attached to 5 kg of weight, was used to guide the pellet into the mixer. Once the pellets were loaded, the chute was removed. Blending was done in an atmosphere of nitrogen to prevent the resins from degradation by air oxidation. Blending was done for a run time of 5 minutes in order to obtain a stable morphology while preventing degradation of the resins. Once the run time was over, the rotor blades automatically stopped rotating. The mixer face plate was quickly removed and the samples were scooped from the different parts of the mixer. In practice, approximately the first half of the blend collected from the blender was ice quenched and used for preparation of samples for microscopy and rheological measurements. The rest of the polymer blended was discarded as it was exposed to high temperature and air and may result in degradation.

4.5 Rheological Characterization

Viscoelastic properties are generally measured by dynamic mechanical testing, in which the material under test is deformed by step function strain, strain rate or stress and the response of the material is measured. Small amplitude oscillatory shear experiments are one of the most widely used experiments to characterize the polymers. In these experiments, a thin sample of material is subjected to a simple rotational sinusoidal shear strain, which is a function of time and is given as

$$\gamma(t) = \gamma_0 \sin(\omega t) \tag{4.2}$$

where, γ_0 is the strain amplitude and ω is the frequency.

This results in the following complex function for the shear stress

$$\tau(t) = \gamma_0(G'(\omega)\sin(\omega t) + G''(\omega)\cos(\omega t)) \qquad (4.3)$$

thereby defining two frequency dependent functions, the shear storage modulus $G'(\omega)$ and the shear loss modulus $G''(\omega)$. The elastic or storage modulus $G'(\omega)$ is in phase with the applied strain and measures the mechanical energy stored during each rotation. The loss modulus $G''(\omega)$ is out of phase with the applied strain and measures the amount of mechanical energy dissipated per cycle.

The oscillation sweep experiments were performed using the Haake RS150 Rotational Rheometer. A plate-plate configuration was used, with a plate size of 20 mm and a gap of 1.5 mm. Since polymers are quite sensitive to air and heat, experiments at higher temperatures and lower frequency were carried out in an atmosphere of nitrogen to avoid thermal degradation. Samples were prepared by melting the polymer at 190°C and pressing the melted resins to form a thin sheet of around 2 mm height. Samples were then, immediately cooled by quenching in ice water. The whole procedure took less than 2-3 mins. A 20 mm diameter circular cutter was used to cut out the sample from the sheet. The samples were visually inspected and those containing air bubbles were discarded, as they would result in erroneous results. These samples were then loaded between the parallel plates and the extra material was gently squeezed out, in order to properly wet the plates and also to obtain the desired gap of 1.5mm. As the rheometer used is a constant stress rheometer, initially stress sweep experiments were performed at various frequencies viz. 0.1Hz, 1Hz, 10 Hz and 45 Hz, in order to obtain the linear viscoelastic range of the polymer. Once the linear viscoelastic range of the polymer was determined, frequency sweep tests were then done in a frequency range of 0.00147Hz to 100 Hz. The frequency sweeps were done at temperature of 190°C. The stress obtained for the different frequency ranges never produced more than 15% strain. It was verified that the polymers response were in the linear region for this value of strain.

4.6 Morphology Characterization

The direct visualization of phases in blends can be done with the different microscopy techniques. Though there are some other indirect methods such as light scattering, DSC etc, they are not always suitable and not as reliable as direct imaging. Vessely (1996) has done an excellent review on the different microscopy techniques, which are primarily light microscopy, transmission electron microscopy and scanning electron microscopy.

Phase dispersion was characterized using Scanning Electron Microscopy (SEM). The model of microscope used is Hitachi S 450, and is equipped with a manual camera. The samples were prepared by fracturing the quenched blends in liquid nitrogen. If the blend did not fracture while in the liquid nitrogen, then it was impacted by a hammer and fractured while still cold. The pieces of the fracture were glued on to the aluminum stub by a double sided adhesive tape. The opposite side was trimmed, so that the total height of the sample did not exceed 3 mm. The samples were then coated with a thin layer of gold/palladium alloy in an evacuated cathodic chamber. The coating provides a conductive path and prevents overcharging and overheating of the sample during SEM examination.

The stubs with the samples were then placed on the sample holder, which slides into a dove tail slot in the SEM chamber. Normally two kinds of electrons, secondary and backscattered, are generated during the examination and, depending on the samples, either of them may be used. For the examination of our samples, we only used the secondary electrons. A beam voltage of 20 KV and a suitable magnification to measure the particle diameter was used for all the samples. The samples were scanned in all directions and several photographs of each sample were taken using a 35mm manual camera. The film was then developed and the photographs scanned for image analysis.

The crystalline structure of the blends and its components were observed using an optical microscope and polarized light. The samples for the optical microscopy were prepared using a hot plate. Around 2 mg of sample was cut from the blend or the homopolymer and melted in between two glass slides at a temperature of 190°C, under 5 kg of load for 1-2 min. The samples were either ice quenched (fast cooled) or air quenched (slow cooled) to ambient temperature, to observe the spherulites. Some of the samples were heated in the hot plate to around 190°C and then cooled back at different rates of cooling that is -10°C/min and -1°C/min, to further examine the effect of the cooling rate on the crystallization kinetics.

Results and Discussions

Chapter 5

5.1 Physical Properties of the Virgin Resins

The physical properties of the six Linear low density polyethylenes and two Polypropylenes were determined using the methods described in Chapter 4. The samples have been abbreviated according to the melt flow index (MFI) and comonomer type (B-Butene, H–Hexene, O-Octene) for convenience. The resin's MFI, densities and the supplier's information are given in Table 5.1. The range of melting temperatures, maximum endothermic peak temperatures and percent crystallinity for all the virgin resins, as calculated from the DSC measurements, are also presented in Table 5.1. It should be noted that a higher percent crystallinity indicates a tightly packed ordered chain structure and therefore results in higher density, which is in line with the results presented in Table 5.1.

The storage modulus $G'(\omega)$ for all the LLDPE and PP resins as functions of frequency are presented in Fig. 5.1. It is observed that PE-B1.0 and PE-O0.8 show the highest storage modulus and PE-B20 exhibits the lowest storage modulus. The rest of the LLDPE resins show an intermediate behavior. Further, comparing PPHo with the various LLDPE resins exhibiting intermediate behavior, it is observed that PPHo shows a slightly

Table 5.1 : Material properties of the LLDPE and PP resins

Names	Comonomer	Supplier	Code No	MFI * @190°C	Density (G/cm^3)	Melting Range Temp. (°C)	Peak Melt Temp.(°C)	% Crystallinity
LLDPE								
PE-B1.0	Butene	Nova	PF0118F	1.0	0.918	83.7 - 127.0	123.7	41.2
PE-B20	Butene	Nova	PI2024A	20	0.924	89.4 - 126.0	124.2	42.0
PE-H3.3	Hexene	Exxon	LL8460	3.3	0.938	97.4 - 135.0	129.6	55.7
PE-H6.8	Hexene	Exxon	LL8555	6.8	0.935	95.9 - 133.0	127.2	54.1
PE-O0.8	Octene	Nova	SC9443	0.8	0.920	87.8 - 128.2	125.9	43.1
PE-O5.3	Octene	Nova	SC6003	5.3	0.919	82.0 - 126.8	124.8	43.0
PP								
PPCo	Ethylene	Exxon	PP7194	20**	0.89[a]	151.0 - 171.2	165.1	48.8
PPHo	-	Equistar	PP51B12A	38[b]	0.90[a]	138.6 - 170.4	165.4	60.4

* given by supplier

** MFI at 230 °C / 2.16 kg

a) measured using archimedes principle

b) estimated using shear viscosity vs. shear rate data at 230°C (refer Appendix B)

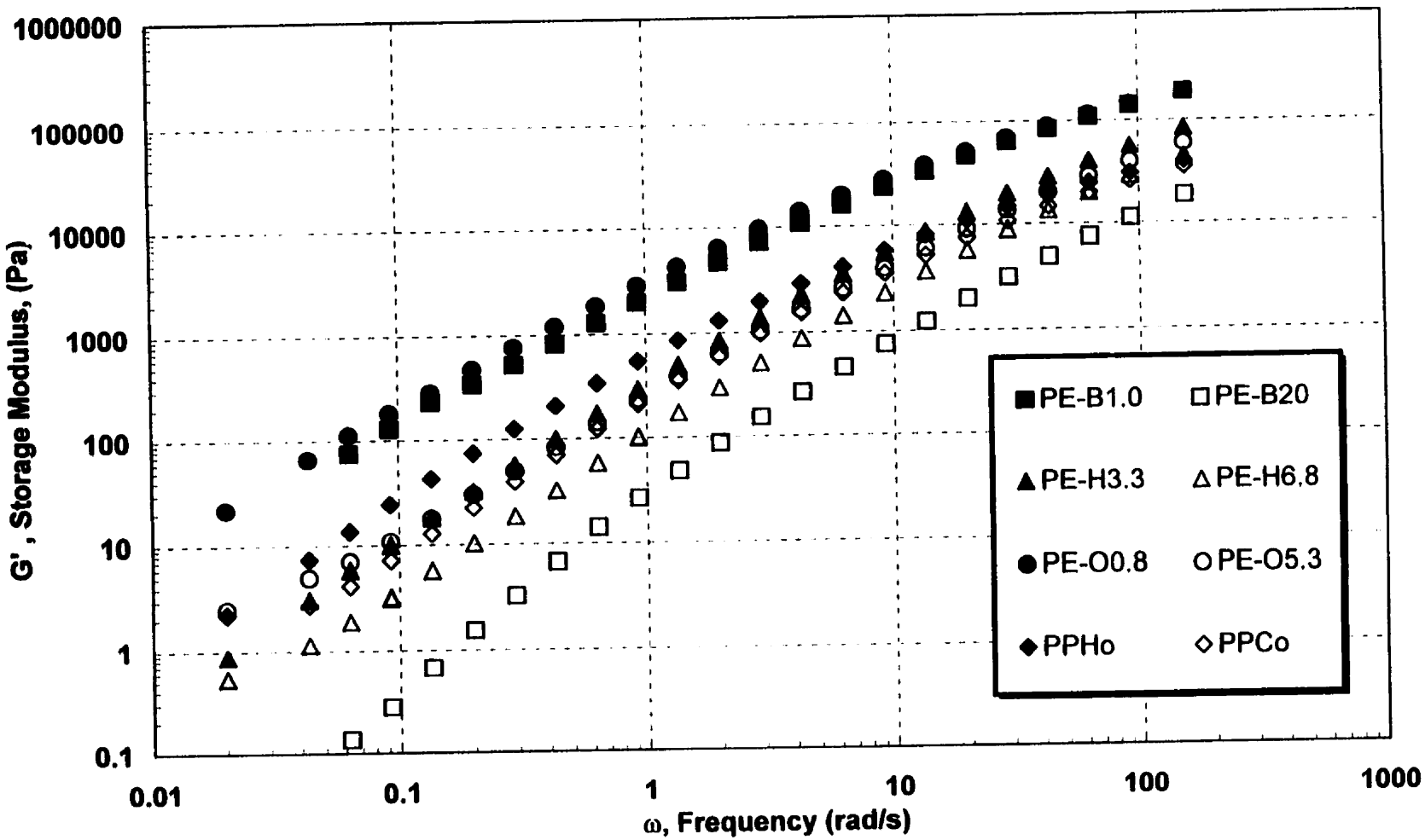

Fig 5.1: Storage Modulus as a function of frequency for the PP and LLDPE resins, at 190°C

higher modulus at low frequency. The shear viscosity $\eta(\dot{\gamma})$ versus shear rate $(\dot{\gamma})$ profiles has been obtained using the Cox-Merz rule (Fig. 5.2). The Cox-Merz rule states that the complex viscosity curves $\eta^*(\omega)$ is equivalent to the shear viscosity curves $\eta(\dot{\gamma})$ for all virgin resins. The shear viscosity at a shear rate of 65 s^{-1} is denoted as η_{65} and are presented in Table 5.2. The zero shear viscosity denoted as η_0, is calculated using equation 5.1 at a temperature of 190°C and is also tabulated in Table 5.2.

$$\eta_0 = \lim_{\omega \to 0} \left| \eta^*(\omega) \right| = \lim_{\omega \to 0} (G''(\omega)/\omega) \qquad (5.1)$$

The order of values for shear viscosity exhibit a similar trend to that observed for storage modulus. It can be noted that PE-B20 is the only resin whose shear viscosity is lower than that of PPHo at higher shear rates ($\geq 65\ s^{-1}$). A higher zero shear viscosity or the higher complex viscosity at low shear rates, reflects the relative difference in molecular weight among the samples (Harrell and Nakajima, 1984). From Fig. 5.2, the resins can be compared according to their molecular weight (MW) as PE-O0.8>PE-B1.0>PE-H3.3>PE-O5.3>PE-H6.8>PE-B20. This is consistent with the weight average molecular weight (M_w) results obtained using Gel Permeation Chromatography (GPC) (Table 5.2). It is also observed that the M_w of the polyethylene ranges from 47,000 to 107,300.

Zeichner and Patel (1986) correlated the breadth of the MWD for PPHo resins with the value of the "crossover modulus" G_c which is the value of storage modulus (G') and loss modulus (G'') at the crossover frequency ω_c where G' and G'' are equal. They defined the polydispersity index (PI) as

$$PI = 10^5/G_c\ (Pa) = 10^6/G_c\ (dynes/cm^2) \qquad (5.2)$$

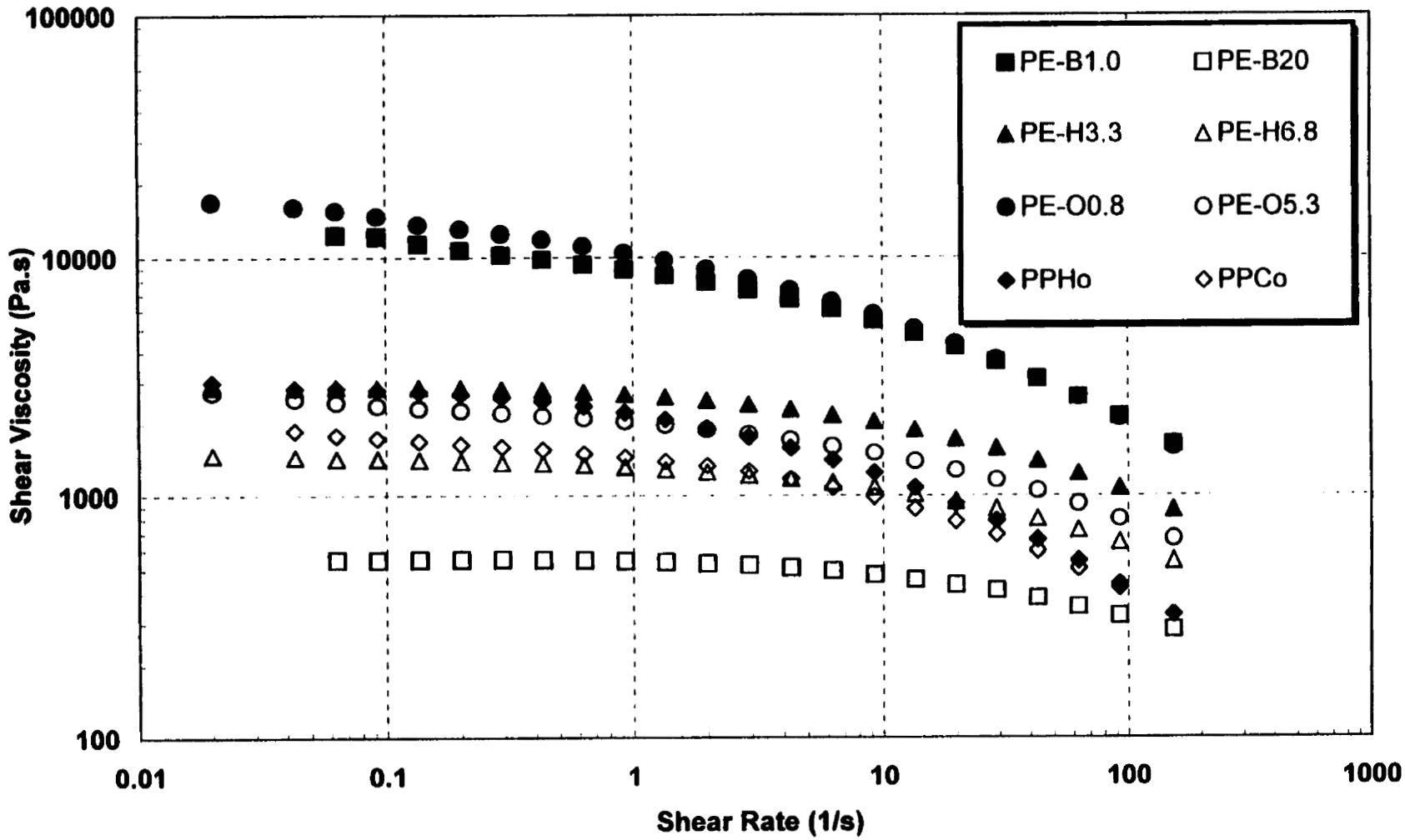

Fig 5.2 : Shear viscosity as a function of shear rate for the LLDPE and PP resins, at 190°C

Table 5.2 : Viscosity and molecular structure of the LLDPE and PP resins

Resin	Rotational Rheometer Results		GPC Results			TREF Results		
	η_0-190°C (Pa.s)	η_{65}-190°C (Pa.s)	M_n x 10^{-3} (G/mol)	M_wx10^{-3} (G/mol)	PI	CoHo Ratio	CH3/ 1000C	Dispersity**
PE-B1.0	17812	2930	34.4	107.15	3.12	9.7	14.8	Broad
PE-B20	559	352	13.6	47.1	3.48	14.7	15.2	Broad
PE-H3.3	3770	1235	23.8	72.2	3.03	1.32	6.1	Narrow
PE-H6.8	1834	720	19.4	61.3	3.17	2.0	10.8	Narrow
PE-O0.8	21286	2594	30.6	107.3	3.51	3.99	12.4	Broad
PE-O5.3	2905	926	22.1	66.1	3.00	6.8	13.2	Broad
PPCo	2381	505	-	-	2.7	-	-	-
PPHo	4008	541	-	-	4.1	-	-	-

η_{65} : $\eta^*(\omega)$ at ω =65 rad/s

η^{**} : dispersity is only for the copolymer section and is relative to the other LLDPE resins

Generally, this relationship has been found valid only for the polypropylene resins (Dumoulin *et al.*, 1984b). The PI of the polypropylenes has been calculated using equation 5.2 and results are presented in Table 5.2. The PI of the LLDPE resins presented in Table 5.2, have been obtained from GPC experiments. The PI values of LLDPE resins are relatively low and show little variation. In contrast PPHo has a higher PI value, indicating a broader MWD. This can be also observed from the shear viscosity vs. shear rate curves of PE-H3.3 and PPHo (Fig. 5.2). While the two resins have similar zero shear viscosity, the shear thinning behavior of PPHo is more pronounced and also starts at an earlier shear rate as compared to PE-H3.3, which is a clear indication of its broader MWD.

The characterization of branching distributions in LLDPE resins was done using Temperature Rising Elution Fractionation (TREF) results. The normalized TREF profile for the LLDPE resins is shown in Fig. 5.3. The profiles were normalized by subtracting the baseline signal and dividing these reduced Infrared (IR) signals by the area under the reduced IR-T curve. All the LLDPE resins TREF profiles show a bimodal branching distribution (Fig. 5.3). It is also observed that the homopolymer peak, which is the peak at high temperature, is quite narrow while the copolymer peak is very broad. This is an indication of the broad distribution of side chain branching. The bimodal distribution has been observed, earlier by Usami *et al.* (1986) and Rao (1999). The narrow elution peak temperature has been attributed to ethylene homopolymer of high crystallinity and the bimodality due to the character of the Ziegler Natta catalysts. The order of crystallinity predicted from the area of the elution peak at high temperatures is PE-B20<PE-B1.0<PE-O5.3<PE-O0.8<PE-H6.8<PE-H3.3. This is in accordance with the DSC crystallinity data with an exception for PE-B20 data.

The comonomer content in the LLDPE resins can be estimated by evaluating the copolymer : homopolymer ratio, referred to as the CoHo ratio. On the TREF profile the lowest point on the curve between the homopolymer and copolymer peaks is used to

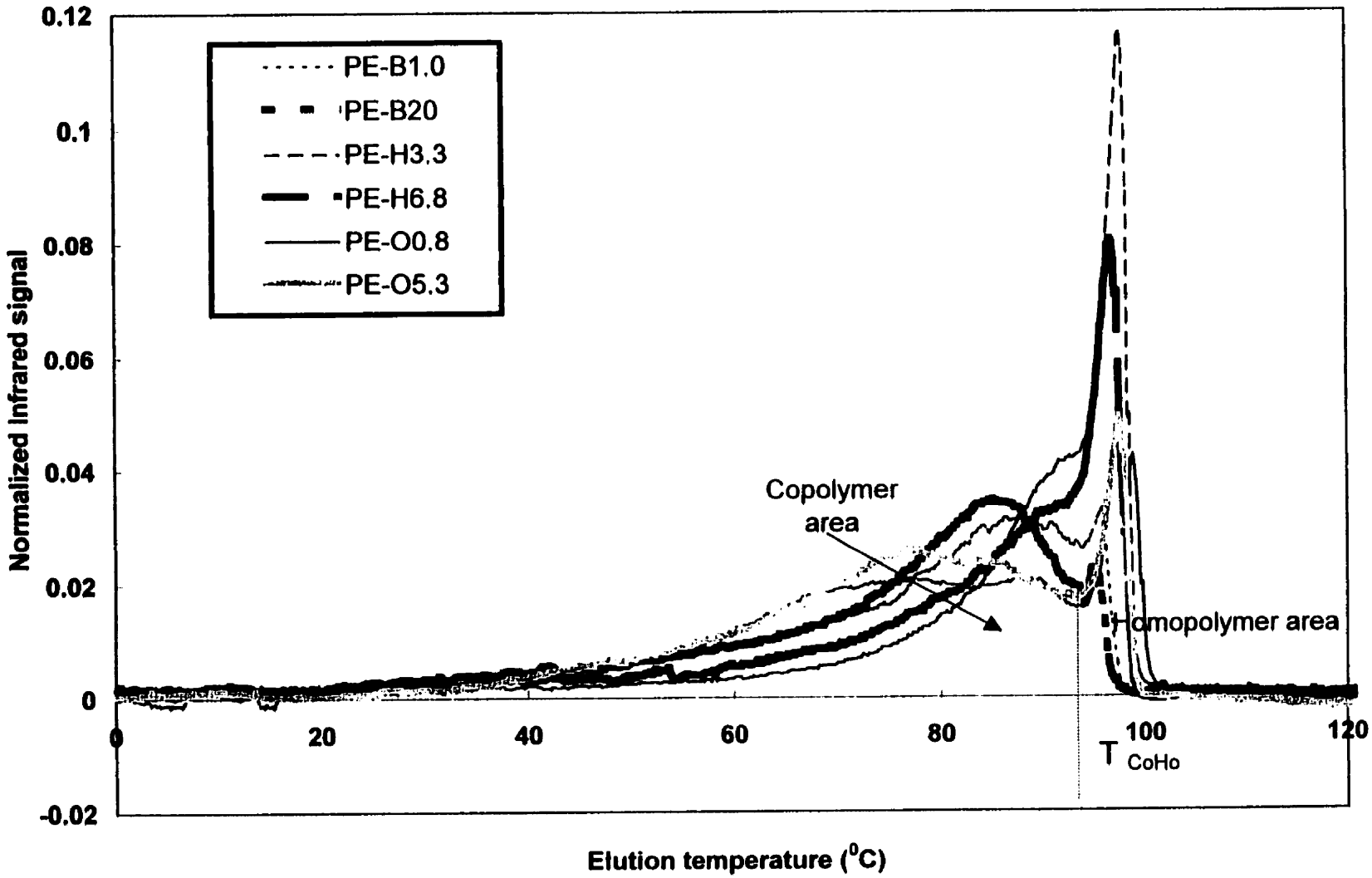

Fig 5.3 : Normalized TREF profiles for the six LLDPE resins studied

separate the copolymer and hompolymer elution temperature respectively (indicated by the vertical line drawn through T_{coho} in Fig. 5.3). The area under the TREF curve before and after the vertical T_{coho} line represents the fraction of copolymer and homopolymer respectively. The ratio of these areas, on the other hand gives an estimate about the branching of the polymer. The CoHo ratios were calculated using numerical integration using trapezoidal rule and are given in Table 5.2. Several repetitive temperature readings were there in the raw TREF data, so the data were averaged numerically. A copy of this program is given in Appendix C.

It is observed that PE-B1.0 and PE-B20 (i.e. the Butene copolymers) show the highest CoHo ratios and also a low crystallinity based on the DSC results, indicating high amount of branching. (Rao, 1999). The CoHo ratios are observed to vary according to the type of comonomer; Hexene<Octene<Butene and the crystallinity on the other hand varies in the reverse order. This is in concurrence, because the increased comonomer content signifies increased branching and thus would result in lower crystallinity. Further, the spread of the copolymer peak, which gives an estimate of the branching distribution, is relatively broad for Butene and Octene comonomer resins as compared to that of the Hexene comonomer resins. This indicates that Hexene comonomer resins have a relatively uniform branching distribution as compared to Butene and Octene resins.

Further, the concentration of the methyl groups in the copolymers was determined using the correlation given by Huang *et al.* (1997). The methylene sequence length (MSL) calibration method of Bonner *et al.* (1993) was used by them for converting T_{el} to the methyl group content.

$$\frac{1}{T_{el}} = \frac{1}{T_o} + c\frac{\ln(MSL)}{MSL} \tag{5.3}$$

where T_{el} is the elution temperature, T_o and c is the calibration parameter and MSL is basically the number of bond lengths of the crystallizeable sequence between the SCB. The constants for the above equation were found by Huang *et al.* (1997) and are given as T_o = 374.1 K and c = 0.0006583. The MSL has been further related to the methyl group concentration for linear polyethylene as

$$\frac{CH_3}{1000\,C} = \frac{2000}{MSL+2} \tag{5.4}$$

The analytical form for short chain branched PEs changes slightly for different comonomer types but the above correlation is found to be reasonably good for random intramolecular distributions of methylene sequence length, as found in LLDPE made with Ziegler–Natta catalyst (Huang *et al.*, 1997). The number of methyl groups per thousand carbon ($CH_3/1000C$) is estimated using these equations and is tabulated in Table 5.2. It is observed that $CH_3/1000C$ follows a trend Butene>Octene>Hexene. However, it should be kept in mind that this method is not the most reliable way to calculate the branching content quantitatively. Discrepancies have been observed by Rao (1999) when comparing the results to the manufacturer's data, though qualitatively it was found to be quite reliable. He attributed it to the fact that the calibration curves used to evaluate the branching were based on low molar mass hompolymer samples, and the use of these curves for differing comonomers and higher crystallinity might place undue emphasis on certain elution temperatures.

5.2 Polymer Blends

Blends were prepared in a ratio of 5, 20, 50, 80, 95% of PPHo by volume with the different grades of LLDPEs. The torque profiles obtained during mixing, the morphology of the blends and the rheological results are all presented in the following sections.

5.2.1 Torque profiles in the batch mixer

The Haake mixer is equipped with transducers to measure the torque during blending. The typical torque profiles (Bousmina *et al.*, 1999) as a function of time for mixing resins is shown in Fig. 5.4. When the polymer is introduced in the blender, the resins offer a certain resistance to the free rotation of the blades and therefore the torque increases. When this resistance is overcome, the torque required to rotate the blades at the fixed speed decreases and reaches steady state for a short time. The torque then again increases due to the melting of the surface of the granules, which coalesce giving bigger lumps. When sufficient heat has transferred for all granules to melt, a macroscopic melt continuum is obtained. As a result, the torque again reaches a steady state, though for a longer time. Subsequently, or when the sample is mixed for a long period, degradation takes place. The torque may increase or decrease depending upon whether cross-linking or chain scission degradation takes place. This is in agreement with the Shih *et al.* (1991) classification for mixing profiles. They had proposed four distinct rheological regimes that have been indicated in Fig. 5.5.

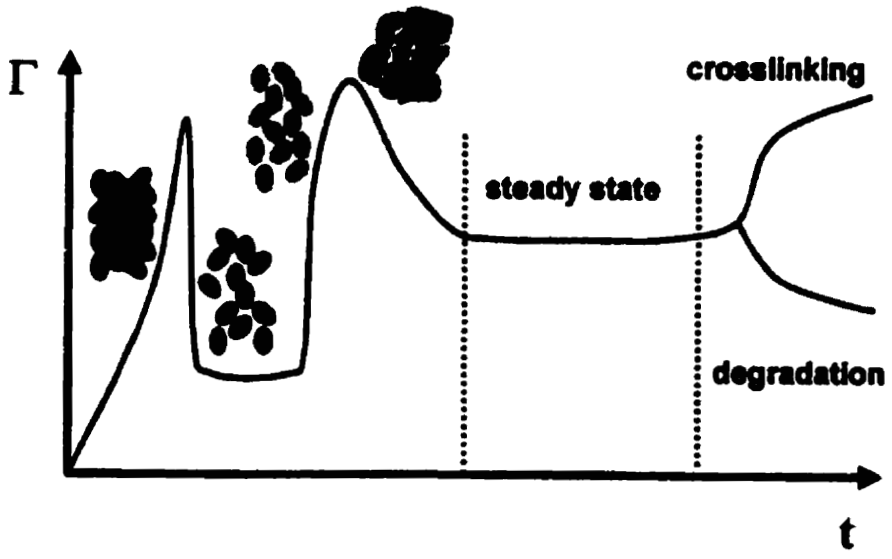

Fig. 5.4: Typical variation of the measured torque as a function of time (from Bousmina *et al.*, 1999)

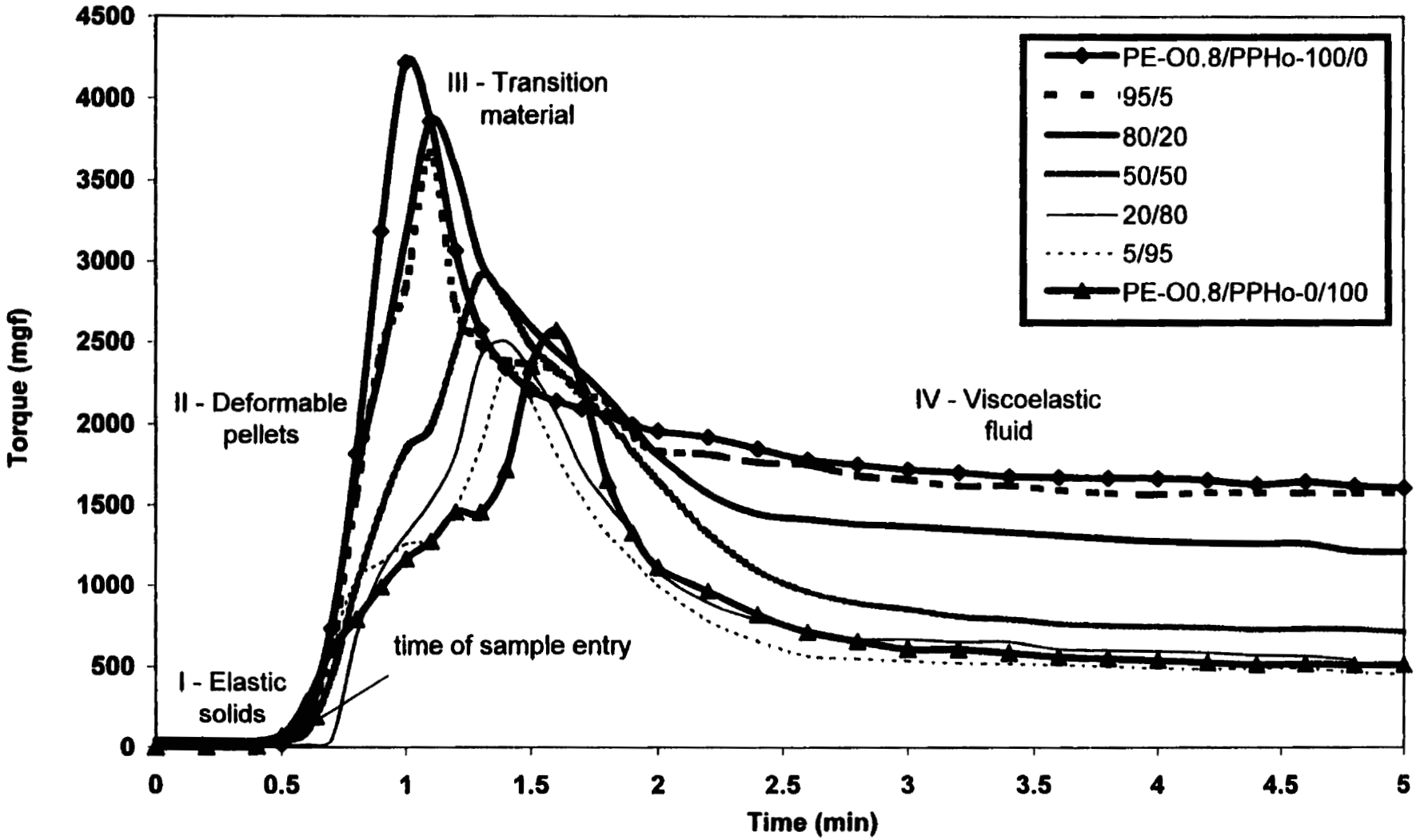

Fig 5.5 : Torque profiles for PE-O0.8/PPHo blends prepared at 190°C

Blending was done for a period of 5 min., as this time was considered sufficient for proper mixing. Researchers (Favis, 1990; Scott and Macosko, 1995) have reported that significant amount of size deformation and disintegration occurs within the first two minutes of polymer melt mixing. Moreover, longer blending time at high temperature would result in degradation of the sample, which is generally characterized by formation of brown films.

The torque profiles observed for the PE-O0.8/PPHo blends and its components are shown in Fig. 5.5. The rest of the torque profiles are attached as Appendix D. The second torque peak can be clearly seen, however, the first maxima was not observed as it is always very short and is seldom obtained in practice. It can be further observed from Fig. 5.5 that the torque becomes nearly constant after 3 to 3.5 minutes of mixing. This is an indication that the blend has melted completely and is properly mixed.

As LLDPE is dispersed in PPHo, we observe that there is a reduction in the torque peak and it also occurs at an earlier time. Shih *et al.* (1991) also observed this trend and attributed it to the lower softening temperature of the dispersed phase as compared to the matrix. This results in the melting of the LLDPE (dispersed phase) first and engulfing the PPHo (matrix), leading to a better lubrication and thus resulting in reduced deformation/torque. The melted LLDPE layer around the PPHo further provides an efficient layer for heat transfer resulting in the speed-up of the melting of PPHo, thus causing the peak to occur at an earlier time. A reduction in the torque peak is also observed, even with the addition of PPHo to LLDPE, where LLDPE is the matrix and PPHo is the dispersed phase. However, in this case we observe that the torque peak shifts to the right and the inception of the constant torque zone is delayed. This may be attributed to the combined effect of lower melting temperature of LLDPE and lower viscosity of PPHo. The shift of the torque peak to the right may be due to higher melting point of PPHo. The higher melting point of PPHo further results in requirement of more time to melt and hence delay in the attainment of a constant torque zone. The lower peak

as compared to that of virgin LLDPE is probably due to the lower viscosity of PPHo. Experiments conducted with LLDPE as the matrix and PPHo as the dispersed phase, PPHo having a higher viscosity than that of LLDPE, indicate an increase in the torque peak (e.g. : PE-B20/PPHo results in Appendix D). This observation is in line with the above explanation.

It was observed that the steady state torques for the blends tends to lie between that of the hompolymers, and increased or decreased with the addition of the dispersed phase concentration depending upon the shear viscosity. The change in the magnitude of steady state torque can be easily observed for PE-O0.8/PPHo blends (Fig. 5.5) due to a large difference in the shear viscosity. We also observe some torque profiles which are different, however this might be due to the low sensitivity of the machine. The sampling time for the torque curves was six seconds, which is a relatively large sampling period and may have resulted in these differing results.

5.2.2 Thermal behavior

Figs. 5.6 to 5.8 show the thermogram scans of the homopolymer and the blends. Two distinct peaks where observed for the blends. It can be seen that each component of the blend produces an endothermic peak that retains the characteristic shape of the homopolymer. The melting behavior of the blends, also show constant melting points with a maximum standard deviation of 1.53°C. The difference is relatively small and it is a usual expected error/variation within the sample. Thus we can consider that there was no detectable shift in the melting point for all the blends with various comonomers. This indicates that these blends are immiscible and that there is no mixing between the components of the blends at molecular level.

At higher concentration of PPHo it was observed that the endothermic peaks are not always separated and some overlapping portion occurs. The evaluation of the peak area of the components was carried out by dividing the overlapping regions to areas

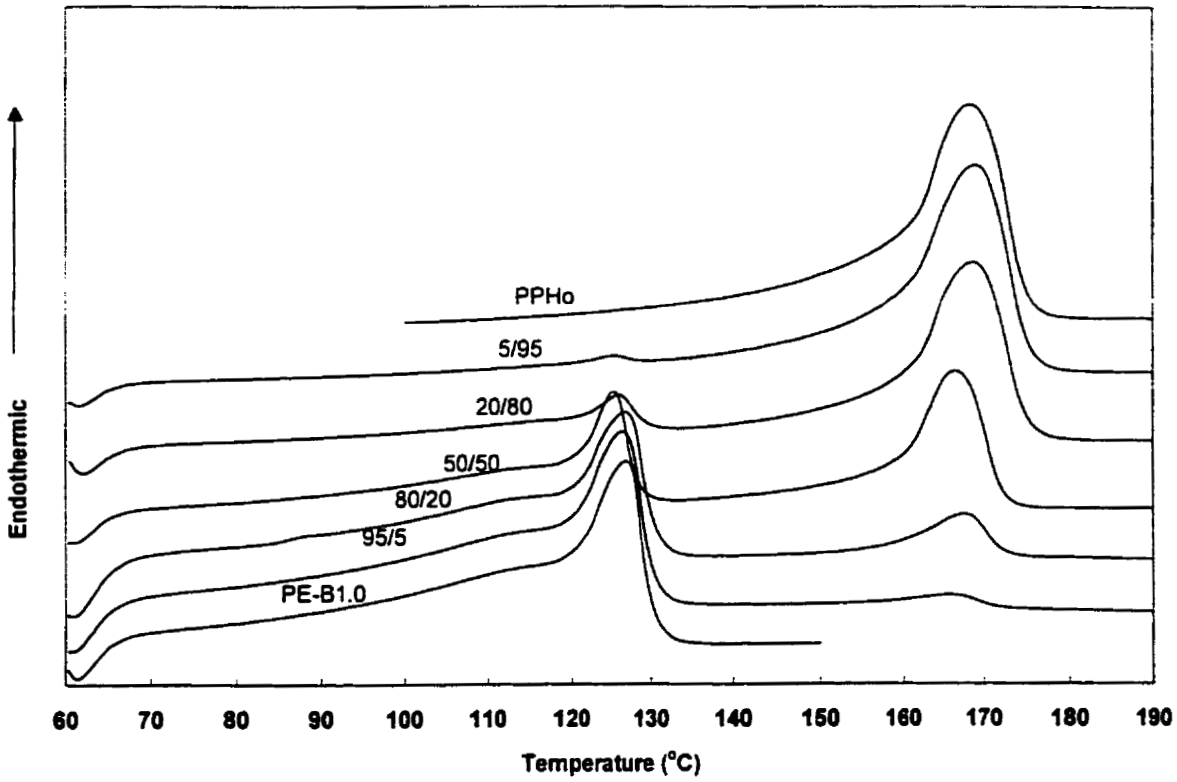

Fig 5.6 : Thermogram scans for PE-B1.0/PPHo blends prepared at 190°C

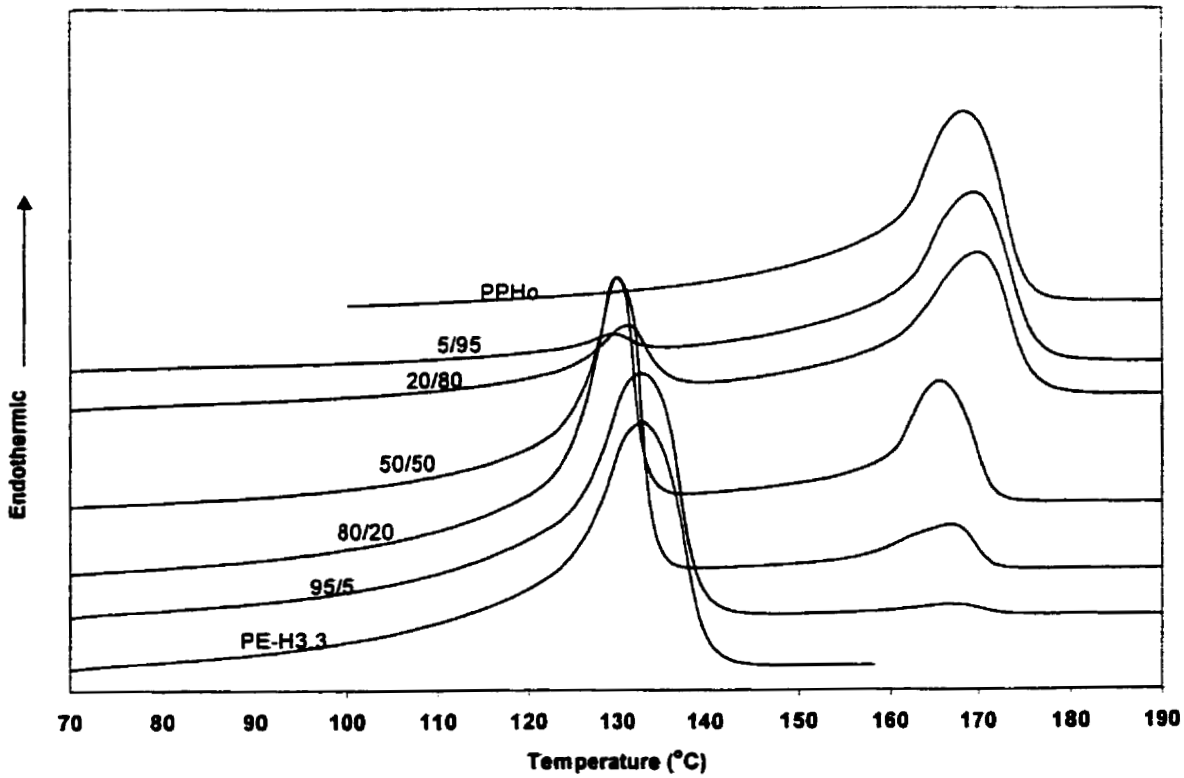

Fig 5.7: Thermogram scans for PE-H3.3/PPHo blends prepared at 190°C

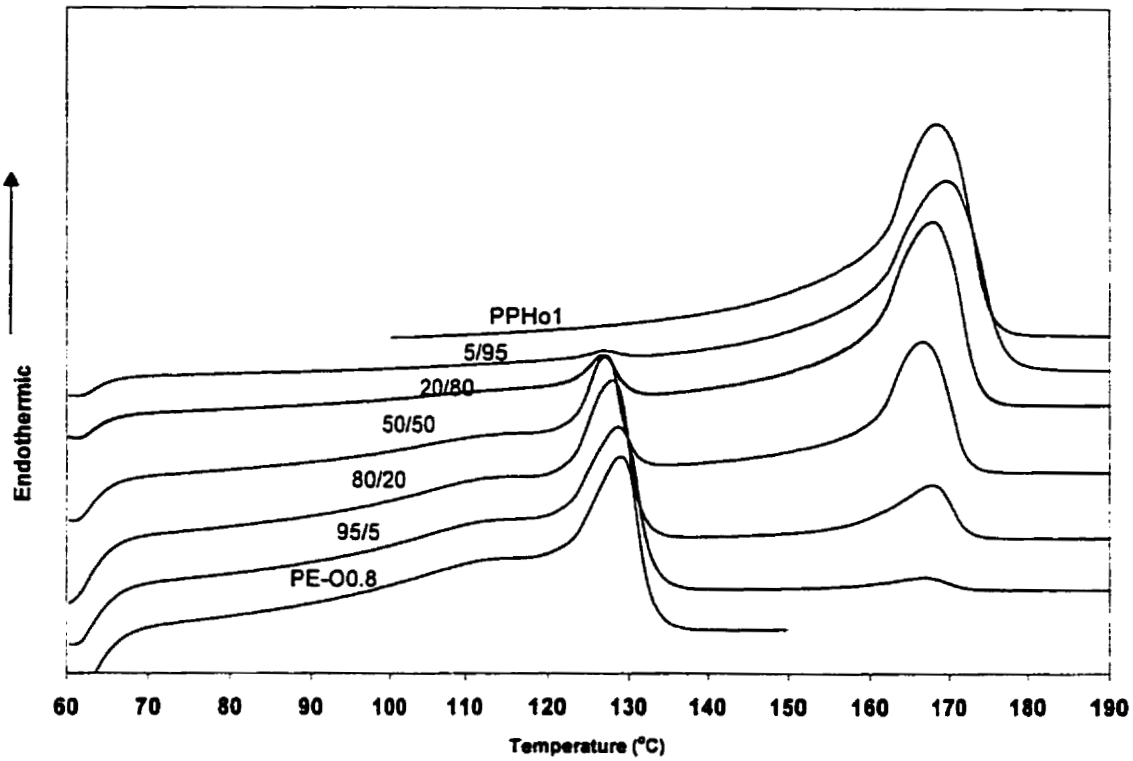

Fig 5.8 : Thermogram scans for PE-O0.8/PPHo blends prepared at 190°C

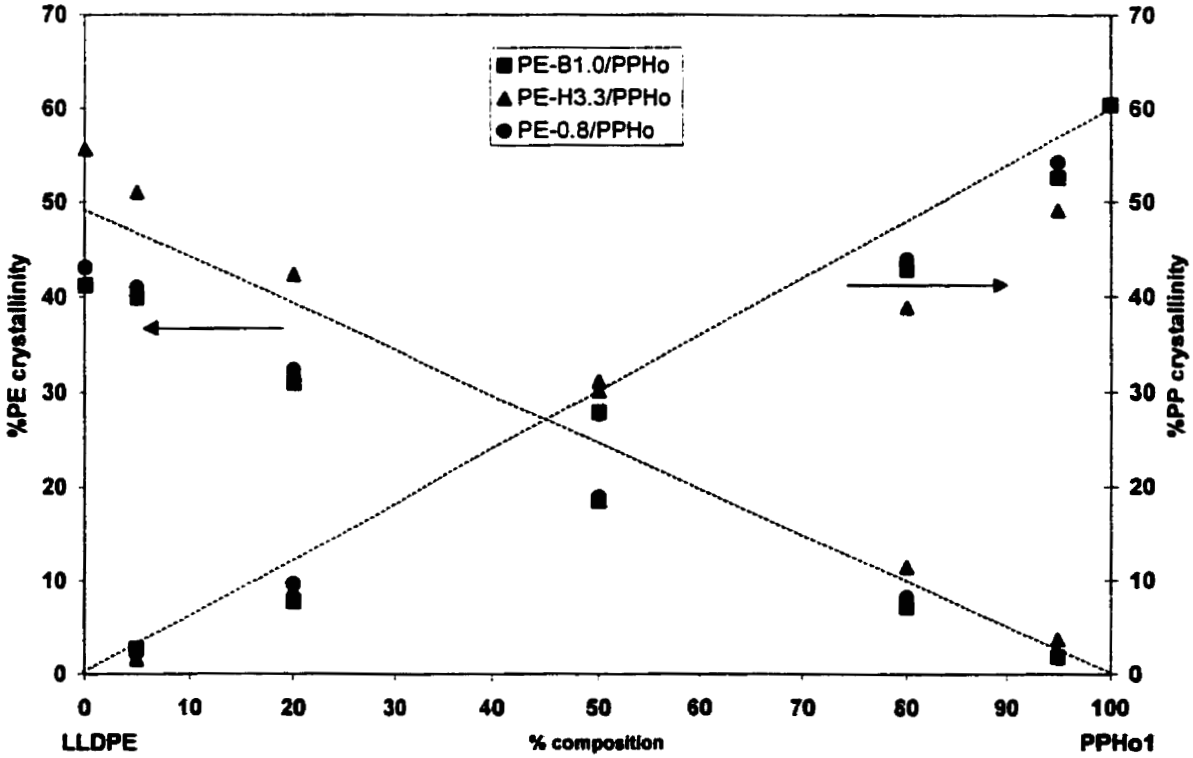

Fig 5.9 : Percentage of crystallinity as a function of blend composition

belonging to each component graphically (Inoue, 1963). The degree of crystallinity variation with the blend composition indicates that the crystallinity of one component decreases slightly with increase of the amount of another component as shown in Fig. 5.9. This was also observed by Inoue (1963), in case of Nylon 6 and Nylon 11 blends, which are both semicrystalline in nature.

5.2.3 Blend Morphology

- ***Morphological features***

In Figs. 5.10 to 5.12, the SEM photographs show the fractured surfaces of all LLDPE/PPHo blends studied at various compositions. One can clearly see that the components are microscopically separated in the blends, indicating immiscibility. And further depending on the volume ratio between the two components of the blend, one of the components is either dispersed in the other component or constitutes the matrix. In the micrographs, the dispersed phase can generally be distinguished as the brighter phase and the matrix as the darker one.

It is observed that in general the dispersoids were spherical, except in that of 50/50 LLDPE/PPHo blends which are more fibrous in nature. The dispersoids were of LLDPE in the blends with 95% and 80% of PPHo and that of PPHo in the blends with 20% and 5% of PPHo. This is in line with the experimental observations of many other researchers. The appearance of these droplets in the surface also depends on the path of the sample fracture. The particle distribution of the dispersoids, was not uniform over the fracture surface but appeared in clusters. This has also been reported by Rao (1999) and Plochocki *et al.* (1989) where they observed that clusters form along the flow streamlines.

It is observed that when LLDPE forms the matrix the texture of the morphology is quite lacy. This kind of morphology was referred by D'Orazio *et al.* (1982) as "beehive morphology" in which the dispersed phase particle is enclosed in the cell. The round PPHo particles which were either de-bonded or fractured and the lacy structure obtained

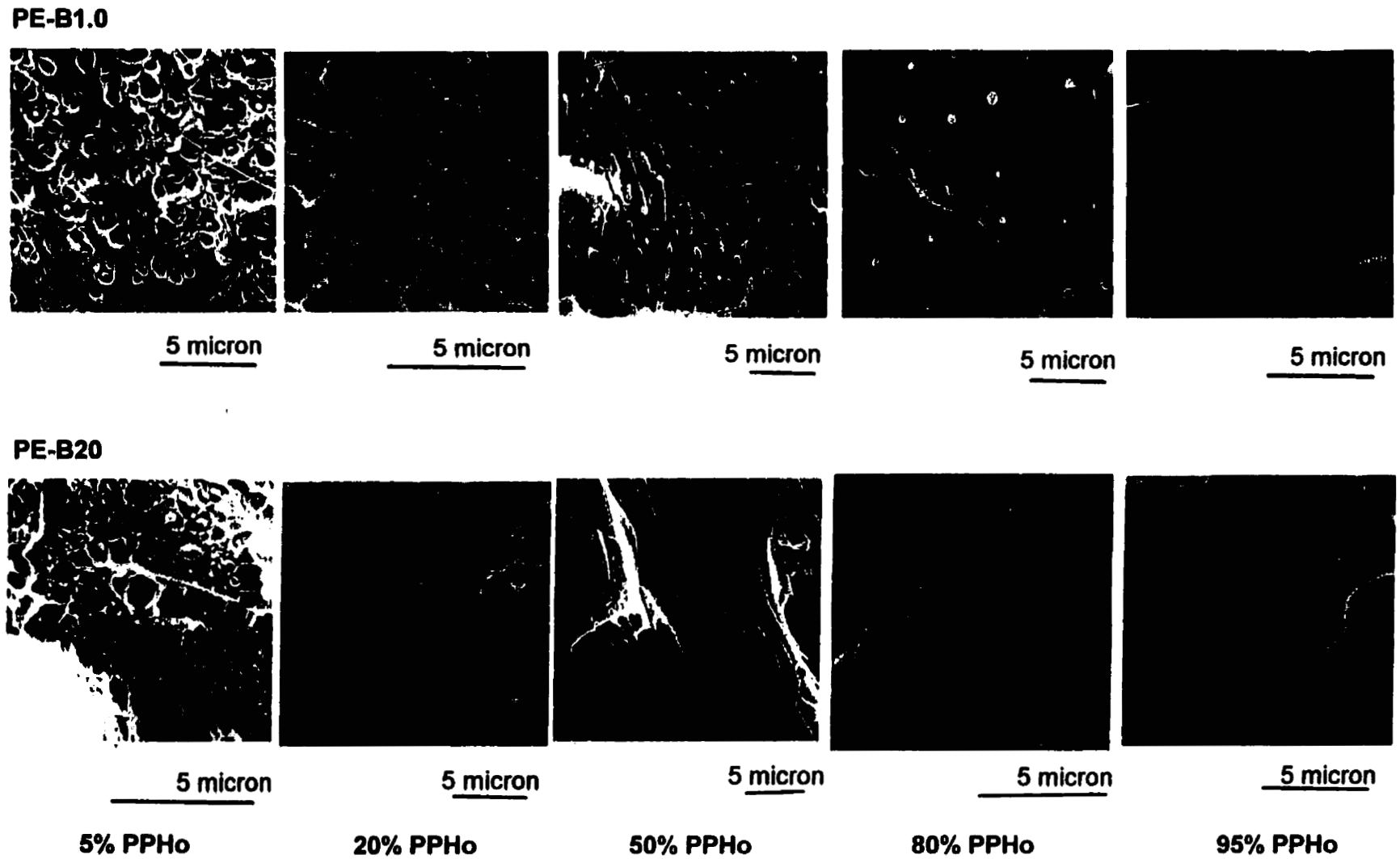

Fig 5.10: SEM photographs of fractured surfaces of PE-B1.0/PPHo and PE-B20/PPHo blends

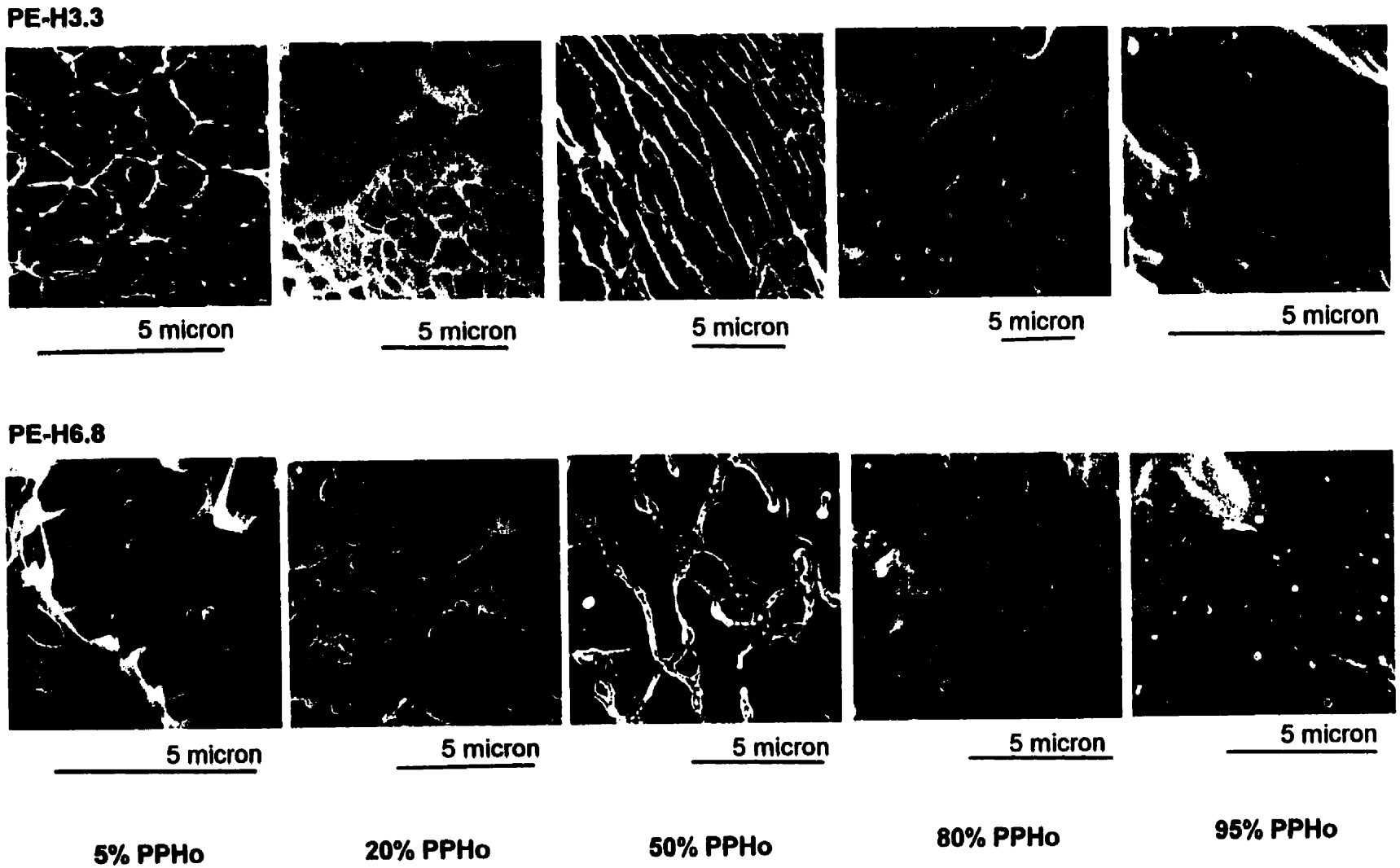

Fig 5.11 : SEM photographs of fractured surfaces of PE-H3.3/PPHo and PE-H6.8/PPHo blends

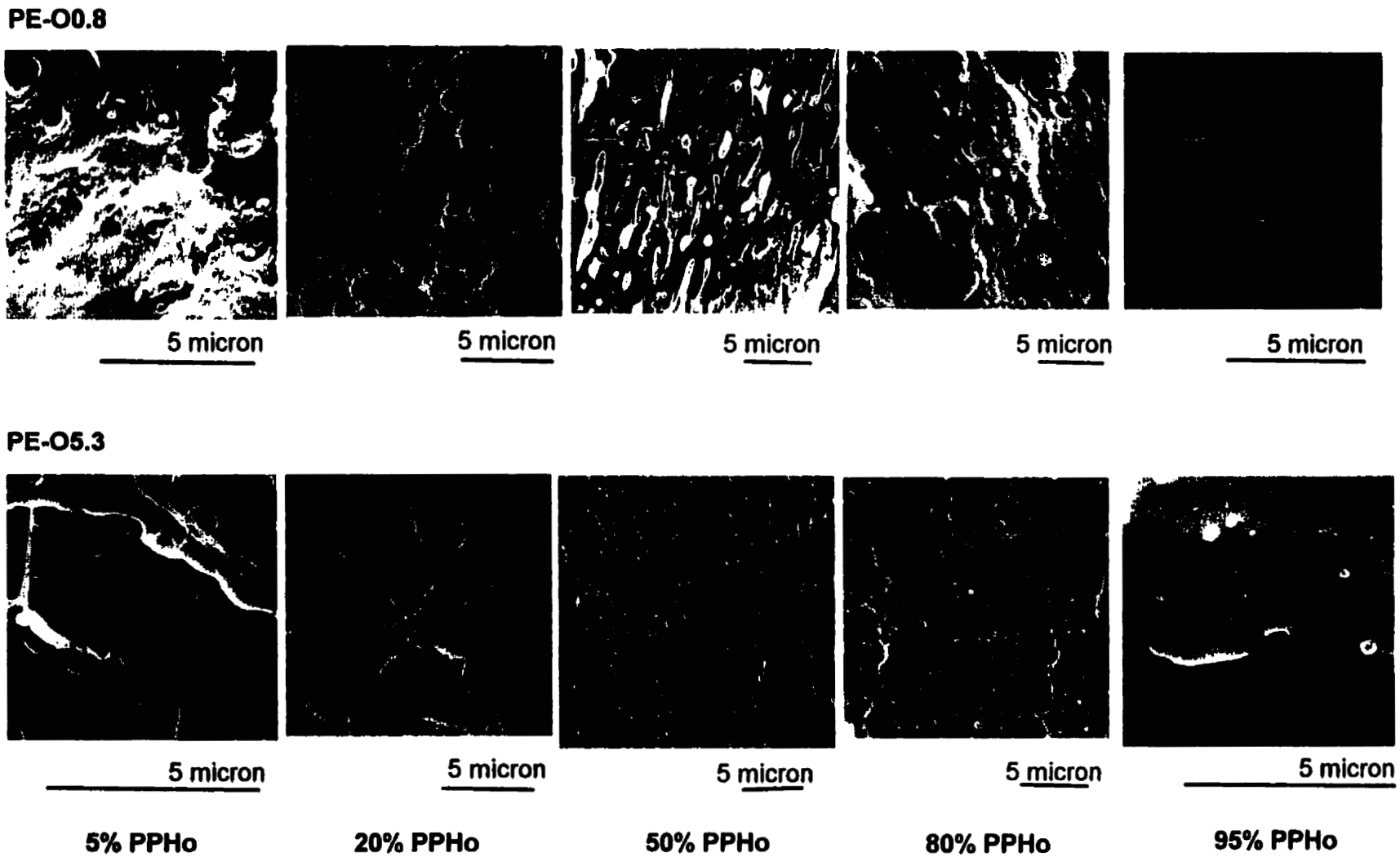

Fig 5.12 : SEM photographs of fractured surfaces of PE-O0.8/PPHo and PE-O5.3/PPHo blends

from the drawn LLDPE are probably due to the ductile fracture mechanism, even though the sample was quenched in liquid nitrogen for 30 min. Liu and Truss (1996) also observed these ductile fracture features, even though they too immersed the sample in liquid nitrogen for long periods of time (25 min). However, when the percentage of the PPHo increases to 80 and 95%, it forms a droplet-in-matrix type of morphology. Besides the dispersed phase, voids are also seen which are in the form of dark holes and indicate that the dispersed phase has been removed from the surface. The presence of voids indicates that during fracture the dispersed particles were not ripped apart but instead overcame the interfacial adhesion between the dispersed phase and the matrix and thus the droplets got dislodged from the matrix. The fractures observed in these cases are brittle in nature as the crack cuts through the matrix, removing the dispersed particle completely.

The 50/50 PE/PPHo morphology was very fibrous and the thickness of the fibrils depended on the type of LLDPE. It is observed that the LLDPE resins with high viscosity (i.e. PE-B1.0 and PE-O0.8), show a thicker fibril type morphology as compared with the rest of LLDPEs (Figs. 5.10 to 5.12). D'Orazio *et al.* (1982) also observed fibrils for HDPE and PPHo blends which seemed to connect the different domains indicating that part of the material, presumably HDPE, was plastically deformed. Further Liu and Truss (1996) observed similar morphology and referred to it as lamella like morphology. Figs. 5.10 to 5.12 show that the PE lamellas were drawn during fracturing while the PPHo lamellas were interconnected as a matrix holding the lamella of PE.

Several unusual morphological features were observed in the various samples of the droplet-in-matrix type of morphology. One of them is the formation of strands which connected one topography to another or connected one dispersed drop to another (Fig. 5.13). Rao (1999) attributed their formation either during the mixing procedure or during the fracturing procedure and proposed two explanations. He suggested that these could be formed when two droplets collided during mixing and the droplets are pulled apart

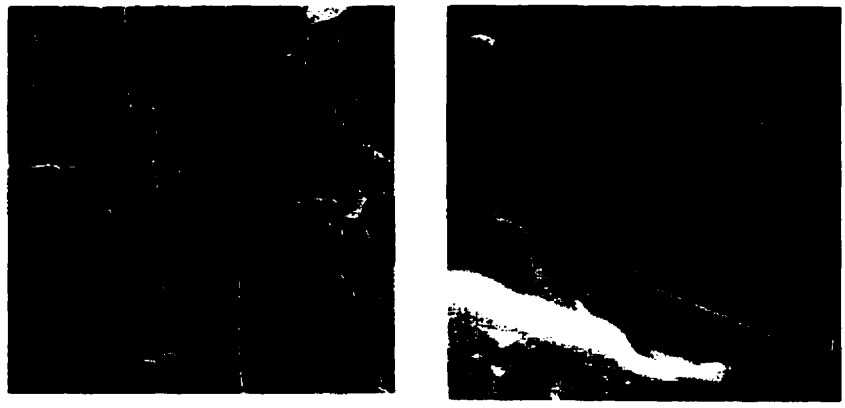

10 micron 5 micron

A: PPHo/PE-O0.8 -80/20 B: PPHo/PE-H3.3 -95/5

Fig 5.13: SEM photographs of fiber formation in LLDPE/PPHo blends

5 micron 5 micron 5 micron

C:PE-O5.3/PPHo1 -80/20 D: PE-B20/PPHo -80/20 E: PE-H6.8/PPHo -95/5

Fig 5.14: SEM photographs of LLDPE/PPHo blends : peculiar spots

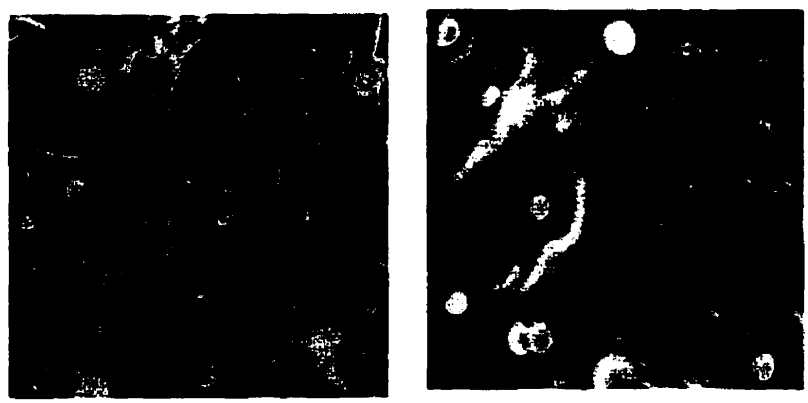

5 micron 5 micron

F: PPHo/PE-H6.8 -80/20 H: PPHo/PE-B1.0 -80/20

Fig 5.15: SEM photographs of LLDPE/PPHo blends : shrinking minor phases and web like structures

without sufficient time for coalescence. These then get stretched and form an interconnecting thread. He further explained with reference to Elmendrop's (1986) work that the time scale for the strand to relax and form droplets was retarded, for threads of higher elasticity. Thus, it is possible to capture these interconnections due to the rapid quenching after the mixing of the blend. The other explanation was based on cases where the interfacial adhesion of the dispersed phase with the matrix is strong. This would cause the droplet to stretch into fiber when a crack is propagated through it and would retract back on the surface and fuse with the first point of contact when the crack is fully developed. In our case, we observe these interconnecting strands in all cases where PPHo is the matrix and LLDPE is the dispersed phase. The only exception to this was the blend with PE-O5.3. It is further observed that the length of the strands in blend of PE-O0.8, were much larger than that of the strands found in the rest of the resins. The differences in the type of strands are probably due to the different mechanisms involved in their formation. Since PE-O0.8 is quite elastic, it may have formed during the mixing procedure. However, the fibers in the rest of the resins are probably a result of their strong interfacial adhesion of the system and are formed during the fracturing of the sample.

In a few cases, some small spots on the dispersed phase were observed (Fig. 5.14). These were seen only in the beehive morphology and not in the drop in matrix morphology. It is likely that these were formed during the ductile fracture mechanism. They might have formed when the dispersoids in the blends where sectioned by the crack during the fracture. The crack would have extended the surface of the drop, snapping it and then its retraction may have formed the spot. Rao (1999) however observed similar features for the drop-in-matrix morphology and attributed them to the breaking of the fibrils that were formed from the drops.

In few cases it was found that the dispersed phase had somewhat shrunk and certain microfibrils connecting the dispersed phase to the interface were present. These

can be clearly seen for blends shown in Fig. 5.15. The dispersoids were generally attached from one side to the matrix and was detached from the other side. In some cases, in the drop-in matrix morphology, there are a few interconnecting strands between the dispersed phase and the matrix. McEvoy and Krause (1997) also observed these features, which were referred as web-like structure, as the strands were quite significant in number. They reported higher impact properties for these systems. Westphal *et al.* (1997) reported higher impact properties in PPHo blends with ultra low density polyethylene (ULDPE) as the dispersed phase and HDPE as the modifier. They attributed the increase in impact strength due to the presence of microfibrils, which increases the coupling across the domain interface and hence toughens the blend. They further concluded that the minor phase of higher crystallinity would exhibit more shrinkage and formation of more webs. Further, for cases where interfacial adhesion is strong, the dispersed phase would stretch to form fibril and attach itself to the matrix to bridge the gap. We observed the formation of the web-like structure only in blends of Butene and Hexene comonomer resins, while the shrinking minor phases without the strands is observed in all blends. These features are probably due to the strong interfacial adhesion between the dispersed phase and the matrix. This further supports our previous inference that the fibers are formed in blends of Butene and Hexene comonomer resins due to their strong interfacial adhesion to PPHo.

The dispersed drop diameters were obtained for all the systems using the image analyzing software " Image Pro". The SEM photographs obtained were scanned and then the analysis was performed. The dispersed particles and the voids contours were traced manually. Manual tracing is the most widely used method for counting and a maximum of 10% error has been estimated by some authors (Sundararaj and Macosko, 1995; Rao, 1999). The numbers of particle analyzed lay between 75-250. The software used calculated the area, the aspect ratio and the length of the major axis. The number average diameter and the volume average diameter were calculated and have been summarized in Table 5.3. To ensure reproducibility of the results, dispersed drop diameters were

Table 5.3: Particle size diameter determined from image analysis of SEM photographs of LLDPE/PPHo blends

PE Resin	% PPHo	No. Avg. Dia. - Dn, (μm)	Std Dev.	Vol. Avg. Dia. - Dv, (μm)	No of Particles	Viscosity Ratio, p
PE-B1.0	5% PPHo	0.330	0.055	0.356	101	0.184
	20% PPHo	0.522	0.105	0.586	102	0.184
	80% PPHo	0.659	0.178	0.800	189	5.41
	95% PPHo	0.321	0.098	0.422	245	5.41
PE-B20	5% PPHo	0.352	0.08	0.419	75	1.53
	20% PPHo	0.620	0.193	0.780	117	1.53
	80% PPHo	0.389	0.103	0.470	80	0.65
	95% PPHo	0.312	0.070	0.361	195	0.65
PE-H3.3	5% PPHo	0.358	0.102	0.438	76	0.43
	20% PPHo	0.680	0.109	0.733	80	0.43
	80% PPHo	0.601	0.114	0.668	151	2.2
	95% PPHo	0.305	0.061	0.341	117	2.2
PE-H6.8	5% PPHo	0.336	0.064	0.373	121	0.75
	20% PPHo	0.494	0.151	0.634	88	0.75
	80% PPHo	0.468	0.130	0.587	179	1.33
	95% PPHo	0.306	0.060	0.349	201	1.33
PE- O0.8	5% PPHo	0.392	0.072	0.437	129	0.21
	20% PPHo	0.784	0.129	0.846	122	0.21
	80% PPHo	0.902	0.219	1.172	208	4.79
	95% PPHo	0.474	0.173	0.684	109	4.79
PE-O5.3	5% PPHo	0.384	0.100	0.463	155	0.58
	20% PPHo	0.651	0.224	0.880	120	0.58
	80% PPHo	0.576	0.112	0.642	247	1.71
	95% PPHo	0.328	0.081	0.386	105	1.71

measured for several samples of the same blend system, obtained from two different batches. A maximum deviation of 7% for the average drop diameter was observed which is within the range of errors attributed to the manual tracing method for counting the particles. It is clearly evident that as the dispersed phase concentration increases, the particle diameter increases. This has been attributed to the enhanced collision-coalescence phenomenon that occurs in more concentrated blends (Luciani and Jarrin, 1996). As the dispersed phase concentration increases, the particle size increases until the largest particles are no longer stable as droplets in the imposed shear field and a fibril and drop type morphology coexist. The increase in the concentration also results in the increase in the particle size distribution, which is evident from the increase in the standard deviation of the number average diameter (Table 5.3). This again has been observed by Sundararaj and Macosko (1995) and has been attributed to the simultaneous breakup and coalescence, resulting in much broader distribution of particle sizes. The small particles are basically a result of breakup in the shear regions and the big particles, on the other hand, are the result of coalescence.

The effect of higher concentrations, which may also result in the formation of continuous morphology, was also studied. In our case, no co-continuous phase was observed for all the compositions of the blend studied. Predictions were made for the point of phase inversion using equations 2.1 and 2.2. The results are presented in Table 5.4. It is clear that the predictions made by both the equations are quite different. For our case equation 2.1 seems to give a better prediction keeping in mind that this model has a limitation of predicting within ± 5 wt% error. However, to confirm the results and to validate the model, blends should be prepared at the predicted compositions to observe the co-continuous morphology.

A plot of drop size as a function of viscosity ratio presented in Figs. 5.16 and 5.17 shows that the number average particle size forms a U shaped trend line. Besides this, it is evident that the type of comonomer has a significant influence on the particle size. The

Table 5.4 : Prediction of point of phase inversion for the type of morphology

Resin	Torque (mgf)	Viscosity (Pa.s)	Blend PPHo: matrix	Torque Ratio	Composition[a] (vol. fraction)	Viscosity Ratio	Composition[b] (vol. fraction)
PE-B1.0	4012	2930	PPHo/PE-B1.0	1.56	61/39	5.41	84/16
PE-B20	2322	352	PPHo/PE-B20	0.904	48/52	0.65	39/61
PE-H3.3	3840	1235	PPHo/PE-H3.3	1.49	60/40	2.28	69/31
PE-H6.8	4454	720	PPHo/PE-H6.8	1.73	42/58	1.33	57/43
PE-O0.8	4214	2594	PPHo/PE-O0.8	1.64	62/38	4.79	83/17
PE-O5.3	3253	926	PPHo/PE-O5.3	1.27	56/44	1.71	63/27
PPHo	2570	541					

a) using Averopoulos equation 2.1

b) using Jordhamo's equation 2.2

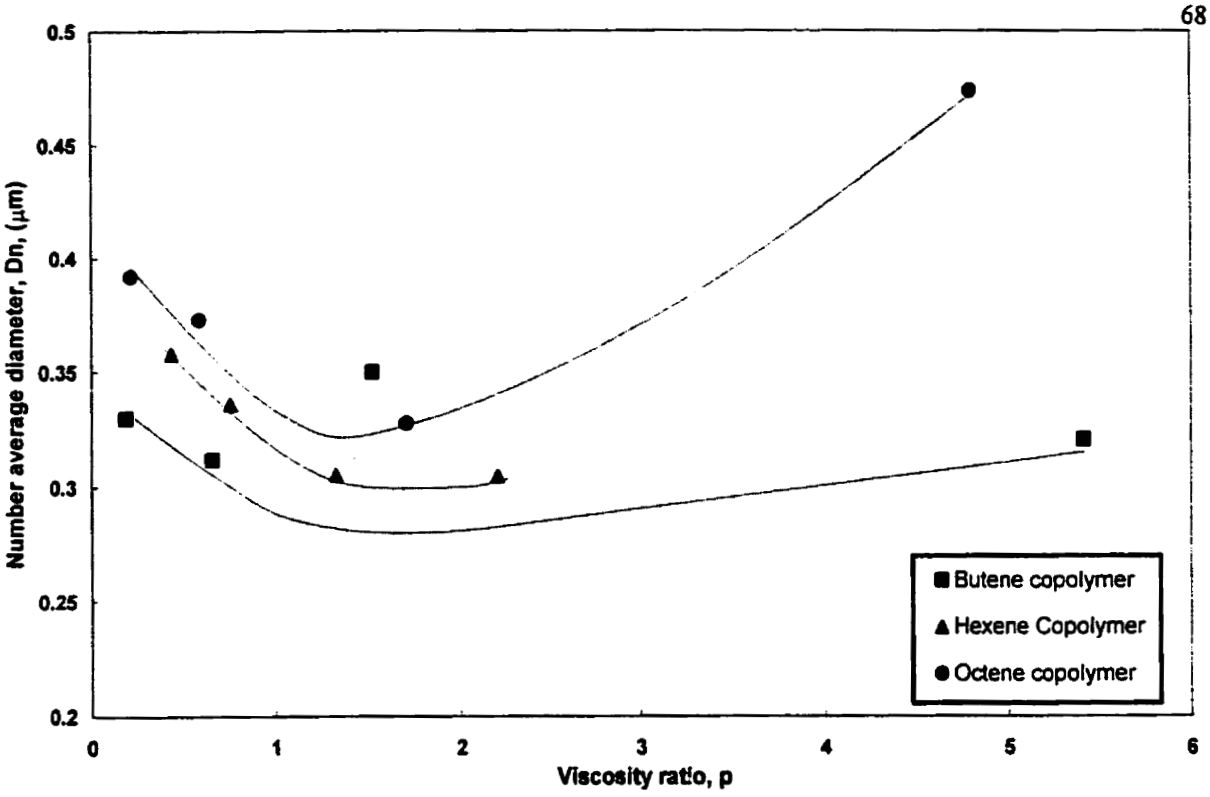

Fig 5.16 : Number average diameter against viscosity ratio for LLDPE/PPHo (5%) blends

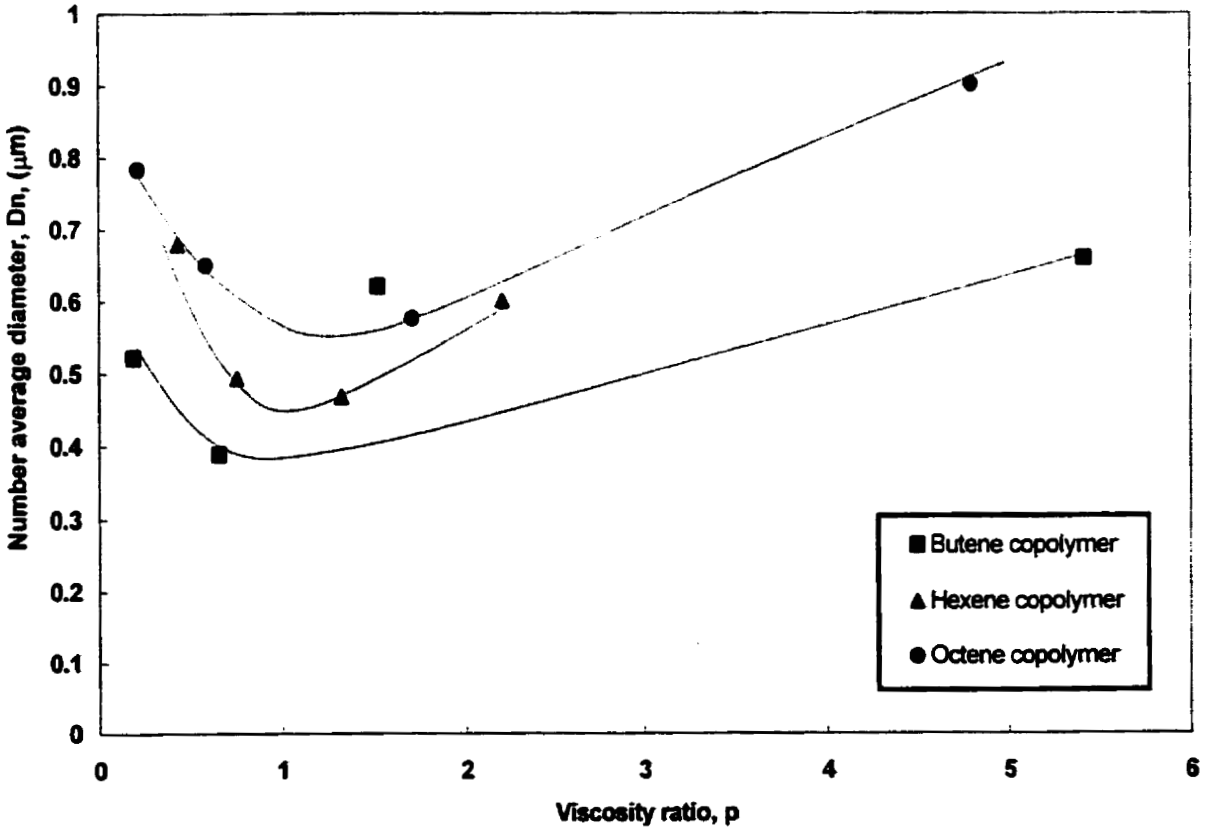

Fig 5.17 : Number average diameter against viscosity ratio for LLDPE/PPHo (20%) blends

average particles size varies in the following order Butene<Hexene<Octene, which is prevalent for both 5% and 20% composition blends. The only exception observed from this trend was for PE-B20/PPHo blends of 5% and 20% (PE-B20) composition where large drop size diameters were obtained as compared to the other blends at around the same viscosity ratio. This deviation may be due to the fact that PE-B20 is the only resin of all the resins studied which has a lower viscosity in comparison to the PPHo. Thus, it may be possible that, due to its low viscosity, the 5 minute time of blending may be large enough to cause degradation. The degradation, however, was not evident either from the torque profile nor was there any indication of the brown film. Fig. 5.18 indicates that the polydispersity in the size of the minor phase increases with the increasing viscosity ratio. Favis and Chalifoux (1987) observed similar increase with a system of PC/PP.

- ***Crystalline morphology***

Figs. 5.19 A and B show the crystalline morphology of the virgin LLDPE and virgin PPHo resins, respectively. The size of the spherulites of PPHo are much larger as compared to those of LLDPE as shown in Figs. 5.19 A and B, where LLDPE and PPHo resins have been slow cooled (air quenched) from 190°C to ambient temperatures. It is further seen that PPHo had two types of spherulites, the smaller ones were identified as the α-spherulites that are the most common form of spherulites and the larger and brighter ones were identified as the β-spherulites. In order to confirm the presence of the β-spherulites, the sample was heated in a hot stage microscope at a rate of 10°C/min and it was observed that the larger spherulites started to melt at 145°C while the rest of the spherulites started melting at approximately 160°C. The above observation clearly confirms that the large distinct spherulites were β-spherulites. Teh (1983) had also observed the β-spherulites, but only in the case of blends (PP/LDPE) and not in the virgin PP. He attributed the formation of the β-spherulites due to the presence of LDPE. However, in our study, the β-spherulites were observed for not only the blends but also for the virgin PPHo. Therefore, it may be inferred that it is not due to the presence of

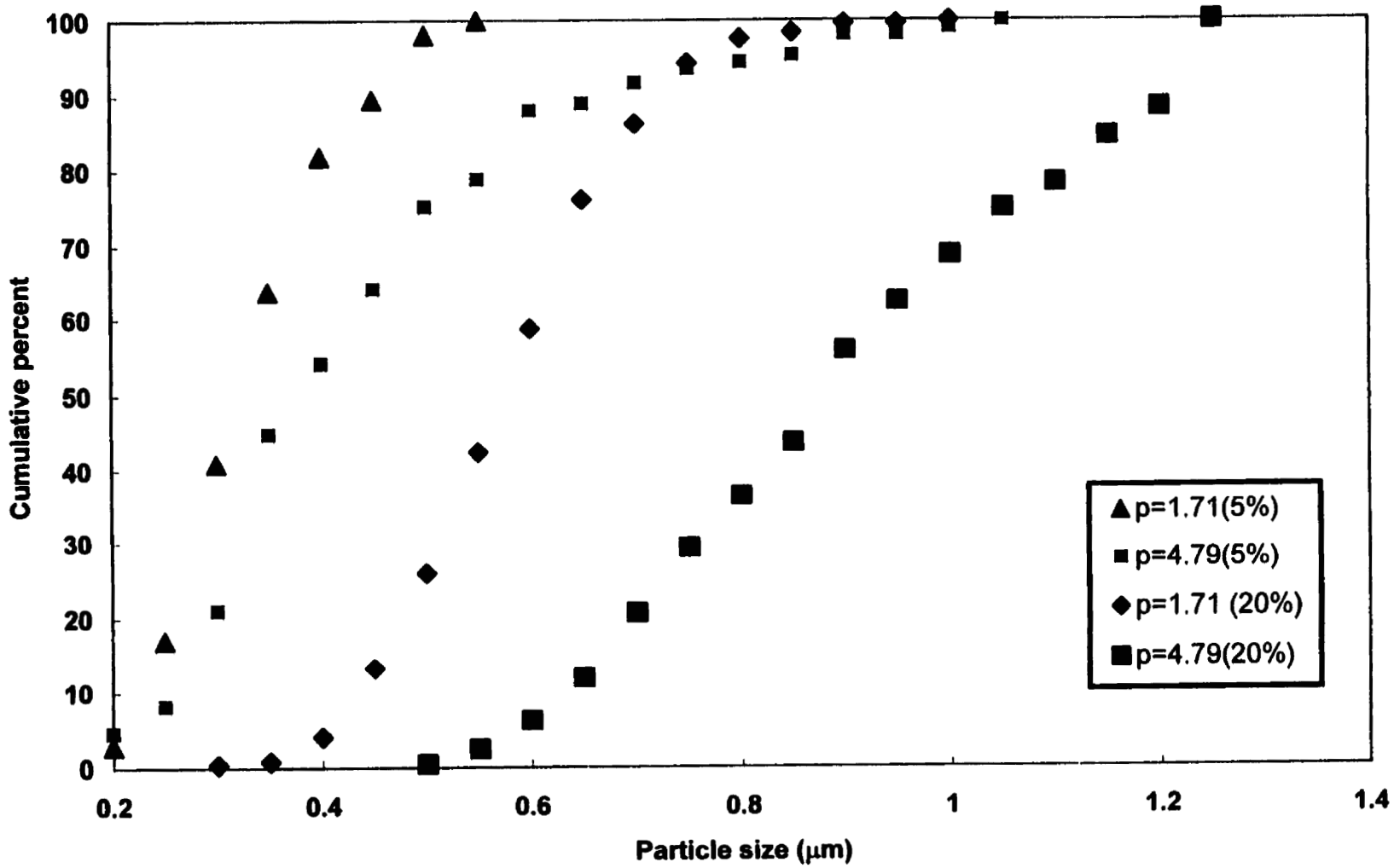

Fig 5.18: Cumulative percent vs. particle size for LLDPE/PPHo blends at different viscosity ratios

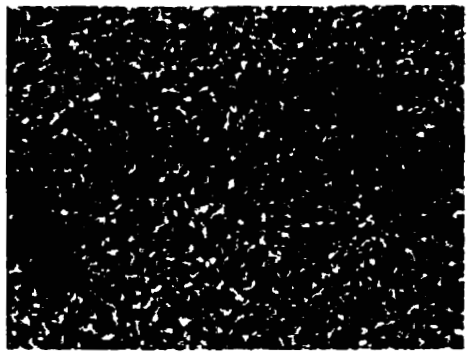

A: PE-0.8 slow cooled, 500x

B: PPHo slow cooled, 500x

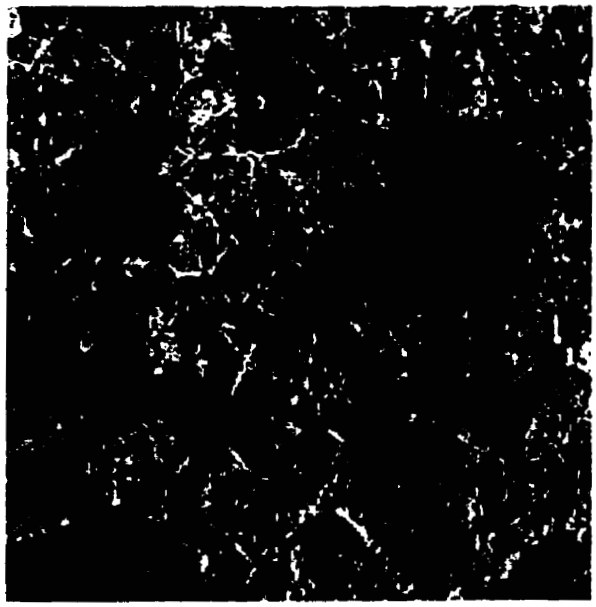

C: PPHo -10 DegC/min, 200x

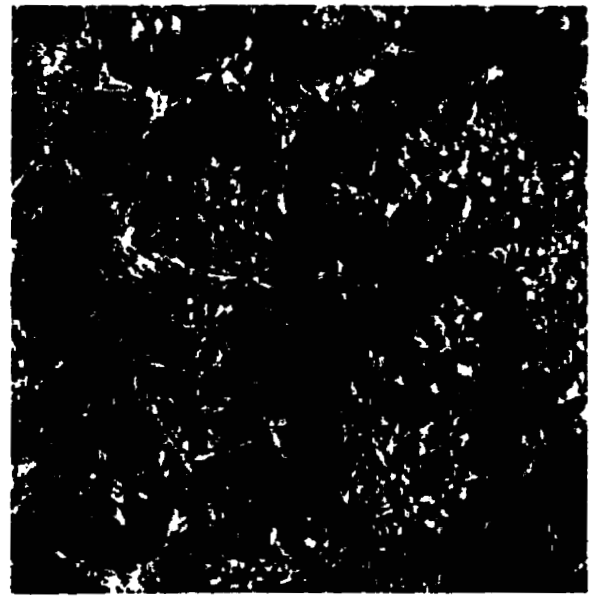

D: PPHo -1 DegC/min, 200x

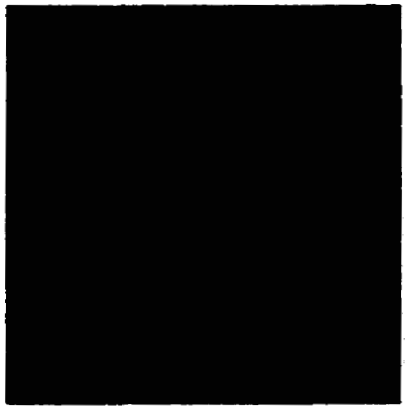

E: PPHo/PE-B1.0 -80/20

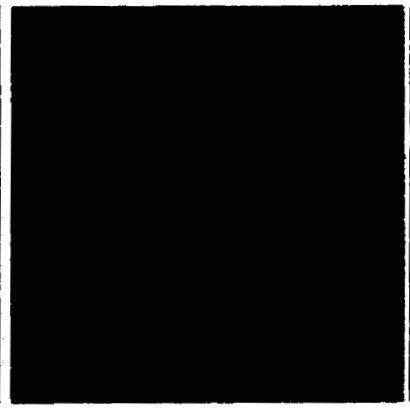

F: PPHo/PE-O0.8 -80/20

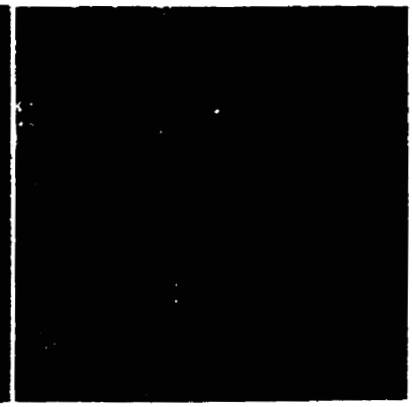

G: PPHo/PE-H3.3 -80/20

fast cooled, 500x

Fig 5.19: Crystalline morphology of PPHo, LLDPE and their blends obtained at different cooling rates

LLDPE resin which results in the formation β-spherulites. It still needs to be investigated what reasons contribute to the formation of these β-spherulites. Further it can be seen in Figs. 5.20 and 5.19 that the β-spherulites were observed only for the samples that were slow cooled (air quenched) and not for the fast cooled (ice quenched) (Figs. 5.19 E, F, G) samples. This indicates that the rate of crystallization also affects the formation of the β-spherulites. This is supported by Teh *et al.* (1994) review, in which he pointed out that the size and the amount of β-spherulites were independent of composition and only varied with rate of crystallization.

The relative effect of cooling rate on the size of the spherulites of PPHo and its blends were examined. Samples of PPHo were cooled at 1°C/min and 10°C/min (Figs. 5.19 C and D). The spherulites of PPHo for the slower cooled samples (1°C/min) measure around 63 μm whereas for the faster cooled samples (10°C/min) they measure around 32 μm. The growth dynamics of these spherulites was further studied and are presented at various temperatures in Figs. 5.21 and 5.22. It is clearly seen that for samples cooled at a rate of –10 °C/min the non-isothermal crystallization does not begin until the sample reaches a temperature around 135°C. At a cooling rate of –1 °C/min, it begins at around 145°C. Further, the nucleation also seems to be rate dependent and increases with an increase in the cooling rate. The nucleation density for the slow cooled samples was determined to be around 60-70% lower in comparison to the fast cooled samples. This is probably because homogeneous or spontaneous nucleation is preferred at lower temperatures and always produces many more nucleation sites per unit per volume (Progelhof and Throne, 1993). This is in line with our observation that a cooling rate of 10°C/min nucleates at a lower temperature and produces more nucleation sites. Further if the cooling rate is fast enough, the mobility of chains traveling to the growing sites decreases rapidly reducing the size of the spherulite, which would explain why we observe smaller sized spherulites at a faster cooling rate (Progelhof and Throne, 1993).

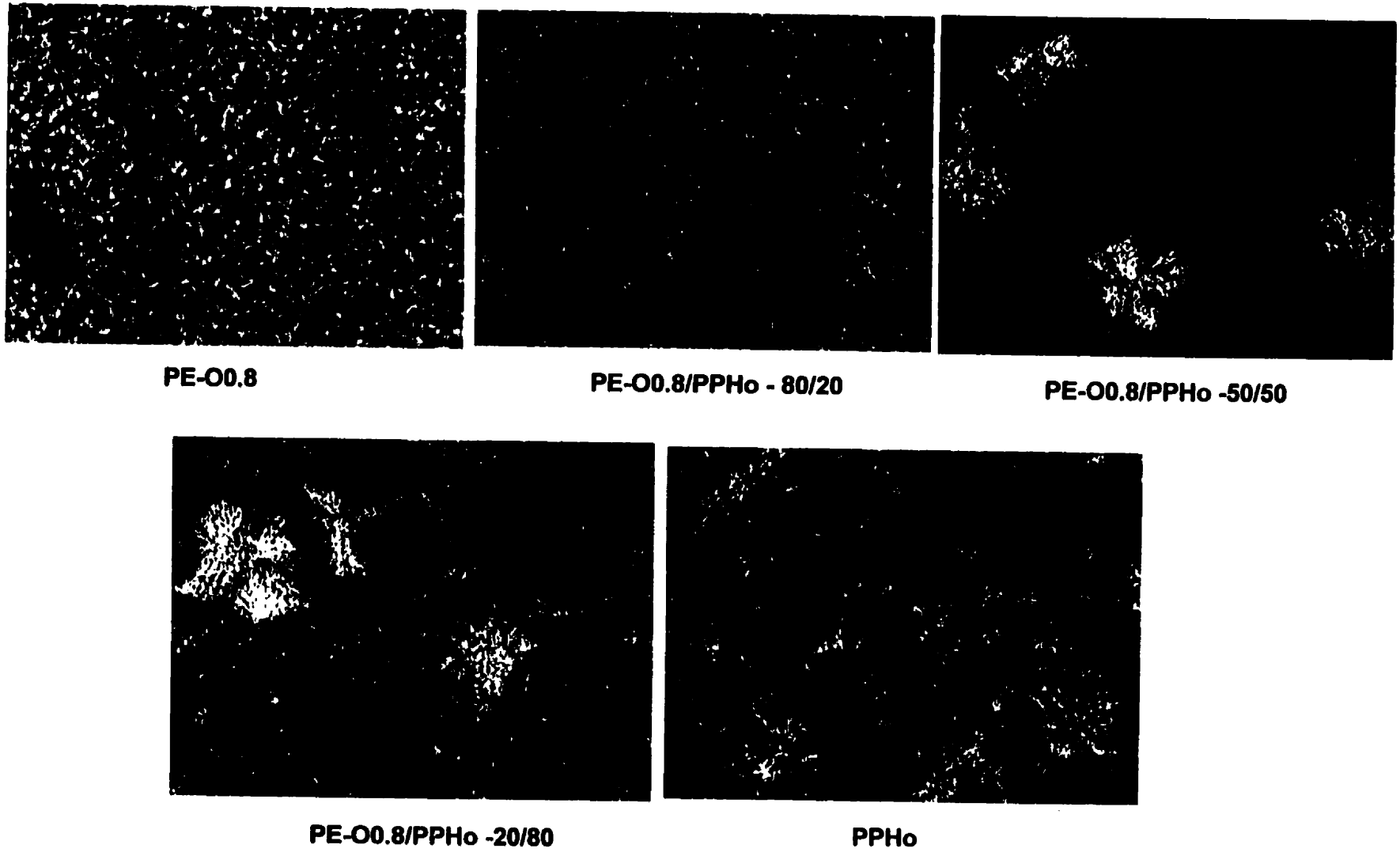

Fig 5.20 : Crystalline morphology of PE-O0.8/PPHo blends obtained when air quenched, at 500X

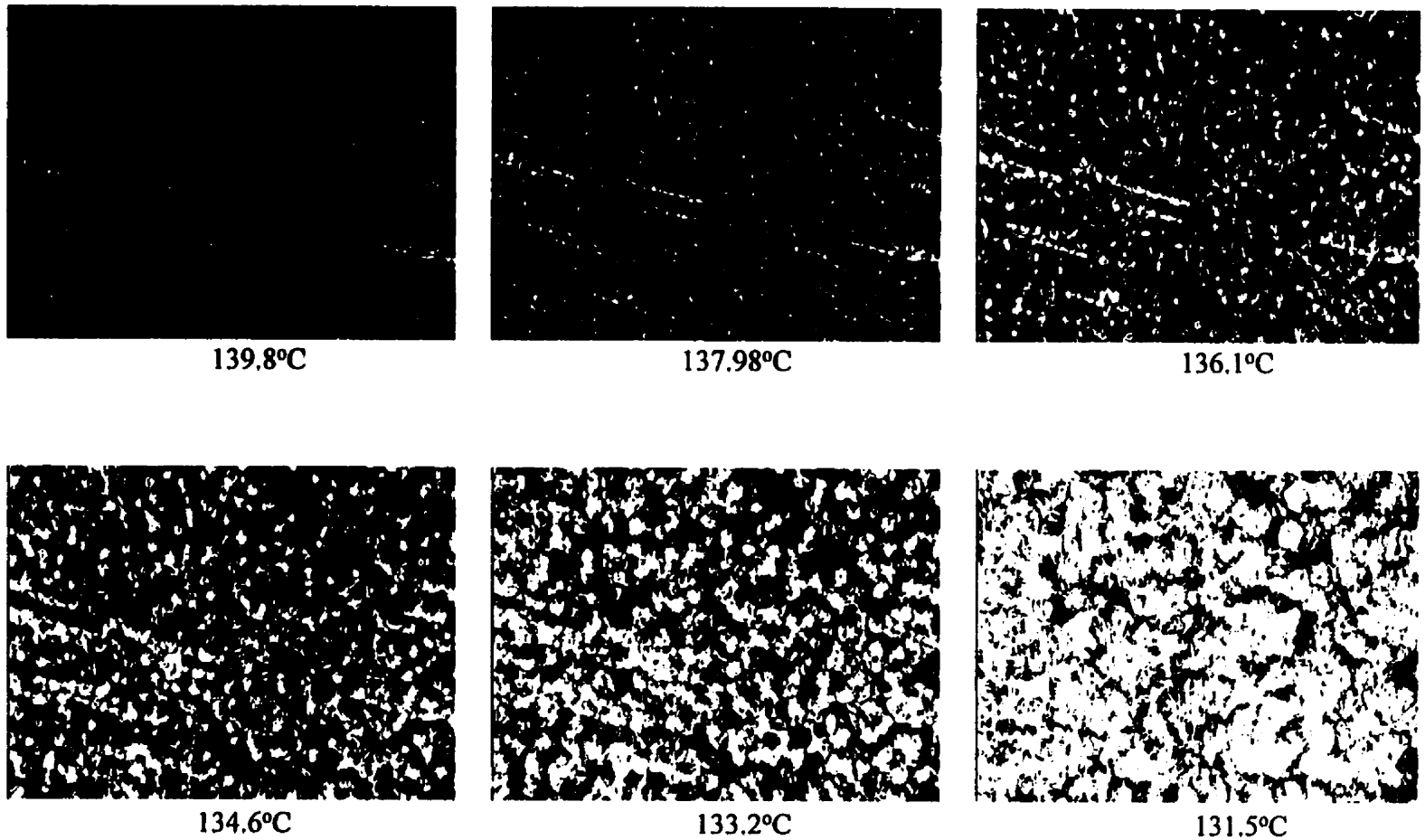

Fig 5.21: Spherulite growth for PPHo at a cooling rate of 1°C/min (200X)

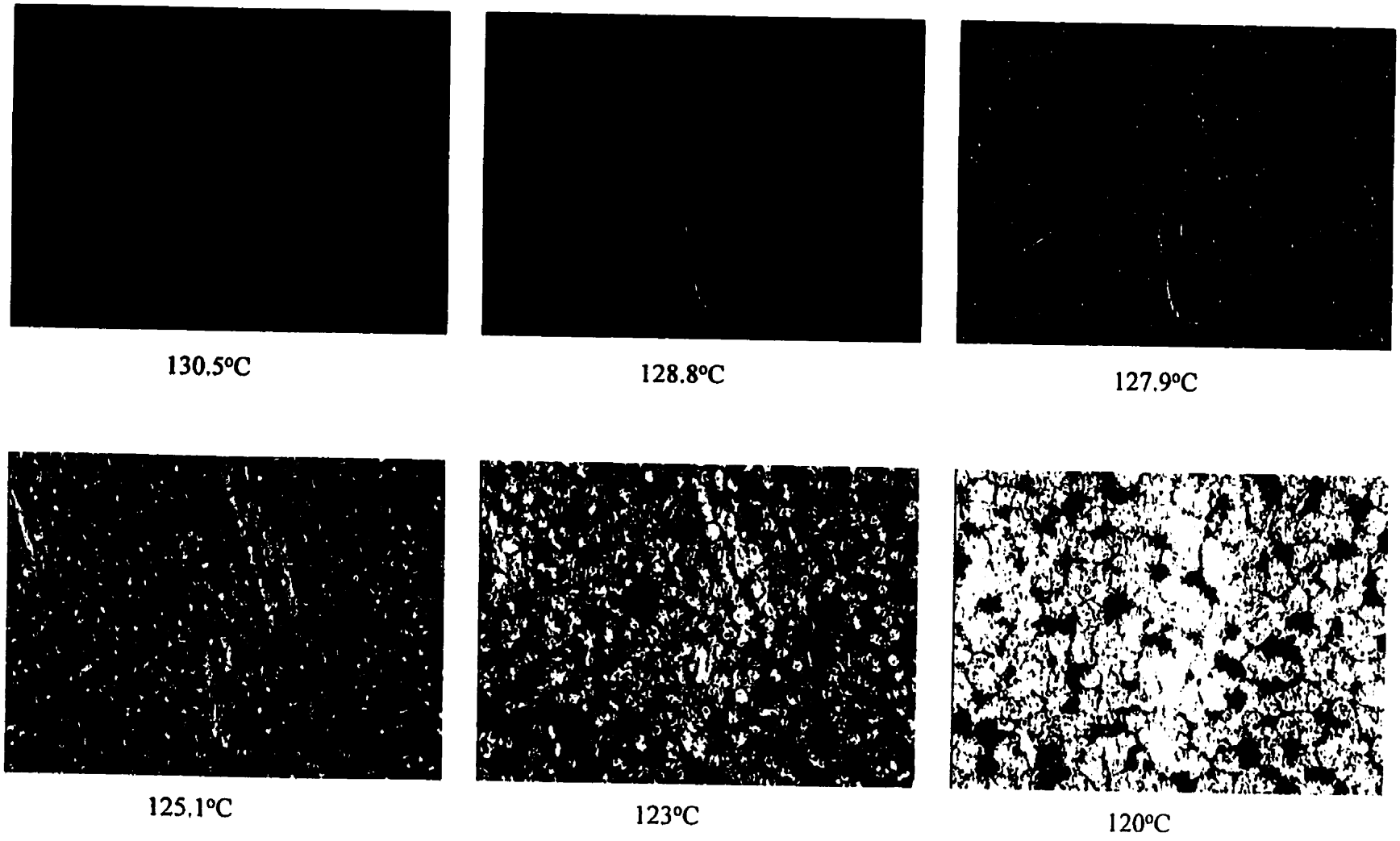

Fig 5.22 : Spherulite growth for PPHo at a cooling rate of 10°C/min (200X)

It has been well documented in the literature that the slow cooling of PE/PP blends results in the formation of larger spherulites, while fast cooling result in the formation of smaller sized spherulites (Teh *et al.*, 1994). Further, it has been observed that blends with smaller sized spherulites results in better mechanical properties (Lovinger and Williams, 1972). Thus, the LLDPE/PPHo blends were only fast cooled to study the effect of the type of comonomer on the size of the spherulites. It was observed that spherulite size of the PPHo on addition of LLDPE reduced significantly which is in line with the literature (Fig. 5.19 E, F, G). However, we could not assess the effect of the comonomer on the size of the spherulite, as the spherulite size became quite small and could not be measured.

5.2.4 Rheological characterization

The storage and loss moduli at 190°C of the PE-H3.3/PPHo blends for all the various compositions (5, 20, 50, 80, 95 % of PPHo) are compared to that of the respective matrix (Fig. 5.23). The storage and the loss modulus for the other blends are presented in Appendix F. It is observed that for relatively low concentration (5 and 20%), the loss modulus of the blends almost coincides with that of the matrix. However, by increasing the amount of dispersed phase the loss moduli decreases or increases depending on the relative viscosity of the dispersed phase to that of the matrix. This is in line with results presented by Lacroix *et al.* (1996). The storage modulus on the other hand is characterized by a shoulder in the low frequency region (terminal zone) compared to that of the matrix and is termed as the secondary plateau. This enhancement in elasticity is attributed to the deformability of the dispersed phase particles (Carreau, 1996). It is further observed from Fig. 5.23, blends characterized with larger viscosity ratios, exhibit secondary plateaus at lower frequencies. This is in line with the study of Graebling *et al.* (1993), where they showed that at high viscosity ratio (p=46), no secondary plateau was observed even for frequency as low as 10^{-2} rad/s. The zero shear viscosity (η_o) and the terminal relaxation time (λ) of the blends were calculated using equations 5.1 and 5.5 and are reported in Table 5.5

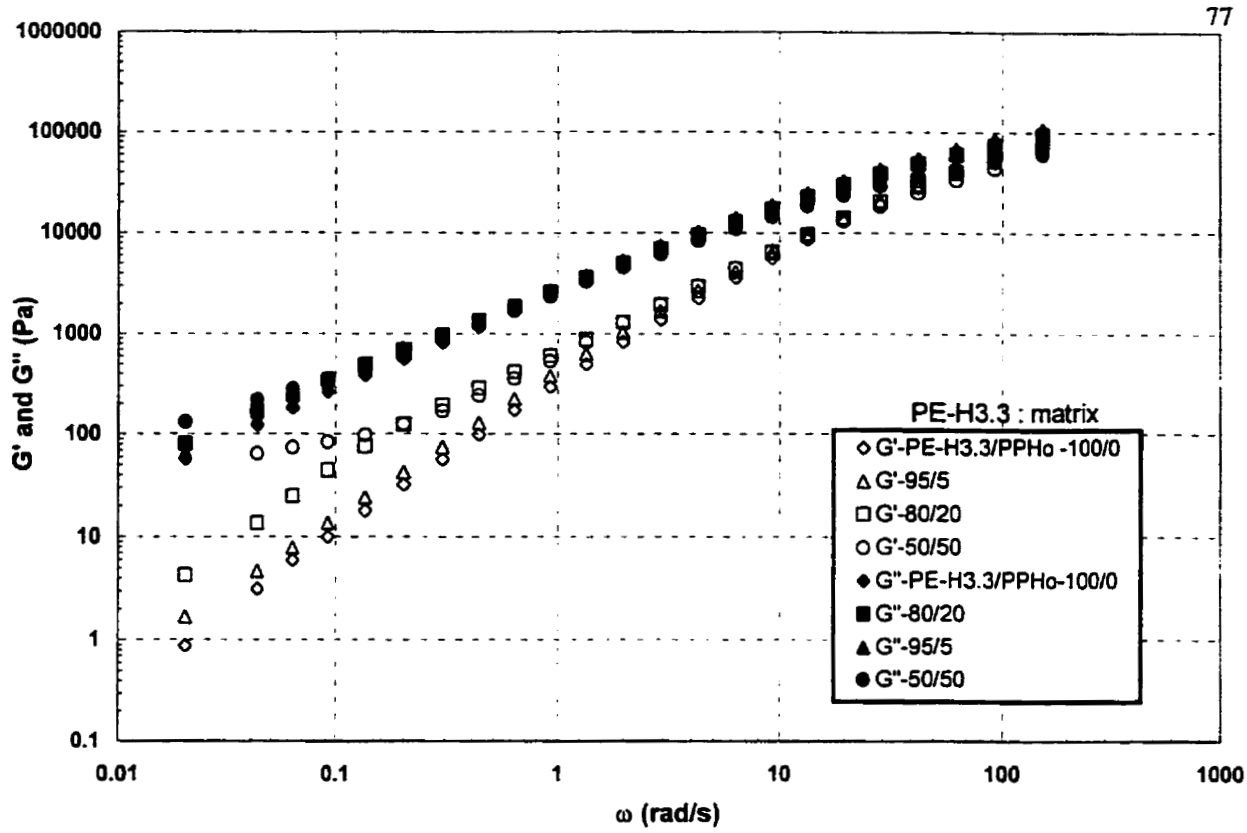

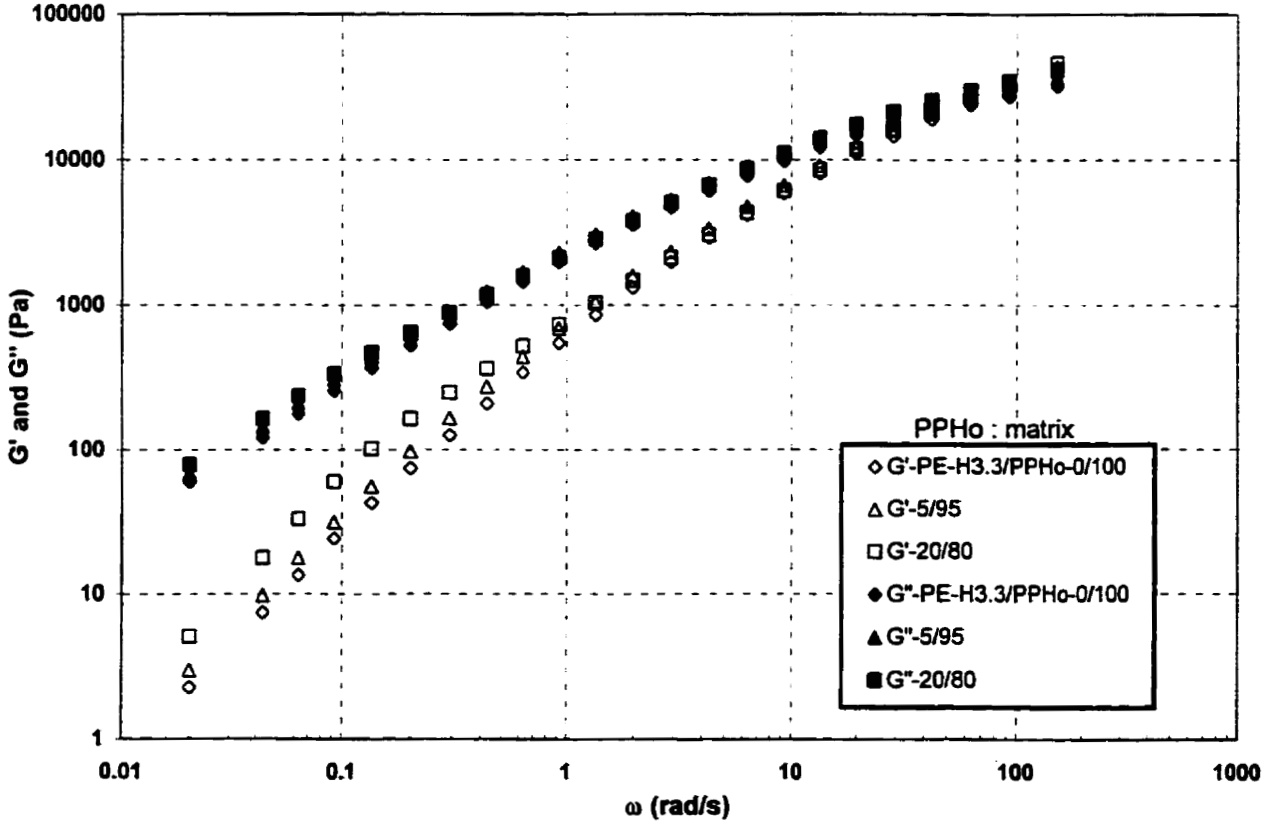

Fig 5.23: Storage and loss moduli for PE-H3.3/PPHo blends at 190°C

Table 5.5 : Rheological parameters of the terminal zone for the components and the blends at 190 °C

Matrix	Dispersed phase	η_0 (Pa.s)	λ (sec)	Matrix	Dispersed phase	η_0 (Pa.s)	λ (sec)
PE-B1.0	0%	17812	0.033	PPHo	0%	4008	0.044
	5% PPHo	18315	0.041		5% PE-B1.0	4294	0.059
	20% PPHo	24005	0.056		20% PE-B1.0	6263	0.072
PE-B20	0%	559	0. 018				
	5% PPHo	480	0.034		5% PE-B20	4609	0.069
	20% PPHo	907	0.0245		20% PE-B20	5233	0.076
PE-H3.3	0%	3770	0.0139				
	5% PPHo	4380	0.0146		5% PE-H3.3	4818	0.068
	20% PPHo	5436	0.0227		20% PE-H3.3	5497	0.050
PE-H6.8	0%	1834	0.0124				
	5% PPHo	1915	0.0136		5% PE-H6.8	4147	0.064
	20% PPHo	2826	0.0194		20% PE-H6.8	5476	0.088
PE-O0.8	0%	21286	0.044				
	5% PPHo	24382	0.048		5% PE-O0.8	5146	0.071
	20% PPHo	28799	0.071		20% PE-O0.8	5394	0.070
PE-O5.3	0%	2905	0.0147				
	5% PPHo	2830	0.0181		5% PE-O5.3	4811	0.066
	20% PPHo	4283	0.0266		20% PE-O5.3	5002	0.073

$$\lambda = \eta_0 \lim_{\omega \to 0} \frac{G'}{G''} \tag{5.5}$$

Results reported in Table 5.5 show that most of the blends have longer relaxation times and higher zero shear viscosities as compared to that of their respective matrix. Similar trends have been reported in the literature and were attributed to the deformability and relaxation of the shape of the inclusions.

Han (1985, 1988) used log G'-log G'' plots to study the relative strength of elasticity to that of viscosity. He found that such plots were independent of temperature and formed straight line for homopolymer and compatible polymer. In this study, however, we have used *tan* δ *(G"/G')* curves to asses the relative strength of the elasticity to that of the viscosity, as the effects were more noticeable in these curves (Fig. 5.24 and Appendix G). It is noted that the blends of PE-B1.0 and PE-O0.8 exhibit the highest elasticity with 20% PPHo whereas the rest of the PE resins exhibited highest elasticity with 80% PPHo. This is expected as blends with matrix of higher elasticity would result in the highest elasticity. However, in some cases (PE-B1.0/PPHo –80/20) the curves at lower frequency, forms a plateau whereas for the others (PE-H6.8/PPHo –80/20) a slight plateau followed by an increase is observed.

Fig. 5.25 gives the curves for complex modulus viscosity versus the compositions at low shear rates ($\omega = 0.1$ rad/s). It is seen that the curves of blends made of components of similar viscosity (i.e. PPHo/PE-O5.3 and PPHO/PE-H3.3) show a positive deviation from linearity with a local minimum at around 50% composition. However, if the viscosity difference between the components is large, the viscosity curves have a somewhat *S*-shape, with the maximum positive deviation towards the low composition ratios. The positive deviation has been observed by many researchers (Xanthos *et al.*, 1997; Levij and Maurer, 1988) and was attributed to the strong interaction between the phases and the maxima was attributed to the presence of co-continuous phase. For our

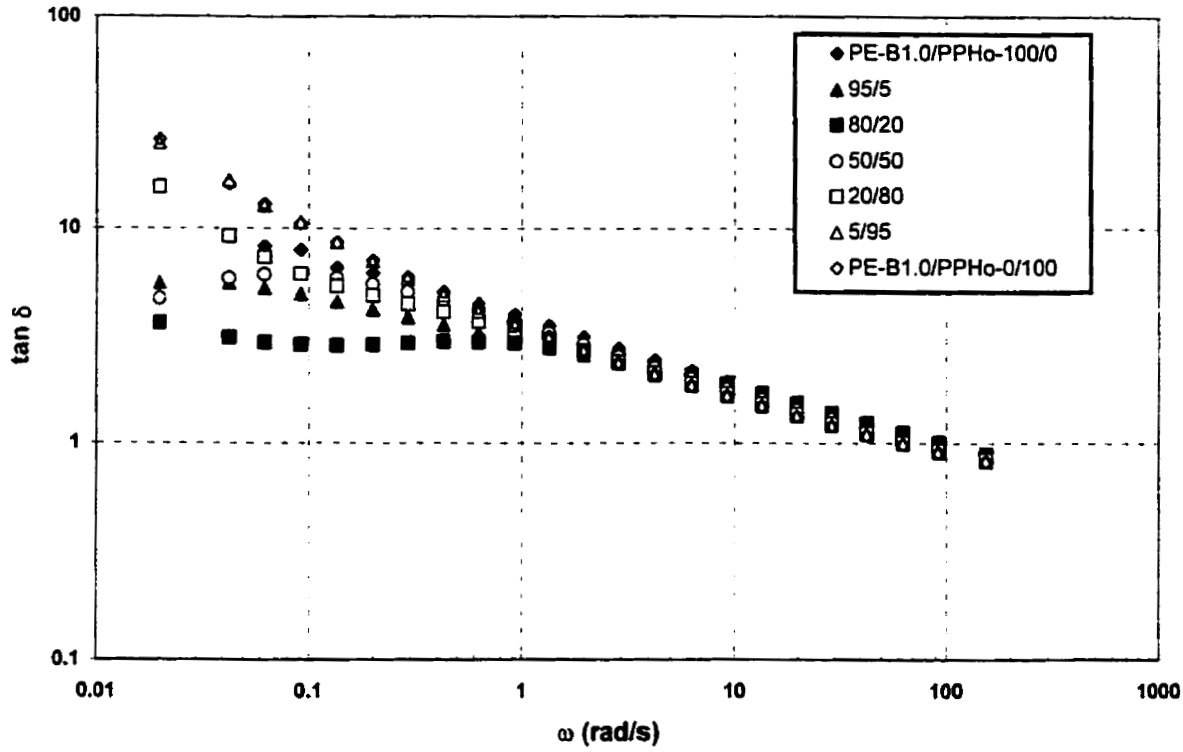

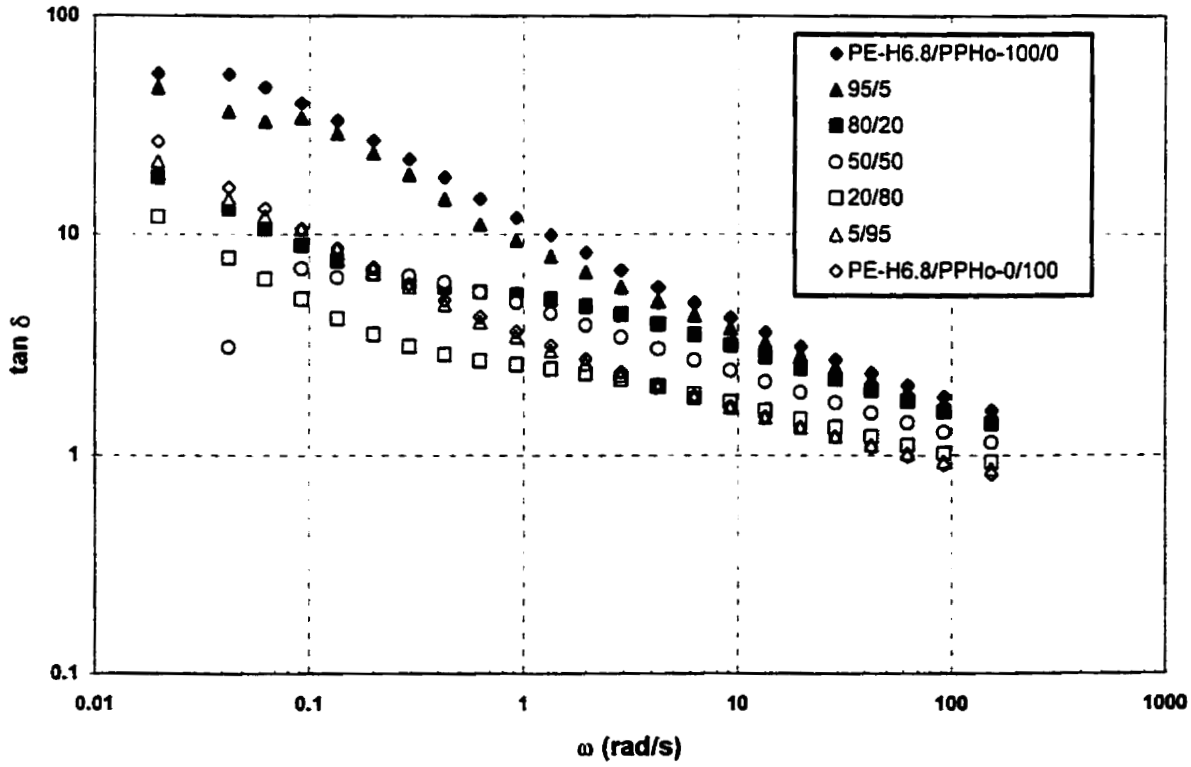

Fig 5.24 : Tan δ as a function of frequency for PE-B1.0/PPHo and PE-H6.8/PPHo blends at 190°C

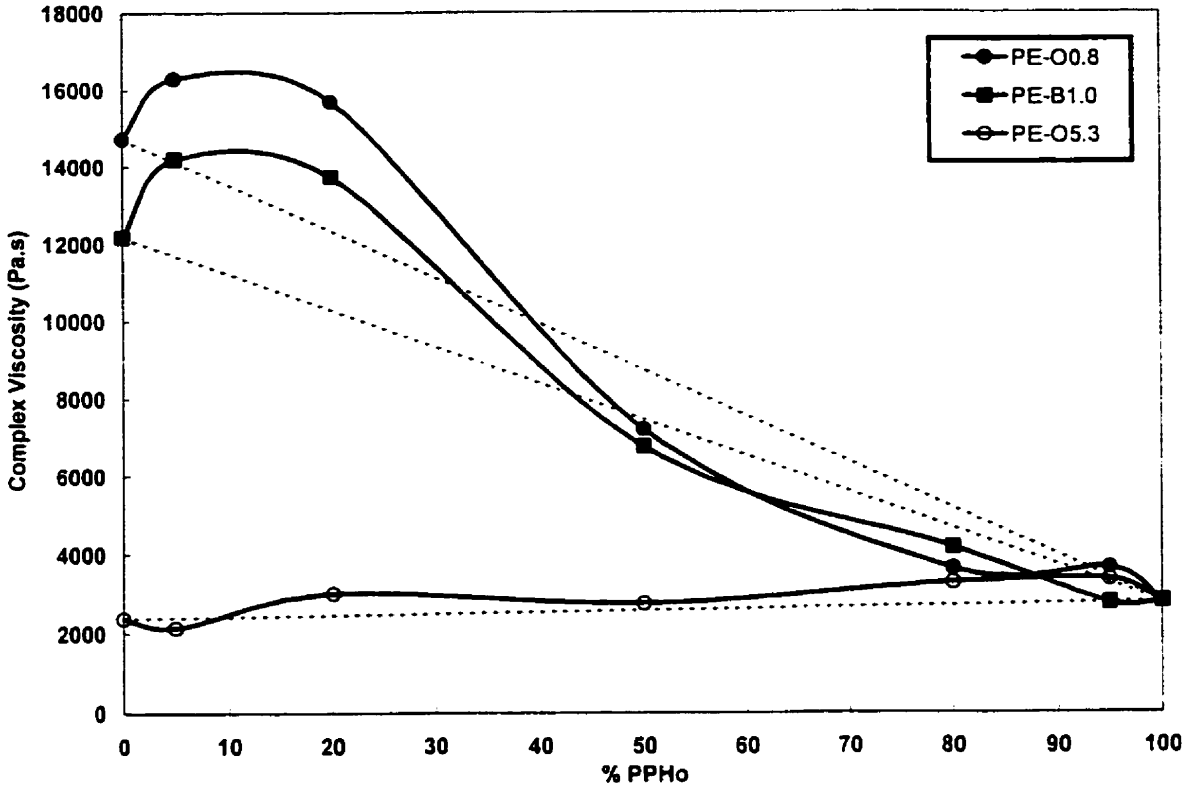

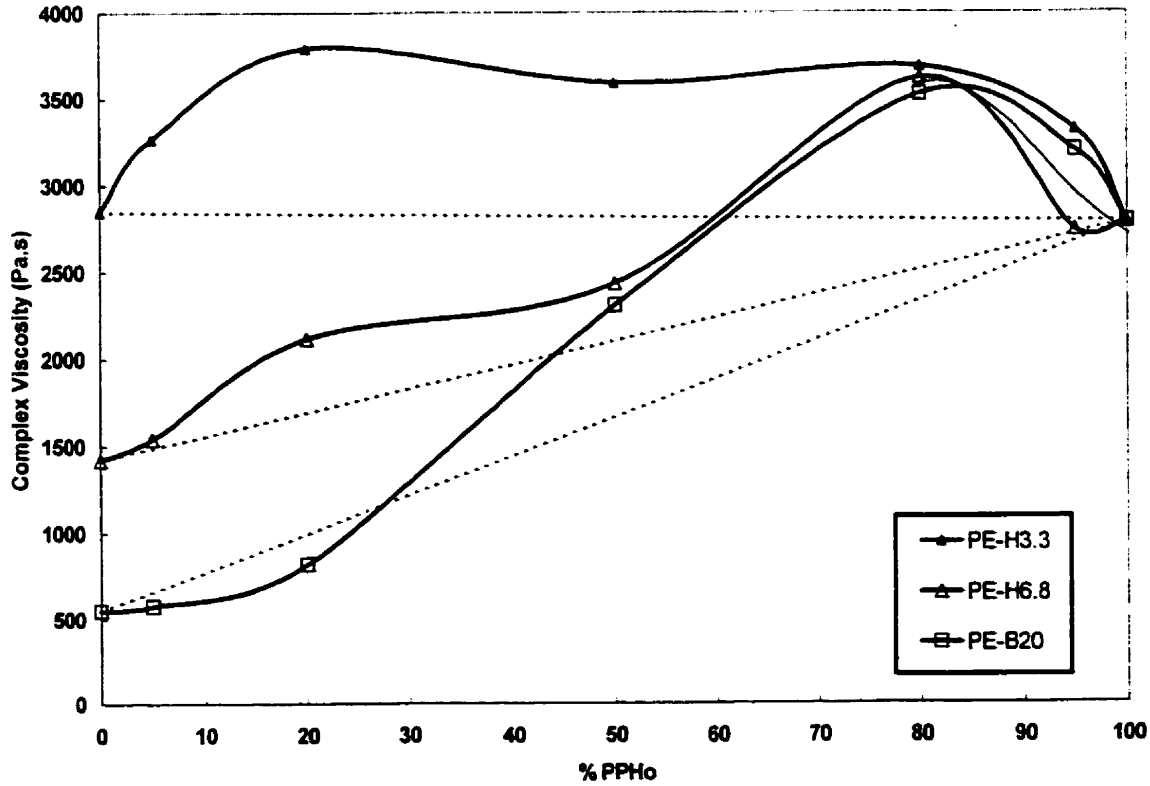

Fig 5.25 : Dependence of complex viscosity of LLDPE/PPHo blend on PPHo content, at ω-0.1 rad/s and at 190°C

system, however, we cannot interpret the maxima in terms of the co-continuous phase, as they were not observed in the SEM micrographs for those compositions. The increase in the viscosity is probably due to hydrodynamic effects within the blends (interactions among the dispersed phase particles) and not due to their intrinsic morphology (cocontinuous phase) as reported by Han (1981). It is seen that minima and inflexion points are observed around 50% composition. These can be correlated with co-continuous phase or phase inversion that were predicted to be observed around 50% composition (Table 5.4). Min *et al.* (1984) also observed a local minima and attributed it to the presence of co-continuous phase.

Rheological study was also performed on LLDPE and PPCo blends to get a better understanding of the rheological characterization. Fig. 5.26 compares the storage modulus of the LLDPE with PPHo and PPCo blends (20% of PPHo and PPCo). It is observed that the storage modulus of the LLDPE/PPCo blends in the low frequency region is always higher than that of the PE/PPHo blends. It can be recollected from Fig. 5.1 that pure PPHo has higher storage modulus as compared to PPCo. As a result it can be inferred that the storage modulus of LLDPE/PPHo blends should be higher. However, different results were obtained. This is probably because PPCo is copolymer with ethylene and it would form a ternary system when blended with PE. A ternary system develops a different and complex morphology as compared to a binary system that normally forms a drop in matrix type. Study of the morphology of these blends using SEM was attempted but we were unable to differentiate between the dispersed droplets and the matrix. This is probably due to the limitations of the SEM and morphological studies of ternary blends are normally studied using Transmission Electron Microscopy (TEM). This would form an interesting topic for future work, as additions of compatibilizers for enhanced compatibility would also result in the formation of ternary blends.

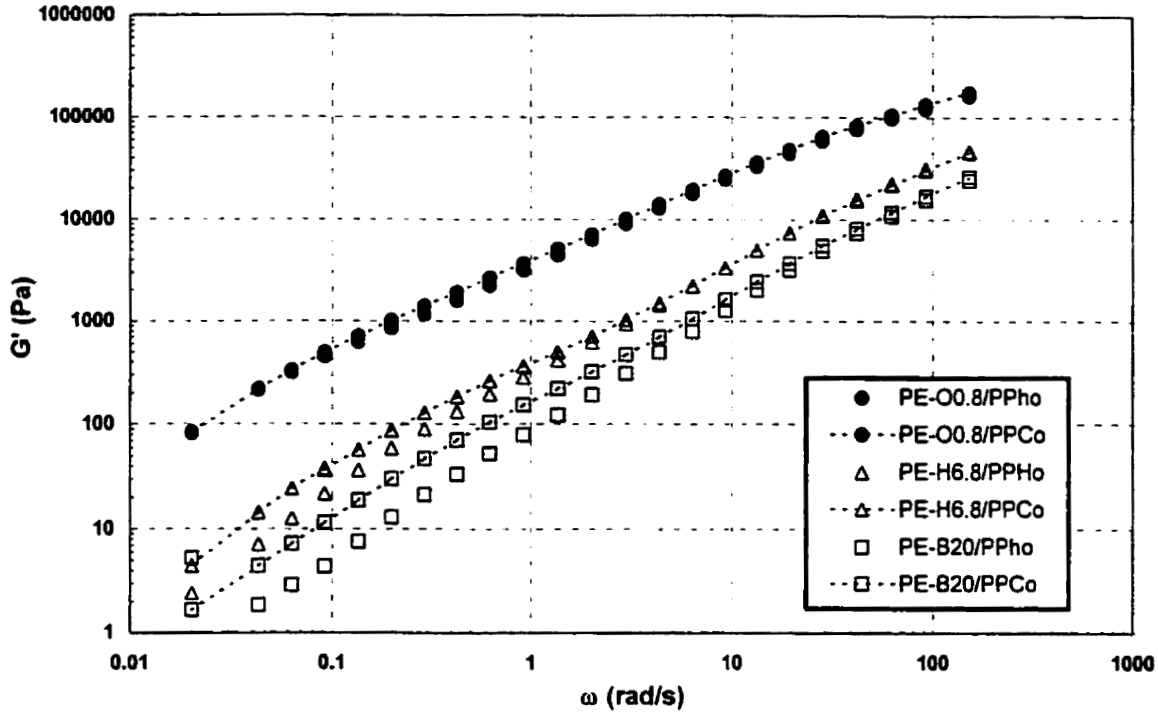

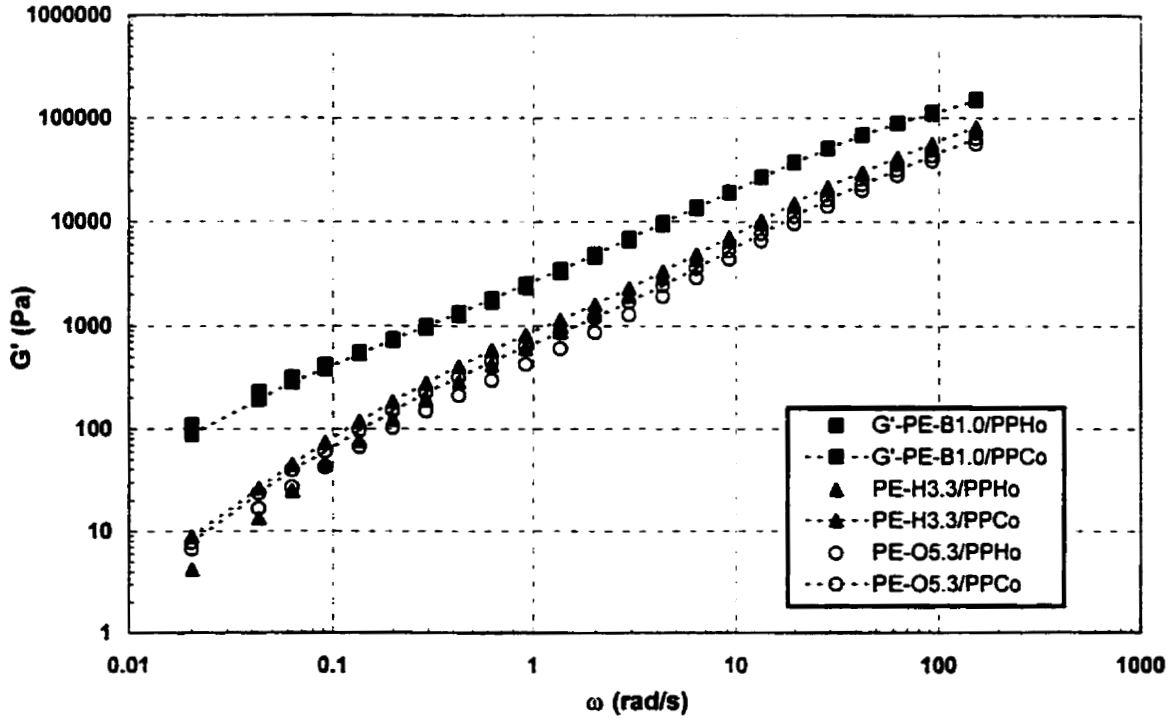

Fig 5. 26 : Storage moduli of LLDPE/PPHo and LLDPE/PPCo blends of 80/20 compositions at 190°C

5.2.5 Interfacial tension

The storage and loss moduli of the blends and their components were fitted to the Palierne model, using the least square method, to determine the interfacial tension between the blend components. Interfacial tension was determined for the four different compositions of all the LLDPE/PPHo blends. The average values of the interfacial tension for the different systems is given in Table 5.6. The results indicate that the blends composed of PPHo and Butene comonomer resins (PE-B1.0 and PE-B20) show the lowest values for the interfacial tensions followed by blends composed of PPHo and LLDPE of Hexene and Octene comonomers respectively. In Fig. 5.27, however, it can be seen that the values for the interfacial tension determined for each blend composition show large variation with no apparent trend. Previous researchers who have used the Palierne model, did not observe much variations in their results (Yamaguchi, 1998; Carreau, 1996; Graebling *et al*, 1994). This is probably because they considered one or two compositions at most, for a given blend system, and did not attempt to characterize the full spectrum of blend composition.

5.3 Discussions

Phase segregation of LLDPE and PP blends in the solid state is quite obvious from the two distinct peaks observed in the thermal profiles of the DSC studies. The immiscible nature is further confirmed from the visual observation of the two phase morphology. The melt immiscibility on the other hand is inferred from the presence of blends secondary plateau and long time relaxation process in the terminal zone. This has been reasoned as an indication of the phase separation in the melt state (Yamaguchi *et al.*, 1996). The reason for melt immiscibility is not so straightforward and has been a subject of great debate. This is probably due to the fact that since these polymers are simple olefins, logically miscibility should be observed in the melt state. Preliminary molecular simulation studies by Choi *et al.* (1995) suggest that the melt incompatibility arise due to

Blend system	Average Interfacial tension (mN/m)
PE-B1.0/PPHo	0.43
PE-B20/PPHo	0.36
PE-H3.3/PPHo	0.59
PE-H6.8/PPHo	0.67
PE- O0.8/PPHo	1.73
PE-O5.3/PPHo	0.57

Table 5.6 : Average interfacial tension of LLDPE/PPHo blends at 190 °C

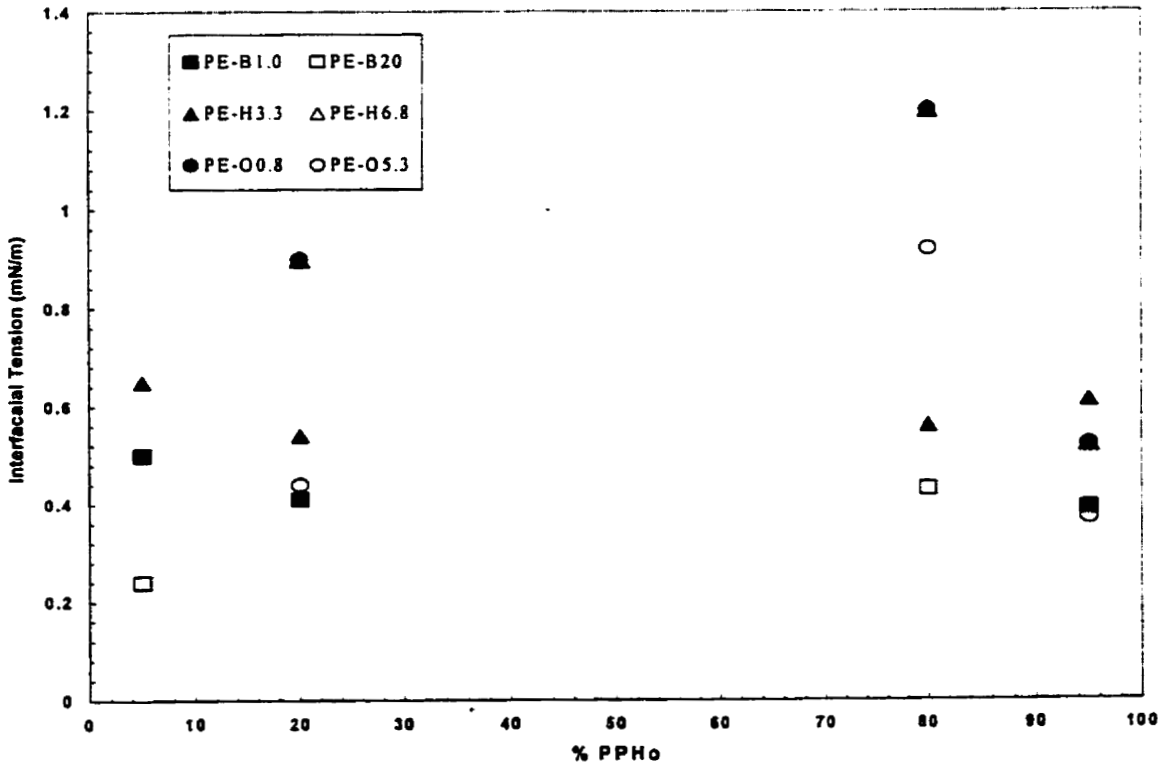

Fig 5.27 : Palierne model's predictions of LLDPE/PPHo interfacial tension, as a function of blend composition, at 190°C

*Note that value calculated for PE-O0.8/PPHo at 5% PPHo is 4.3 mN/m

the long and short ranged order of the polyethylene. This subject is relatively new and efforts are still underway to elucidate the origin of the melt incompatibility.

5.3.1 Relation between rheological properties and morphological features.

The effect of the elasticity of the virgin materials on the morphology of the blend was studied using Van Oene's (1972) criterion (using equation 2.6). The results were used to predict the type of final melt morphology. The approximate first normal stress difference of the components was calculated using the following equation suggested by Laun (1986)

$$\frac{N_1}{\dot{\gamma}^2} = \frac{2G'(\omega)}{\omega^2}\left[1+\left(\frac{G'(\omega)}{G''(\omega)}\right)^2\right]^{0.7} \tag{5.6}$$

According to Van Oene's criterion, for the case when the PPHo is the matrix and LLDPE is the dispersed phase, PE-B20, PE-O5.3 and PE-H6.8 should form a stratified morphology as the dispersed phase elasticity is smaller than that of the matrix phase (Table 5.6). Van Oene's work also states that if a phase β stratifies in phase α then phase α would form droplets in phase β. He referred to them as complementary mixtures. However, we do not observe stratified morphology at any of the predicted compositions, but only observe droplet morphology. Similarly, Favis and Chalifoux (1987) also could not observe stratified morphology for any of the compositions they studied. They attributed the failure of Van Oene's theory to time lapse between sampling and the sample solidification, which might be sufficient for the dispersed phase to relax. Forteleny and Kovar (1992) found that the Van Oene's criteria is not valid for the system of polypropylene, ethylene and propylene elastomers. They further commented that it is very difficult to measure the first normal stress difference at the velocity gradient corresponding to the conditions of the mixing. They attributed this as the reason why the theory of Van Oene can neither be confirmed nor refuted.

Table 5.7: Van Oene theory's predictions for PPHo/LLDPE blend morphology*

Resin	$N_1 \times 10^{-4}$ (Pa)	Type (predicted)
PE-B1.0	33	Droplet
PE-B20	1.64	Stratified
PE-H3.3	9.98	Droplet
PE-H6.8	3.3	Stratified
PE-O0.8	37	Droplet
PE-O5.3	6.8	Stratified
PPHo	7.91	

* PPHo considered as matrix

The viscosity of the blends as a function of composition is another way to relate the blend rheology to its morphology. Han (1981) had related the shape of these curves for two-phase polymer blends to that of the deformation of the dispersed droplets in the shear field. He proposed four different types of behavior which account for a) little interaction between the dispersed droplets and the matrix, b) phase inversion, c) elongation of droplets into fibrils during flow, and d) strong interaction among droplets or interlocked morphology. In our study, we observe that complex viscosity vs. composition curves (Fig. 5.25) show a positive deviation from the mixing rule. The maxima observed in these curves are probably due to the drop interaction and not due to the cocontinuous phase as observed by other researchers. The minima and the inflection point on the other hand have been attributed to the co-continuous phase.

Blend rheological behavior is often related to morphology using the Palierne model. The Palierne model is used by many researchers to either predict the particle size or the interfacial tension between the blend components. While we were able to extract an approximate value of the LLDPE/PP interfacial tensions, the Palierne model's

prediction of the PP/LLDPE interfacial tensions exhibit a lot of variations. The large variations in the interfacial tension values may be due to coalescence effect. It may be possible that for these blend systems coalescence effects may be dominant even at 5% composition. It has been found that the Palierne model is not effective for higher concentration systems (Graebling *et al.*, 1993), where coalescence effect dominates. Hence, it may not be a valid model for calculating interfacial tension for the range of concentration studied.

Results obtained from rheological measurements were analyzed in several ways in order to obtain the maximum information about these blends. It was found that most of the results led to the same conclusion: blending of the polymers results in materials with higher elasticity as compared to that of the matrix. While the change in the PE molecular structure did not seem to have significant effect on the linear viscoelastic properties of the blends, it was found to significantly affect the morphology of the blends.

5.3.2 Relation between molecular structure and morphological features

In the present study, the processing conditions of all blends were controlled and only the material characteristics varied from one system to another. It is well documented that the viscosity ratio plays an important role in determining the particle size and its distribution. The effect of the viscosity ratio on the drop size was evident from the *U-shaped* curve having a minimum drop size value around a viscosity ratio equal to one (Figs. 5.16 and 5.17). It is also observed that for similar viscosity ratio, the type of comonomer significantly affects the drop size of the dispersed phase. The trend followed by the particle sizes for blends composed of different comonomer resins, of LLDPE was observed as Butene<Hexene<Octene. Further, it has been reported by Van Oene (1972) that material properties, such as elasticity, affect the mode of dispersion rather than its homogeneity. Thus, it can be inferred that interfacial tension is the main parameter affecting the morphology of blends. This is in concurrence with the study of Favis and Willis (1990), where the order of effects controlling the morphology of blends followed

were: interfacial tension> viscosity ratio> shear stress. Interfacial tension for the blends studied in the present study can thus be said to vary according to the type of comonomer as: Butene<Hexene<Octene. This trend is further supported by the observance of the unusual features in the blend. The unusual features such as fibers and web like structures, which were observed only in the blends of Butene and Hexene comonomer resins are probably due to a strong interfacial adhesion between the dispersed phase and the matrix. Yamaguchi (1998), based on Helfand and Tagami's (1972) theory and his experimental observations, stated that interfacial tension was inversely proportional to adhesive strength and it was mainly the entanglements that were responsible for the interfacial adhesion. Thus, based on the above reasoning it can be inferred that, blend of Butene and Hexene comonomer have low interfacial tension.

Similar trend for interfacial tension was observed by Rao (1999) with metallocene LLDPE and PP resins. Results presented by Rao (1999) for Ziegler Natta LLDPE/PP Blends, however, were not conclusive. Carriere and Silvis (1997), on the other hand, observed that the interfacial tension varies as: Pentene<Octene<Butene<Propylene. They attributed the decrease of the interfacial tension to the increase in the length of the side chain. The trends indicated by the data in the above studies should be treated with caution, as the different resins had been used, which were produced by different manufacturers by different processes and thus would have had different molecular structure (M_n, MWD, comonomer content and branch distribution).

In addition to the type of comonomer, the effect of comonomer content and comonomer distribution on the blend morphology are examined. For the resins used in this study, it was found that the branch content in the LLDPE resins follows the following order: Butene>Octene>Hexene (Table 5.2). It is also found that Hexene comonomer resins have relatively uniform branching distribution as compared to Butene and Octene comonomer resins, which can be assessed using the spread of the copolymer peak (Fig. 5.3). In light of these results, it can be inferred that the high comonomer content in

Butene comonomer resins contributes to their low interfacial tension. A higher comonomer content leading to lower interfacial tension had also been observed by Carrier and Silvis (1997). They attributed it to the increase of more chain ends and a lower average MW between the chain ends. The above observation can also be supported by the work of Yamaguchi *et al.* (1996), where they reported that resins with a comonomer content higher than 50 % were miscible with PPHo. Based on the above argument, it can be inferred that the high comonomer content in the Octene-LLDPE resins should contribute to lower their interfacial tension with PP resin. Yet, the Octene LLDPE resins appear to have higher interfacial tension than the Hexene LLDPE resins. This probably is either due to the variation in the length of the side chain branches or due to the uniform branching distribution of the Hexene comonomer as compared to the Octene comonomer.

It has been reported in the literature that the interfacial tension is also affected by the number average molecular weight (M_n) and molecular weight distribution (MWD). In general, the interfacial tension has been found to increase with an increase in the M_n (Arashiro and Demarquette, 1999, Ellingson *et al.*, 1994). This effect, however, becomes less important at higher molecular weights. It has been further observed that the interfacial tension decreases with an increase in the polydispersity, for constant number average molecular weight resins (Arashiro and Demarquette, 1999). In our study, since the polydispersities of the LLDPEs are quite close (3 to 3.51), its effect on the morphology cannot be assessed. It is difficult to assess the effect of the M_n on interfacial tension based on the results of the Palierne model due to the great variation in the interfacial tension values. Based on the particle size results, it is also difficult to assess the effect of the MW independent to the viscosity ratio. LLDPE resins with higher MW appears to produce blends with coarser morphology. However, these blends also have a viscosity ratio less close to the optimal value of one which could explain the increase in the dispersed phase particle size.

Conclusions and Recommendations

Chapter 6

The aim of the current work is to get a better understanding of linear low density polyethylene and polypropylene blends in terms of the resin's molecular structure, blend morphology and processing characteristics. Commercial LLDPE resins of varying comonomer type were used together with two PP resins. The results indicate that, regardless of the type of comonomer, these blends are immiscible. This is inferred by the two melting peaks observed in the blends, which remain the same as that of the virgin resins. The two-phase structure was further observed in the SEM micrographs. The blends show the drop-in-matrix and beehive type of morphology depending on the composition, due to the different fracture mechanism. It is observed that the particle size and particle size distribution both increase with the increase in composition. This is attributed to the enhanced coalescence and collision probability at higher concentrations. Certain unusual features such as the fibres, shrinking dispersed phase inside the matrix and web-like fibrils were also observed. These were however, observed only in the blends of Butene and Hexene comonomer and are probably due to the strong interfacial adhesion between the dispersed phase and the matrix.

The blend's morphological characteristics were found to vary as a function of the viscosity ratio and the resin's molecular structure. The experimental results indicated that the minimum particle size in the blend would be obtained when the matrix and dispersed

phase viscosities are matched. Experimental results also showed that the particle size in the blend varies from one type of comonomer resins to another and follows the order: Butene<Hexene<Octene. It is inferred that the interfacial tension for the PP homopolymer and LLDPE resins increases as the length of the LLDPE short side branches increases. For the resins used in this study, it was further found that resins with high comonomer content, but slightly longer side branches, produce blends with larger particle size as compared to resins with lower comonomer content but with shorter branches and uniform branche distribution. This study clearly indicates that Butene comonomer LLDPE resins having high comonomer content would result in better impact properties. This hypothesis further needs to be verified by testing the impact properties of the blends.

The rheological characterization of the blends shows an increase in storage modulus as compared to the matrix in the lower frequency region. This indicates enhanced elasticity, and is attributed to the deformability of the dispersed phase. No significant effect of the type of comonomer on the rheological properties was observed. Results obtained from the rheological and morphological characterization were used to determine the resins interfacial tension using the Palierne model. The validity of the Palierne model for the blend systems studied, however, is questionable. On comparing the average interfacial tension, it was observed that blends of PP homopolymer with Butene comonomer LLDPE resins show the lowest interfacial tension but no trend was detected for blends composed of Hexene and Octene comonomer resins. Furthermore, large variations were observed when comparing the predicted interfacial tension for any specific blend system while varying its composition. It is recommended that assessment of the Palierne model should be done using PE/PP blends with lower dispersed phase compositions than those used in this study.

The crystalline morphology of both virgin resins used and their blends was found to be mostly affected by the cooling conditions. The cooling rate is instrumental in

determining the spherulite size of the resins. The PP samples cooled at a fast rate had a smaller spherulite size as compared to those cooled at a slower rate. This is probably due to the decreased mobility of the chain travelling to the nucleation site. Blends exposed to fast cooling conditions also show a smaller sized spherulite. This is probably due to the simultaneous crystallization of LLDPE and PP. The effect of comonomer on the crystalline morphology, however, could not be assessed. Consequently, the study on the crystalline morphology of the blends used in this work remained mostly qualitative. The crystalline morphology strongly impacts on the resins mechanical properties. It would thus be interesting to further study the effect of the molecular structure of the LLDPE on the size of the spherulites of the blends by performing isothermal crystallization studies.

In order to further improve the performance of these blends, compatibilizers may be added in the blend formulation. Compatibilizers reduce the interfacial tension to facilitate dispersion, stabilize the generated morphology and finally enhance the adhesion between the phases. Very limited literature is available on addition of compatibilizers in LLDPE/PP blends. Study in this field would be useful in putting these blends to better utilisation.

Recycling of these blends is another important issue that needs to further be studied. While polymer recycling often involves blending, several factors affect the viability of the final product: presence of contaminants, additives, material degradations. In the present work, the effect of these factors on the morphology and rheology of the blends were not studied. Findings from the study of blends made with virgin resin, however, provide a foundation for future studies aiming at improving the mechanical property of the recycled blends. A study involving the recycled LLDPE/PP blends with and without the compatibilizers would form an interesting future work.

References

N. Alle and J. Lyngaae-Jorgensen, "Polypropylene and polyethylene blends, I. Flow behavior in capillaries"; *Rheol. Acta*, 19, pp. 94-103, 1980.

N. Alle, F. E. Andersen and J. Lyngaae-Jorgensen, "Polypropylene and polyethylene blends, III. Die swell behavior and morphology after capillary flow"; *Rheol. Acta*, 20, pp. 222-230, 1981

E. Y. Arashiro and N. R. Demarquette, "Influence of molecular weight and polydispersity on interfacial tension between polystyrene and polyethylene"; *ANTEC*, pp. 3780-3784, 1999.

G. N. Avgeropoulos, F. C. Weissert, P. H. Biddison and G. C. A. Bohm, "Heterogeneous blends of polymers: Rheology and Morphology", *Rubber Chem. Technol.*, 49, 93-104, 1976.

L. E. Bailey, D. G. Cook, J. Pronovost and A. Rudin, "Elongational flow properties of low density polyethylene and linear low density polyethylene from non isothermal melt spinning experiments", *Poly. Engg. and Sci.*, 34, 19, pp. 1485-1491, 1994.

M. Bains, S. T. Balke, D. Reck and J. Horn, "The compatibility of linear low density polyethylene-polypropylene blends: Viscosity ratio plots"; *Poly. Engg. and Sci.*, 34, 16, pp. 1260-1268, 1994.

D. W. Bartlett, J. W. Barlow and D. R. Paul, "Mechanical properties of blends containing HDPE and PP"; *J. Appl. Polym. Sci.*, 27, pp. 2351-2360, 1982.

Z. Bartczak and A. Galeski, "Changes in interface shape during crystallization in two component polymer systems"; *Polymer*, 27, pp. 544-548, 1986.

M. H. Baumann, "Plastic solid waste management –The role of source reduction, reuse, recycling, biodegradability and incineration in the future", *ANTEC*, pp. 2821-2824, 1999.

J. G. Bonner, C. J. Frye and G. Capaccio., "A novel calibration for the characterization of polyethylene copolymers by temperature rising elution fractionation"; *Polymer*, 34, 16, pp. 3532-3534, 1993.

M. Bousmina, A. Ait-Khadi and J. B. Faisant, "Determination of shear rate and viscosity from batch mixer data"; *J. Rheology*, 43, 2, pp. 415-433, 1999.

M. Bousmina and R. Muller, "Linear viscoelasticity in the melt of impact PMMA. Influence of concentration and aggregation of dispersed rubber particles"; *J. Rheol*, 37, pp. 663-679, 1993.

D. C. Bugada and A. Rudin, "Branching in Low density polyethylene by ^{13}C-NMR"; *Eur. Polym. J*, 23, 10, pp. 809-818, 1987.

J. A. Covas, J. F Aggasant, A. C Diogo, J. Vlachopoulos and K. Walters, "*Rheological fundamentals of polymer processing*"; Kluwer Academic Publishers, 1995.

C.J.Carriere and H.C. Silvis, " The effects of short chain branching and comonomer type on the interfacial tension of polypropylene-polyolefin elastomer blends"; *J. Appl. Polym. Sci.*, 66, pp. 1175-1181, 1997.

P.J. Carreau, " Rheological properties of multiphase polymeric systems: facts and challenges"; *Proc. XIIth Intl Congr. On Rheology*, 3-6, 1996.

P. Choi, H. P. Blom, T. A. Kavassalis and A. Rudin, "Immiscibility of poly(ethylene) and poly(propylene): A molecular dynamics study", *Macromolecules*, 28, pp 8247-8250, 1995

V. Choudhary, H. S. Varma and I. K. Varma., "Polyolefin blends: effect of EPDM rubber on crystallization, morphology and mechanical properties of polypropylene/EPDM blends"; *Polymer*; 32, 14, pp. 2534-2545, 1991

J. H Daane, F. C. Schilling and L. L. Blyler, "Effect of branches on the flow activation energy and melt elasticity of PE"; *ANTEC*, pp. 282-284,1977.

J. M. Dealy and K. F. Wissburn, "*Melt Rheology and its role in Plastics Processing – Theory and Applications*"; Chapman and Hall, 1995.

F. Defoor, G. Groeninckx, H. Reynaers, P. Schouterden, And B. Van der Heijden, "Thermal and morphological characterization of binary blends of fractions of 1-octene LLDPE", *J. Appl. Polym. Sci.*, 47, pp. 1839-1848, 1993.

M. Doi and T. Ohta., "Dynamics and rheology of complex interfaces"; *J.Chem Phys*, 95, pp. 1242-1248, 1991.

L. Dong, D. C. Bassett and R. H. Olley, "On nucleation and isothermal changes in supercooling in a partially miscible polypropylene/polyethylene blend"; *J. Macromol. Sco. –Phys.*, B 37, 4, pp. 527-542, 1998.

M. M. Dumoulin, C. Farha and L. A. Utracki., "Rheological and Mechanical properties of ternary blends of linear low density polyethylene/polypropylene/ethylene-propylene block polymers"; *Poly Engg Sci*, 24, 17, pp. 1319-1326, 1984.

M. M. Dumoulin, L. A. Utracki. and C. Farha, " Melt rheology and mechanical properties of LLDPE/PP blends Part 1- Properties of one and two component systems"; *ANTEC*, pp. 443-446, 1984

M. M. Dumoulin, P. J. Carreau and L. A. Utracki., " Rheological properties of Linear Low density Polyethylene/Polypropylene blends Part2 : Solid state behavior"; *Poly Engg Sci*, 27, 20, pp. 1627-1633, 1987.

L. D'Orazio, R. Greco, C. Mancarella, E. Martuscelli, G. Ragosta and C. Silvestre, "Effect of the addition of ethylene –propylene random copolymers on the properties of high density polyethylene/isotactic polypropylene: Part 1-Morphology and impact behavior of molded samples"; *Poly Engg and Sci.*, 22, 9, pp. 536- 544, 1982.

R. J. Ehring, *Plastics Recycling*; Hanser Publishers, New York, 1992.

P. C. Ellingson, D. A. Strand, A. Cohen, R. L. Sammler and C. J. Carriere, "Molecular weight dependence of PS/PMMA interfacial tension probed by imbedded fiber retraction"; *Macromolecules*, 27, pp. 1643-1647, 1994.

J. J. Elmendrop, "A study on polymer blending microrheology"; *Polym. Engg. Sci.*, 26, 6, pp. 418-426, 1986.

B. D. Favis, "The effect of Processing Parameter on the morphology of an immiscible blend"; *J. Appl. Polm. Sci.*, 39, pp. 285-300, 1990.

B. D. Favis, " Polymer alloys and blends: recent advance"; *Can. J. Chem. Engg.*, 69, 619-625, 1991.

B. D. Favis and J. P. Chalifoux, "The effect of viscosity ratio on the morphology of Polypropylene/Polycarbonate blends during processing"; *Poly. Eng. and Sci.*, 27, 20, pp. 1591-1600, 1987.

B. D. Favis and J. M. Willis, "Phase size/composition dependence in immiscible blends: experimental and theoretical consideration"; *J. Polym Sci.*, Poly. Phy. Edn., 28, pp. 2259-2269, 1990.

B. D. Favis and D. Therrien., "Factors influencing structure formation and phase size in an immiscible polymer blend of polycarbonate and polypropylene prepared by twin screw extruder"; *Polymer*, 32, 8, pp. 1474-1481, 1991.

V. Flaris and Z. H. Starchurski, "The mechanical behavior of blends of polyethylene and polypropylene and an ethylene-propylene block copolymer at –20 °C"; *J. Appl. Polym. Sci.*, 45, pp. 1789-98, 1992.

Chr. Friedrich, W. Gleinser, E. Korat, D. Maier and J. Wese, "Comparison of sphere size distributions obtained from rheology and transmission electron microscopy in PMMA/PS blends"; *J. Rheol.*, 39, pp. 1411-1425, 1995.

I. Fortelny, Z. Cerna, J. Binko and J. Kovar., "Anomalous dependence of the size of droplets of dispersed phase on intensity of mixing", *J. Appl. Polm. Sci.*, 48, pp. 1731-1737, 1993.

I. Fortelny and J. Kovar, "Effect of the composition and properties of components on the phase structure of polymer blends"; *Eur. Polym. J.*, 28, 1, pp. 85-90, 1992.

M. Fujiyama and Y. Kawaski, "Rheological properties of polypropylene/high density polyethylene blend melts I. Capillary flow properties"; *J. Appl. Polm. Sci.*, 42, pp. 467-480, 1991.

A. Galeski, M. Pracell and E. Martuscelli, "Polypropylene spherulite morphology and growth rate changes in blends with low density polyethylene"; *J. Polym. Sci.*, 22, pp. 739-747, 1984.

P. G. Ghodgaonkar and U. Sundraraj., "Prediction of dispersed phase drop diameter in polymers: The effect of elasticity"; *Poly. Eng. and Sci.*, 36, 12, pp. 1656-1665, 1995.

G. Glockner, "Temperature rising elution fractionation: A review"; *J. Appl. Polym. Sci.*, 45, pp. 1-24, 1990.

D. Graebling, A. Benkira, Y. Gallot and R. Muller, "Dynamic viscoleastic behavior of polymer blends in the melt- experimental results for PDMS/POE-DO, PS/PMMA and PS/PEMA blends"; *Eur. Polym. J.* 30, pp. 301-308, 1994.

D.Graebling, R.Muller and J.F. Palierne, "Linear viscoleastic behavior of some incompatible polymer blends in the melt. Interpretation of data with a model of emulsion of viscoelastic liquids"; *Macromolecules*, 26, pp. 320-329, 1993.

H. P. Grace, "Dispersion phenomena in high viscosity immiscible fluid systems and application of static mixers as dispersion devices in such systems"; *Chem. Engg. Commun.* 14, pp. 225-277, 1982.

M. Grmela and A. Ait-Kadi, "Comments on the Doi-Ohta theory of blends"; *J. Non-Newtonian Fluid Mech.*, 55, pp. 191-195, 1994.

S. K. Goyal, J. Auger , E. Kardashewski and R. Saetre, "Influence of branch distribution on the rheological and processing behavior of LDPE resins"; *ANTEC*, 1881, 1998.

S. K. Goyal, "The influence of polymer structure on melt strength behavior of PE resins"; *Plastics Engg.*, pp. 25-28, Feb 1995.

J. E. Guillet, R. L. Combs, D. F. Slonaker, D. A. Weemes and H. W. Coover, "Effects of molecular weight distribution and branching on rheological parameters of polyethylene melts. Part I. unfractionated polymers"; *J. Appl. Polym. Sci.*, 8, pp. 757-765, 1965.

C. D. Han, "*Multiphase flow in polymer processing*"; Academic Press, N. York, 1981.

C. D. Han, "Blends of nylon 6 with an ethylene based multifunctional polymer I-Rheology structure relationship"; *J. Appl. Polym. Sci.*, 30, pp. 2431-2455, 1985.

C. D. Han, "Influence of molecular weight distribution on the linear viscoelastic properties of polymer blends"; *J. Appl. Polym. Sci.*, 35, pp. 167-213, 1988.

C. D. Han and Y.W. Kim, "The effect of mixing on the modes of dispersion and rheological properties of two phase polymer blends in extrusion"; *J. Appl. Polym. Sci.*, 19, pp. 2831-2843, 1975.

J. H. Han, C. C. Feng, D. J. Li and C. D. Han, "Effect of flow geometry on the rheology of dispersed two phase blends of polystyrene and polymethylmethylacrylate"; *Polymer*, 36, pp. 2451-2463, 1995.

E. Helfand and Y. Tagami, "Theory of the interface between immiscible polymers-II"; *J.Chem. Phys.*, 56, 7, pp. 3592-3601, 1972.

E. Harrell and N. Nakajima, "Modified Cole-Cole plot based on viscoelastic properties for characterizing molecular architecture of elastomers"; *J. Appl. Polym. Sci.*, 29, 995, 1984.

J. C. K. Huang, Y. Lacombe, D. T. Lynch and S. E. Wanke, "Effects of hydrogen and 1-butene concentrations on the molecular properties of polyethylene produced by catalytic gas phase polymerization"; *Ind. Eng. Chem. Res.*, 36, pp. 1136-1143, 1997.

M. Inoue, "Properties of melt blends of crystalline high polymers - Fusion and crystallization behaviors"; *J. Poly. Sci.*, 1, pp. 3427-3438, 1963.

G. M. Jordhamo, J. A. Manson and L. H. Sperling, "Phase continuity and inversion in polymer blends and simultaneous interpenetrating networks"; *Poly. Eng. and Sci.*, 26, pp. 517-523, 1986.

H. J. Karam and J. C. Bellinger, "Deformation and breakup of liquid droplets in a simple shear field"; *Ind. Engg. Chem. Fundam.*, 7, pp. 576-581, 1968.

M. Kryszewski, A. Galeski, T. Paula and J. Grebowicz, "Transport phenomenon on interface in blends of polyethylene and polypropylene"; *J. Colloid Interface Sci.*, 44, pp. 85-94, 1973.

K. Khait and S. H. Carr, "Value added materials made from recycled plastics"; *ANTEC*, pp. 3086-3090, 1997.

Y. S. Kim, C. I. Chung, S. Y. Lai and K. S. Hyun, "Melt rheological and thermodynamic properties of polyethylene homopolymers and poly(ethylene/α-olefin) copolymers with respect to molecular composition and structure"; *J. Appl. Polym. Sci.*, 59, pp. 125-137, 1996.

W. C. Kulhlke, "World volume polymer markets slow"; *ANTEC*, pp. 3030-3033, 1999.

N. Kukaleva, E. Koisor and F. Cser, "Properties of blends of high crystallinity polypropylene and metallocene catalyzed linear low density polyethylene"; *PPS*-14, Yokohoma, Japan, pp. 501-502, 1998.

C. Lacroix, M. Bousmina, P.J. Carreau, B. D. Favis and A. Michel, "Properties of PETG/PVA blends: 1.Viscoleastic, morphological and interfacial properties"; *Polymer*, 37, 14, pp. 2939-2947, 1996.

C. Lacroix, P. J. Carreau and A. Michel, "Linear viscoelastic behavior of molten polymer blends: A comparative study of the Palierne and Lee and Park models"; *Rheol Acta*, 36, pp. 416-428, 1997.

C. Lacroix, M. Grmela and P. J. Carreau, "Morphological evolution of immiscible polymer blends in simple shear and elongational flow"; *to be published in Journal of Non Newtonian Fluid Mechanics*, 2000.

M. Laplante, *M.Sc. Thesis*; University of Calgary, Calgary, 1998.

H. Laun, "Prediction of elastic strains of polymer melts in shear and elongation"; *J. Rheol.*, 30, 3, pp. 459-501, 1986.

H. M. Lee and O. O. Park, "Rheology and dynamics of immiscible polymer blends"; *J. Rheol*, 38, pp. 1405-1425, 1994.

M. Levij and F. H. J. Maurer, "Morphology and rheological properties of polypropylene-linear low density polyethylene"; *Poly. Engg. Sci.*, 28, 10, pp. 670-678, 1988.

Y. Li and P. Liu., "Rheological behavior of composites of recycled high density polyethylene and recycled tire particles", *ANTEC*, pp. 1082-1085, 1997.

Y. Liu and R. W. Truss, "Study of dispersion morphologies of isotactic polypropylene and linear low density polyethylene blends by scanning electron microscopy"; *J. Appl. Polym. Sci.*, 60, pp. 1461-1473, 1996.

A. J. Lovinger and M. L. Williams, "Tensile properties and morphology of blends of polyethylene and polypropylene"; *J. Appl. Polym. Sci.*, 25, pp. 1703-1713, 1980.

A. Luciani, M. F. Champgane and L. A. Utracki, "Interfacial tension in polymer blends. Part 1: theory"; *Polym. Networks blends*, 6, 1, pp. 41-50, 1996.

A. Luciani, M. F. Champgane and L. A. Utracki, "Interfacial tension in polymer blends. Part 2: measurements"; *Polym. Networks blends*, 6, 1, pp. 51-62, 1996.

A. Luciani and J. Jarrin, "Morphology development in immiscible polymer blends"; *Poly. Eng. and Sci.*, 36, 12, pp. 1619-1626, 1996.

E. Martuscelli, "Influence of composition, crystallization conditions and melt phase structure on solid morphology, kinetics of crystallization and thermal behavior of binary/polymer blends"; *Polym. Engg. Sci.*, 24, 8, pp. 563-586, 1984.

R. L. McEvoy and S. Krause, "Impact strength and fracture surfaces of interfaces between polyethylene and polypropylene and some ethylene containing copolymers"; *J. Appl. Polym. Sci.*, 64, pp. 2221-2235, 1997.

N. Mekhilef and H. verhoogt, "Phase inversion and dual phase continuity in polymer blends; theoretical prediction and experimental results"; *Polymers*, 37, 18, pp. 4069-4077, 1996.

I. S Miles and A. Zurek, "Preparation, structure and properties of two-phase co-continuous polymer blends"; *Poly. Eng. and Sci.*, 28, pp. 796-805, 1988.

K. Min, J. L. White and J. F. Fellers, "High density PE/PS blends: Phase distribution morphology, rheological measurements, extrusion and melt spinning behavior"; *J. Appl. Polym. Sci.*, 29, pp. 2117-2142, 1984.

W. Minoshima, J. L. White and J. E. Spruiell, "Experimental investigation of the influence of molecular weight distribution on the rheological properties of polypropylene melts"; *Poly. Engg. Sci.*, 20, 17, pp. 1166-1176, 1980.

A. J. Muller, C. Latorre, G. Mendez, J. Rotino and J. L. Rojas, "Structure-property relationships in PP/LLDPE blends"; *ANTEC*, pp. 2418-2422, 1994.

O. F. Noel and J. F. Carley, "Properties of polypropylene-polyethylene blends"; *Poly. Eng. and Sci.*, 15, 2, pp. 117-126, 1975.

J. L. Palierne, "Linear rheology of viscoelastic emulsions with interfacial tension"; *Rheo. Acta*, 29, pp. 204-214, 1990.

F. Pardos, "Plastics in the world to 2020", *ANTEC*, pp. 3034-3038, 1999.

A. P. Plochocki, S. S. Dagli, J. E. Curry and J. Sarita, "Effect of mixing history on phase morphology of a polyalloy and a polyblend"; *Polym. Eng. Sci.*, 29, 10, pp. 617-624, 1989.

A. P. Plochocki, S. S. Dagli and R. D. Andrews, "The interface in binary mixtures of polymers containing a corresponding block copolymer: Effects of industrial mixing processes and of coalescence"; *Polym. Eng. Sci.*, 30, 12, pp. 741-752, 1990.

R. C. Progelhof and J. L. Throne, "*Polymer Engineering Principles: Properties, Processes and Tests for Design*", Hanser Publications, 1993.

P. Potscke, K. Wallheinke, H. Fritsche and H. Stutz, "Morphology and properties of blends with different thermoplastic polyurethanes and polyolefins", *J.Appl. Polym. Sci. 64, pp 749-762, 1997*

O. R. Quayle, 'Parachors of organic compounds", *Chem. Rev.*, 53, pp. 439-459, 1953.

H-J Radusch, "Morphology development during processing of recycled polymer"; *Frontiers in the Science and Technology of Polymer Recycling*, Kluwer Academic Publishers, Netherlands, pp. 191-211, 1998.

D. Rana, K. Cho, B. H. Lee and S. Choe, "Is metallocene polyethylene blend with HDPE more compatible than with PP"; *ANTEC*, pp. 2462-2465, 1998.

N. Rao, "Interfacial tension, blending and morphology of linear low density polyethylene and polypropylene", *M.Sc Thesis*, University of Alberta, 1999.

D. R. Rueda, F. J. Balta-Calleja and A. V. L. Malers, Study of blends based on recycled polyethylene wastes-Part I Variation of mechanical properties with composition"; *J.Mat Sci.* 29, 4, pp. 1109-1113, 1994.

C. E. Scott and C. W. Macosko, "Morphology development during the initial stages of polymer-polymer blending"; *Polymer*, 36, pp. 461-470, 1995.

B. L. Schurmann, U. Niebergall, N. Severin, Ch. Burger, W. Stocker and J. P. Rabe, "Polyethylene (PEHD)/polypropylene (iPP) blends: mechanical properties, structure and morphology"; *Polymer*, 39, 22, pp. 5283-5291, 1998.

G. Serpe, J. Jarin and F. Dawans, "Morphology -processing relationships in Polyethylene-Polyamide Blends"; *Poly. Eng. and Sci.*, 30, 9, pp. 553-565, 1990.

R. A. Shanks, J. Liu and L. Yiu, "Miscibility and co-continuous morphology of polypropylene-polyethylene blends", *ANTEC*, pp. 2553-2555, 1998.

C. K. Shih, D. G. Tynan and D. A. Denelsbeck, "Rheological properties of multicomponent polymer system undergoing melting or softening during compounding"; *Poly Engg Sci*, 31, 23, pp. 1670-1673, 1991.

R. N. Shroff and M. Shida, 'Effect of molecular weight and molecular weight distribution on elasticity of polymer melts"; *ANTEC*, pp. 285-289, 1977.

U. Sundararaj, C. W. Macosko, R. J. Rolando and H. T. Chan, "Morphology development in Polymer blends"; *Poly. Eng. and Sci.*, 32, 24, pp. 1824-1823, 1992.

U. Sundararaj and C. W. Macosko, "Drop breakup and coalescence in Polymer Blends: The Effects of concentration and Compatibilization"; *Macromolecules*, 28, pp. 2647-2657, 1995.

T. Tavgac, *Ph.D. Thesis*, Department of Chemical Engineering, University of Houston, Houston, Texas, 1972.

G. I. Taylor, "The viscosity of a fluid containing small drops of another fluid"; *Proc Roy. Soc.*, 138A, pp. 41-48, 1932.

J. W. Teh, "Structure and properties of polyethylene-polypropylene blend"; *J. Appl. Poly. Sci.*, 28, pp. 605-618, 1983.

J. W. Teh, A. Rudin, and J. C. Keung, "A review of polyethylene –polypropylene blends and their compatibilization"; *Adv. Poly. Tech.*, 13, 1, pp. 1-23, 1994.

S. Torza, R. G. Cox and S. G. Mason, "Particle motions in sheared suspensions: Transient and steady deformation and burst of liquid drops"; *J. Coll. Int. Sci.*, 38, 395, 1972.

W. H. Tuminello, "Relating rheology to molecular weight properties of polymer"; *Encl. of Fluid Mech.*, 9, pp. 211-242, 1990.

C. Tzoganakis., J. Vlachopoulos and A. E. Hamiele, "Effect of molecular weight distribution on the rheological and mechanical properties of PP"; *Poly Engg & Sci.*, 6, 29, pp. 390 -396,1989.

K. Udipi and A. M. Zolotor, "Polymers and the environment – the next decade", J. Poiym. Sci., Polym Symp., 75, pp. 109-117, 1993

T. Usami, Y. Gotoh and S. Takayama, "Generation mechanism of short chain branching distribution in linear low density polyethylenes"; *Macromolecules*, 19, pp. 2722-2726, 1986.

L. A. Utracki, *Polymer Alloys and Blends;* Hanser Pub, Munich, 1989.

L. A. Utracki, M. M. Dumoulin and P. J. Carreau, "Tensile properties of LLDPE/PP blends"; *ANTEC*, pp. 1419-1422, 1987.

L. A. Utracki and Z. H, Shi, "Development of polymer blend morphology during compounding in a Twin screw extruder. Part I. Droplet dispersion and coalescence-A review"; *Polym Eng Sci*, 32, 24, pp. 1824-1832, 1992.

H. VanOene, "Modes of dispersion of viscoelastic fluids in flow"; *J. Coll. Int. Sci.*, 40, 3, pp. 448-467, 1972.

J. F. Vega, A. Santamaria, A. Munoz-Escalona and P. Lafuente, "Small amplitude oscillatory shear flow measurements as a tool to detect very low amounts of long chain branching in polyethylene"; *Macromolecules*, 31, pp. 3639-3647, 1998.

A. Valenza, F. P. La Mantia and D. Acierno, "Rheological characteristics of blends of isotactic polypropylene with high density polyethylene"; *Eur. Poly. J.*, 20, 7, pp. 727-731,1984.

D. Vessely, "Microstructural characterization of polymer blends"; *Polym Eng Sci*, 36, 12, pp. 1586-1593, 1996.

K. Wallheinke, P. Potschke and H. Stutz, "Influence of compatibilizer addition on particle size and coalescence in TPU/PP blends"; J. Appl. Polym. Sci. 65, pp. 2217-2226, 1997.

S. P. Westphal, M. T. K. Ling, S. Y. Ding and L. Woo, "Further studies on metallocene ULDPE/PP blends impact-morphology relationships"; *ANTEC*, pp. 2631-2635, 1997.

S. Wu, "Interfacial and surface tensions of polymers"; *J. Macromol. Sci.–Revs. Macromol. Chem.*, C10, 1, pp. 1-73, 1974.

S. Wu, "Formation of dispersed phase in incompatible polymer blends: Interfacial and Rheological Effects"; *Poly. Eng. and Sci.*, 27, 5, pp. 335-343, 1987.

K. L. Yam, B. K. Gogoi, C. C. Lai and S. E. Selke, "Composites from compounding wood fibers with recycled high density polyethylene"; *Poly. Eng. and Sci.*, 30, 11, pp. 693-699, 1990.

M. Yamaguchi, "Effect of molecular structure in branched polyethylene on adhesion properties with polypropylene", *J. Appl. Polym. Sci.*, 70, pp. 457-463, 1998.

M. Yamaguchi, H. Miyata and K. Nitta, "Compatibility of binary blends of polypropylene with ethylene -α-olefin copolymer"; *J. Appl. Polym. Sci.*, 62, pp. 87-97, 1996.

M. Xanthos, V. Tan and A. Ponnusamy, "Measurement of melt viscoelastic properties of polyethylenes and their blends-A comparison of experimental techniques"; *Poly. Engg. Sci.*, 37, 6, pp. 1102-1112, 1997.

G. R. Zeichner and P. D. Patel, Proc. 2nd World Congr. Chem Eng., Montreal, 6, 373, 1981.

APPENDIX – A

Differential Scanning Calorimetry (DSC) experiments and data processing

A Mettler 12E Differential scanning calorimeter along with its TA89E software which is directly integrated with the DSC was used for the measurement.

- ***Crucible design/sample preparation***

Aluminum crucibles of 40 μL size were used as test cells/ reference cells for the measurements. Aluminum is the standard material used due to its high heat transfer properties. The samples were prepared by molding the polymer pellets into a sheet at 190 °C and then punching out a diameter to fit the crucible base completely. It is important that the sample fits the crucible properly so that there is homogenous heat transfer to the sample. The weight of the samples ranged from 10 mg to 18 mg. The crucible was then mechanically sealed with aluminum caps with pinholes. The pinholes are normally made so that the crucible doesn't get over pressurized in case of any vaporization. If the weight of the samples exceeded 10 mg the reference cells were filled with an inert material usually alpha aluminum oxide

- *Calibration*

Calibration was done with a pure indium sample of approximately 6mg weight. Indium was placed in the aluminum crucibles with perforated lid. It was heated between 150 °C and 160 °C at a heating rate of 1 °C per minute. The system software TA89E calculated the calibration constants required for the calculation. However, the calibration constant or calorimetric sensitivity can also be calculated manually at the melting point of the indium (156.6 °C) using the following equation

$$E_{In}(\mu V / mW) = \frac{area\ of\ melting\ peak(\mu V.s)}{weight\ of\ indium(mg)\ x\ heat\ of\ fusion\ of\ indium(mW.s / mg)}$$

where the heat of fusion of indium = -28.43 J/g

- ***DSC measurements/evaluation.***

Depending upon the type of polymer, the start, end temperature and the heating /cooling rates were programmed into the DSC. Normally, the samples were heated to around 170 /190 °C at a rate of 10 °C/min and cooled at the same rate to 50 °C. The output of the DSC was recorded in terms of the measurement signal U (μV) and the temperature (°C). To obtain the thermogram in terms of heat flow and temperature the measurement signal had to be calculated using the equation

$$Q = \frac{U}{E(T)\ x\ m}$$

where E(T) is the calorimetric sensitivity in μV/mW, m is the mass of the sample in mg and Q is the heat flow per unit mass in W/g.

E(T) can be further resolved into a temperature dependent and temperature independent component according the following equation

$$E(T) = E_{In} \cdot E_{rel}$$

where E_{In} is the value of E at the melting point of indium, i.e. 156.6 °C and is determined during the calibration and E_{rel} can be calculated using the equation

$$E_{rel} = A + B*T$$

where A = 1.078 and B = -5.512×10^{-4} and T is in °C.

The data obtained was in the machine language format, so a standard procedure involving the use of a basic program was done. The program and other details of the data processing can be referred from the work of Laplante (1998).

APPENDIX – B

Melt Flow Index (MFI) calculation of PPHo

- ***Equations used for estimating MFI for PPHo resin at 230°C***

$$\eta = m\dot{\gamma}^{n-1} \quad \text{(B1)}$$

$$\tau = m\dot{\gamma}^{n} \quad \text{(B2)}$$

$$\dot{\gamma} = \frac{4\ MFI}{6x10^5\ \rho\pi R^3} \quad \text{(B3)}$$

where, η is the shear viscosity, $\dot{\gamma}$ is the shear rate, m is fitting parameter, n is the power law index, MFI is the melt flow index, ρ is the melt density , R is the radius of the die and is equal to 1.075 x 10^{-3} m and τ is equal to 1.94 x 10^4 Pa for MFI test.

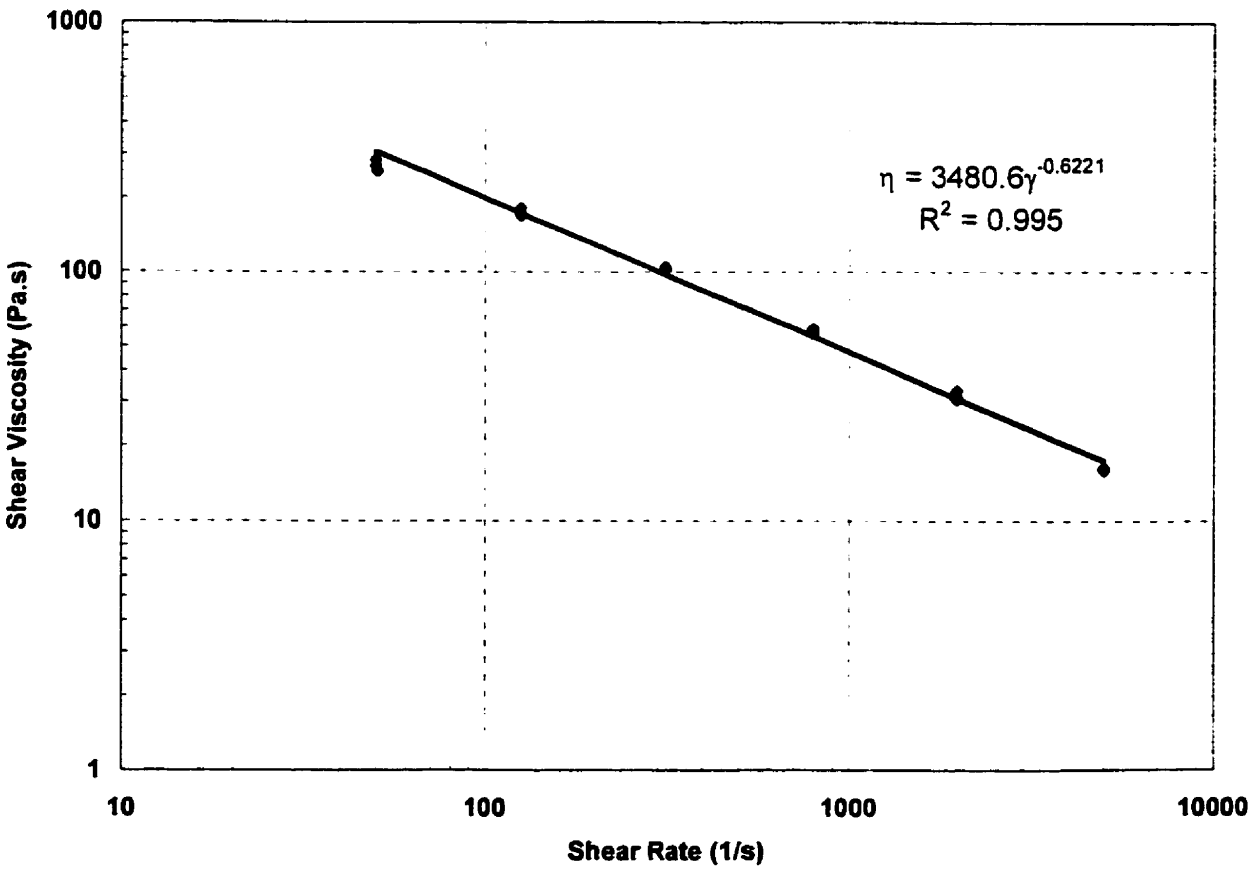

Fig : Shear viscosity against shear rate plot for PPHo at 230 Deg C using capillary rheometer

APPENDIX – C

FORTRAN code for averaging repetitive TREF data

This fortran program reads temperature vs IR signal column from a data file. It then calculates average value of IR signal for a particular temperature.

```
!*********************************************************************
******
!
!  PROGRAM: DATA FILTER
!
!  PURPOSE:  Filtering of repetitive TREF data
!
!*********************************************************************
******

      dimension add(10000)
      dimension avg(10000), x(10000)

      open(UNIT=1, FILE='tref.dat', STATUS='old')
      read(1,*) (x(i),i=1,3158)
      print *, (x(i), i=1,3158)
      close(1)

      open(unit=2, File='out53.dat', Status='new')

      denom=1.d0
      add(2)=x(2)

      do 100 i=1,3158,2
      if(x(i).eq.x(i+2))then
      add(i+3)=x(i+3)+add(i+1)
      denom=denom+1.d0
      else
      avg(i+1)=add(i+1)/denom
      write(2,99) x(i), avg(i+1)
      print *, x(i), avg(i+1)
99    format (2F7.2)
      denom=1.d0
      add(i+3)=x(i+3)
      endif

100   continue
      close(2)
      end
```

APPENDIX – D

Torque profiles of the LLDPE/PPHo blends

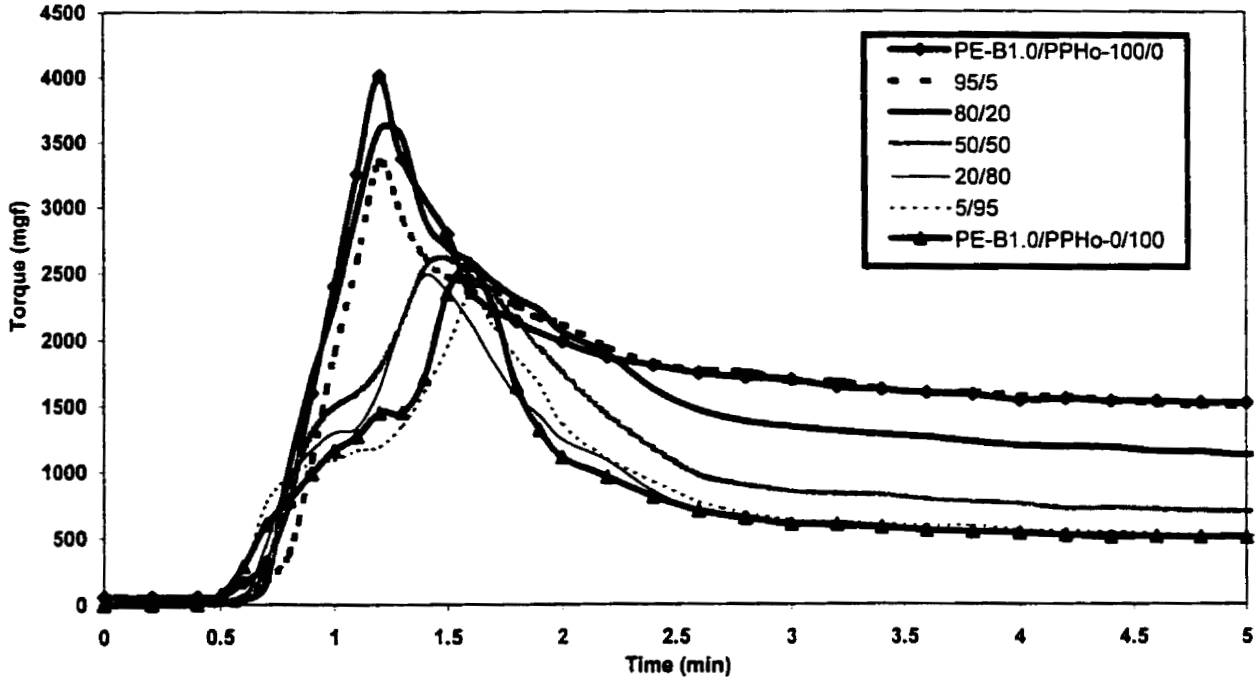

Torque profiles for PE-B1.0/PPHo blends prepared at 190°C

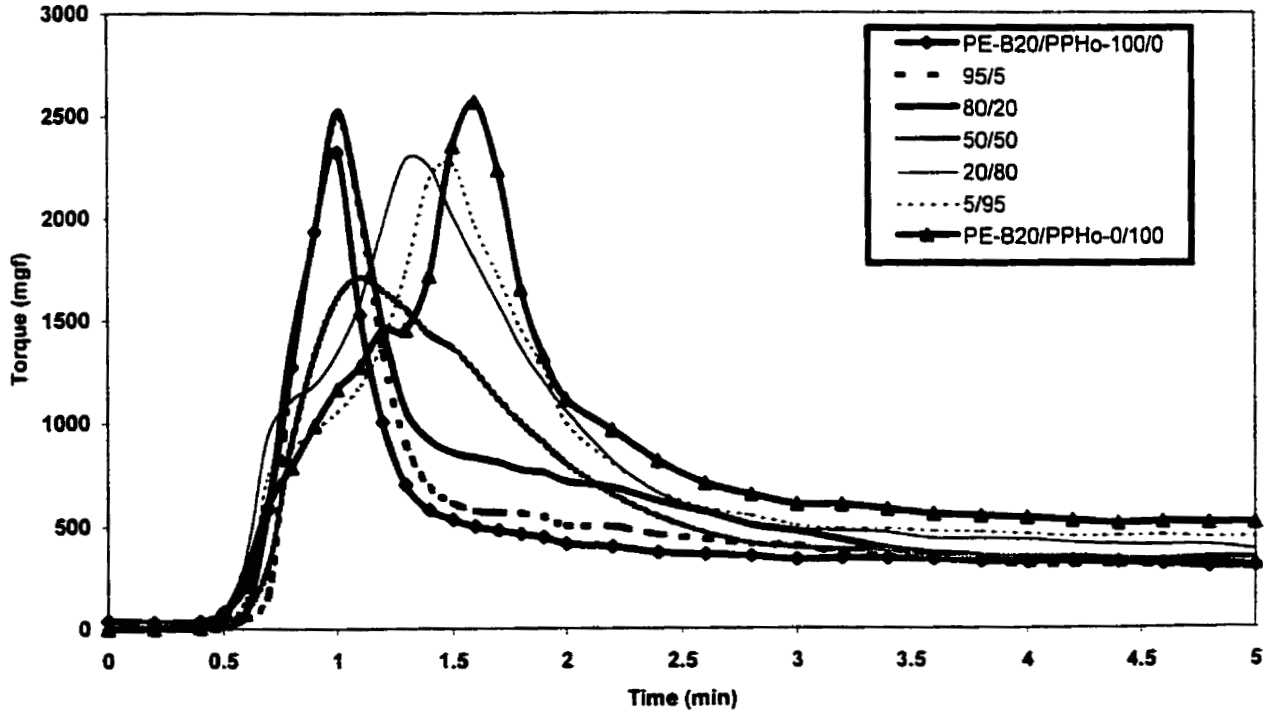

Torque profiles of PE-B20/PPHo blends prepared at 190°C

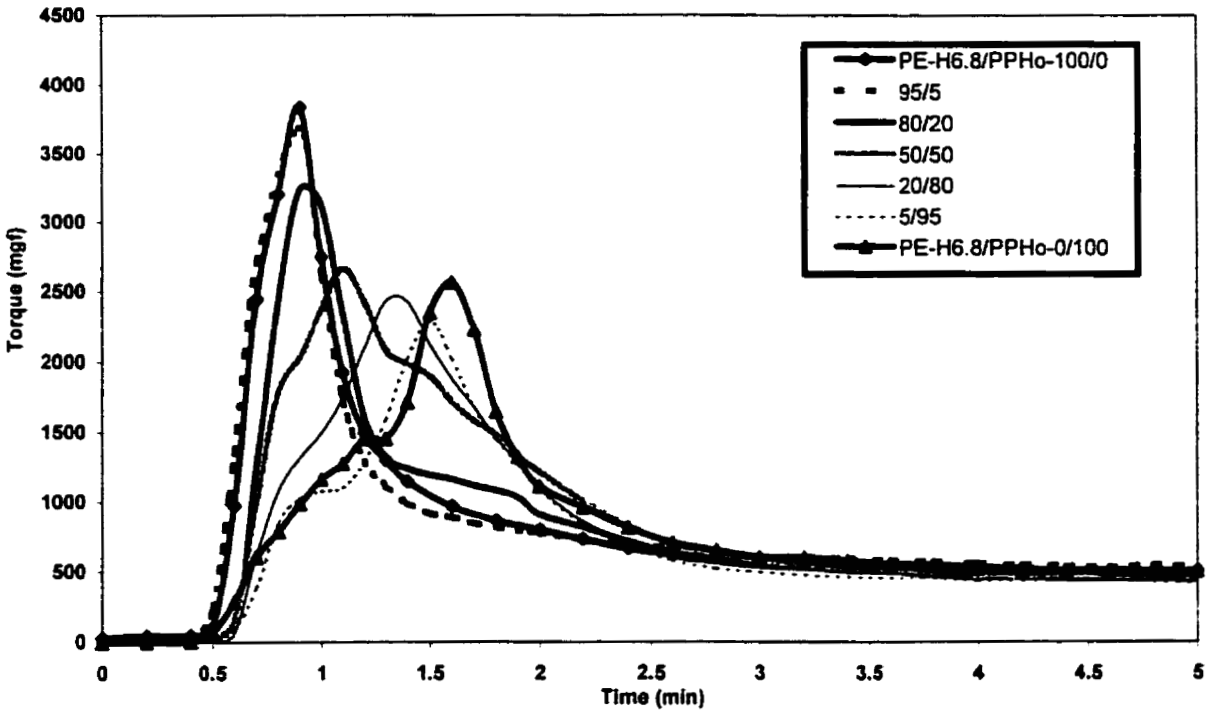

Torque profiles for PE-H6.8/PPHo blends prepared at 190°C

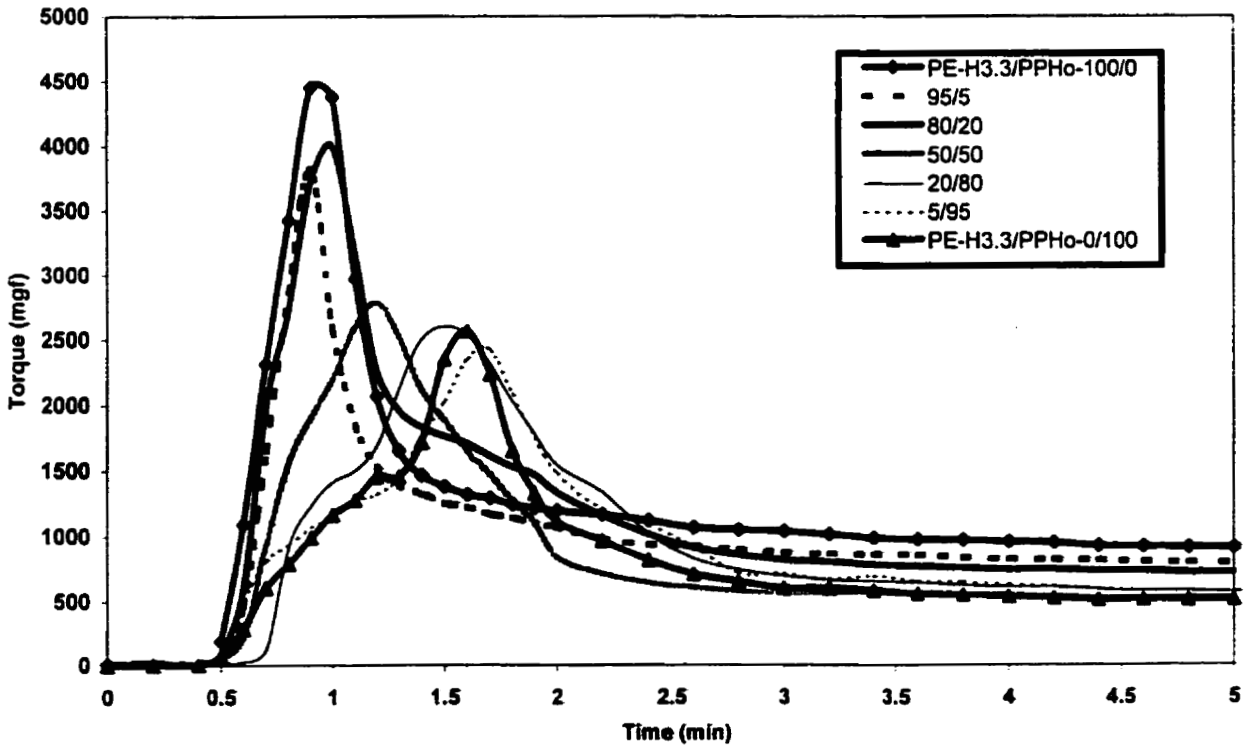

Torque profiles for PE-H3.3/PPHo blends prepared at 190°C

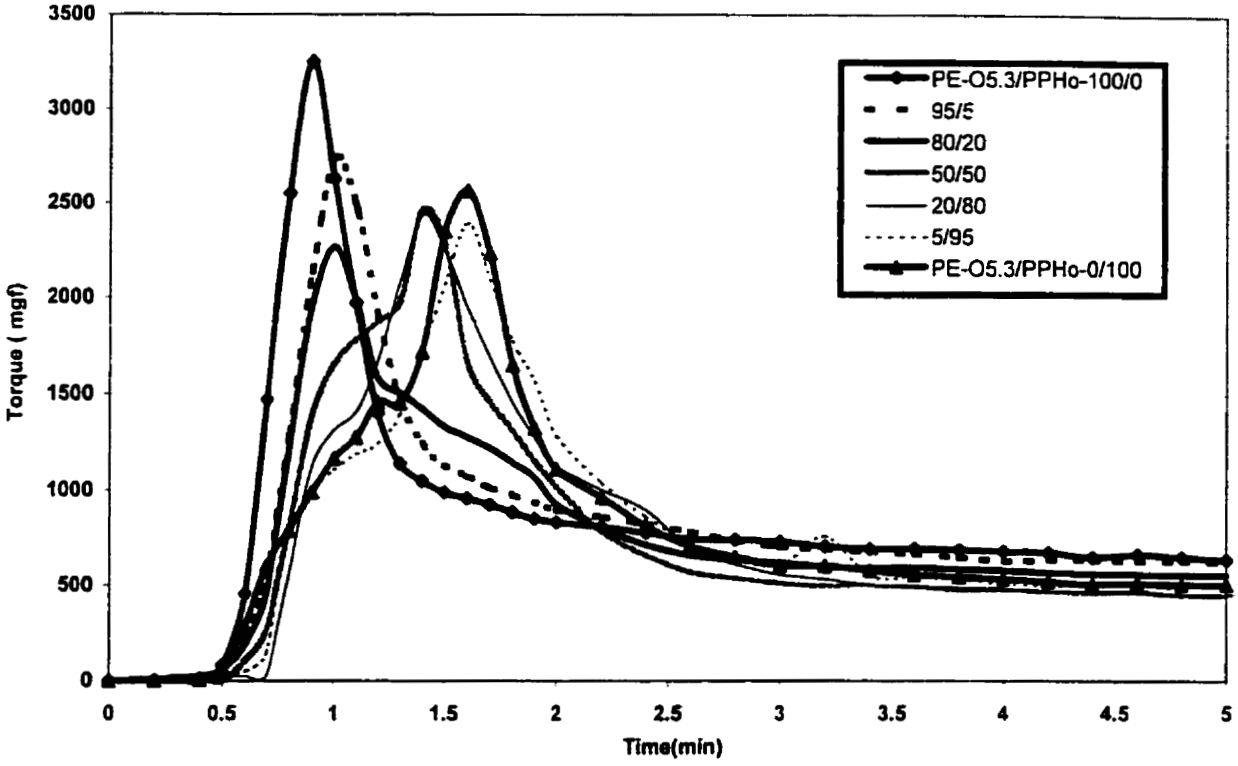

Torque profiles for PE-O5.3/PPHo blends prepared at 190°C

APPENDIX – E

Storage and loss moduli for LLDPE/PPHo blends

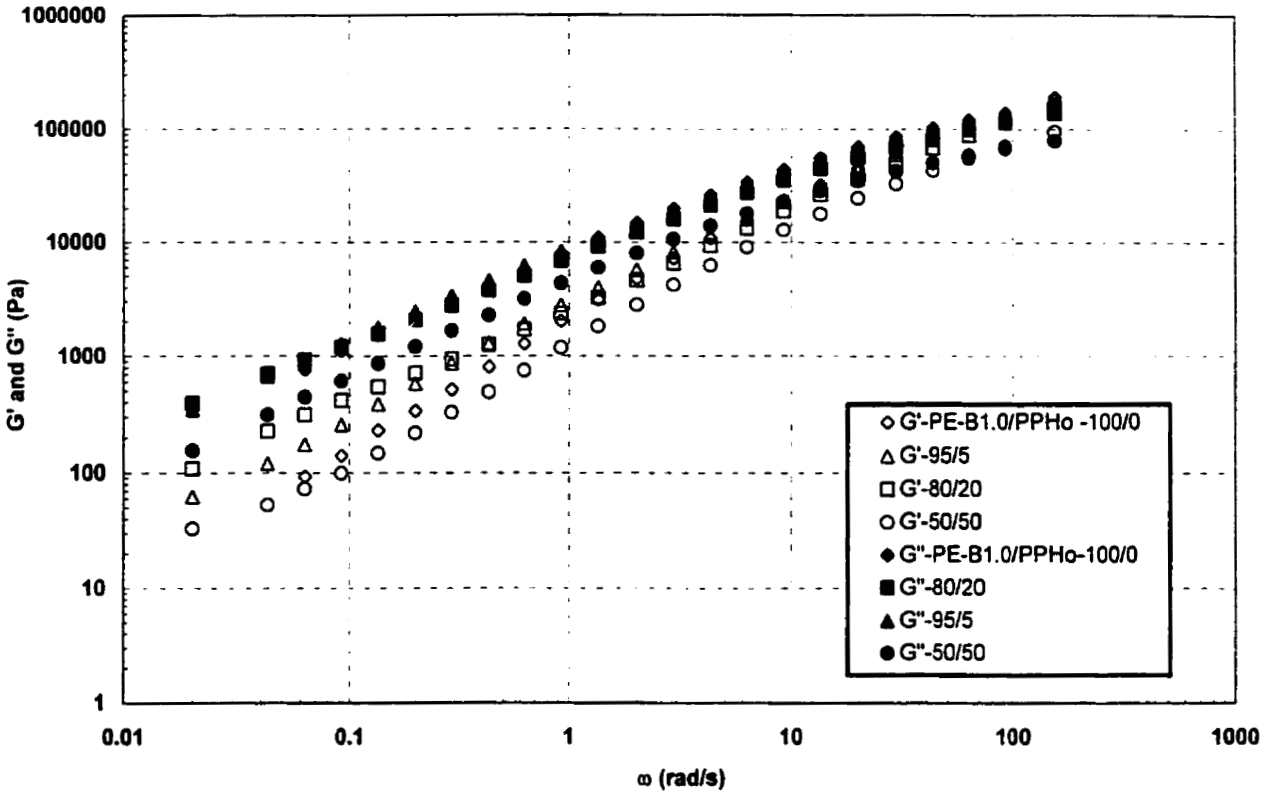

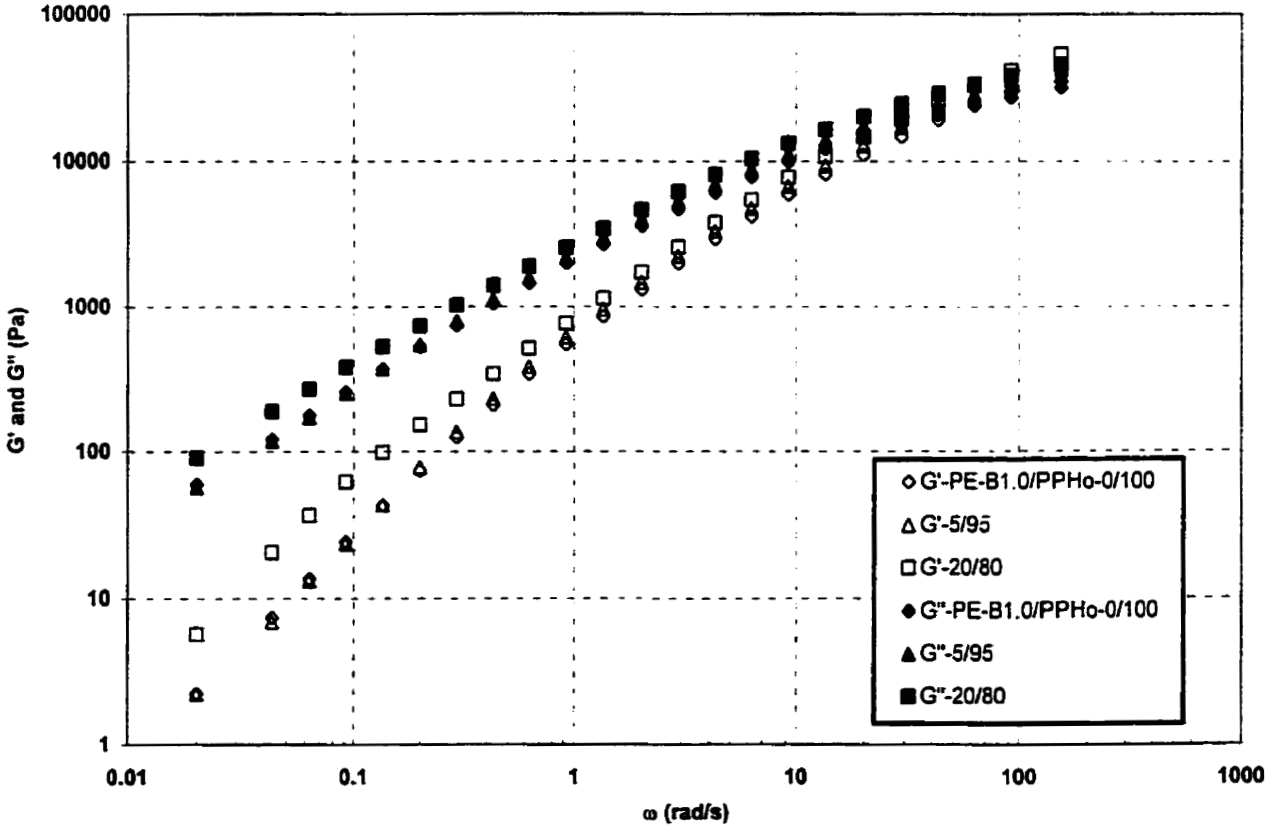

Storage and Loss Moduli for PE-B1.0/PPHo blends at 190°C

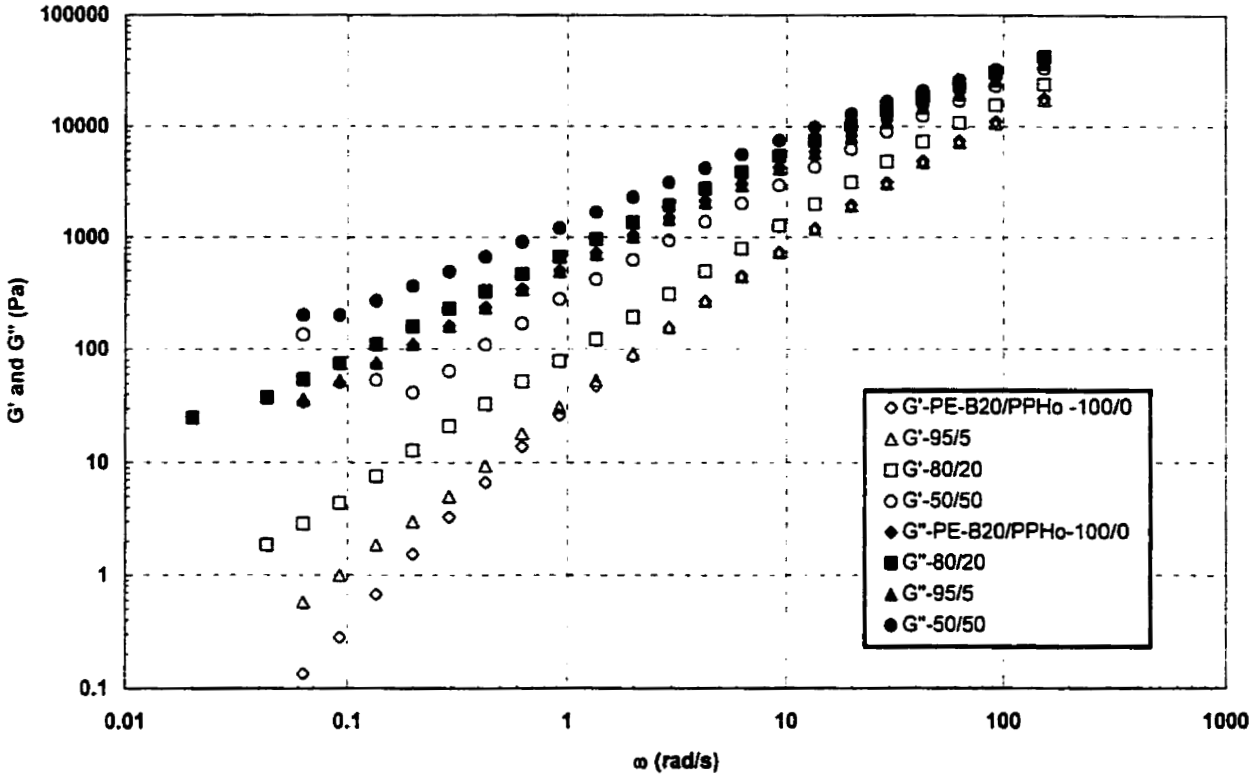

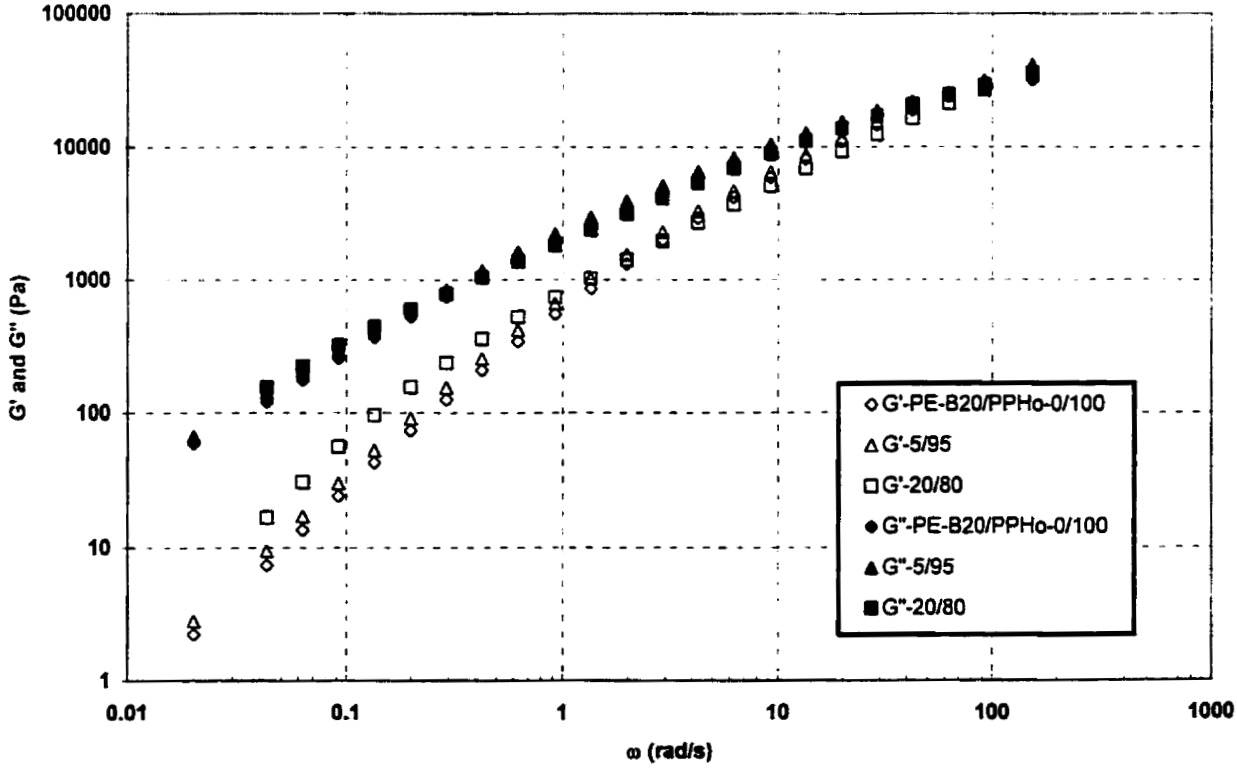

Storage and Loss Moduli for PE-B20/PPHo blends at 190°C

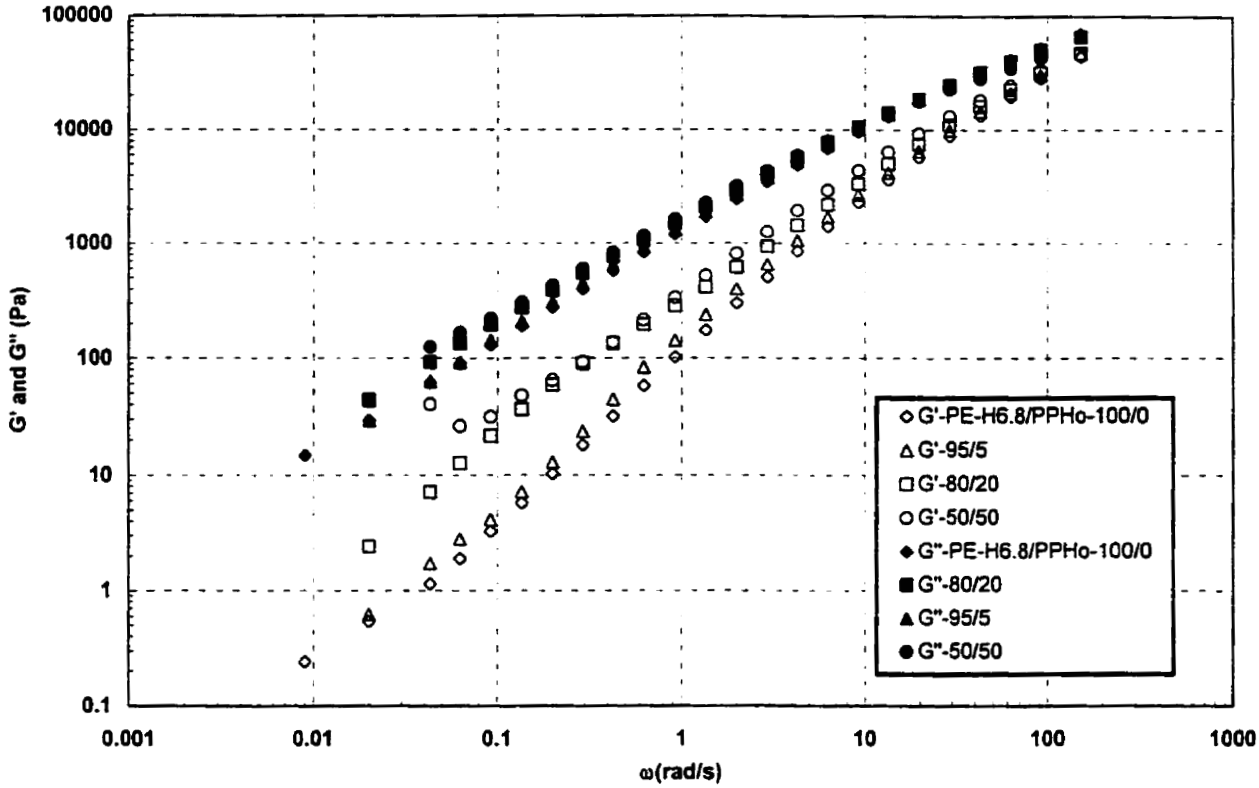

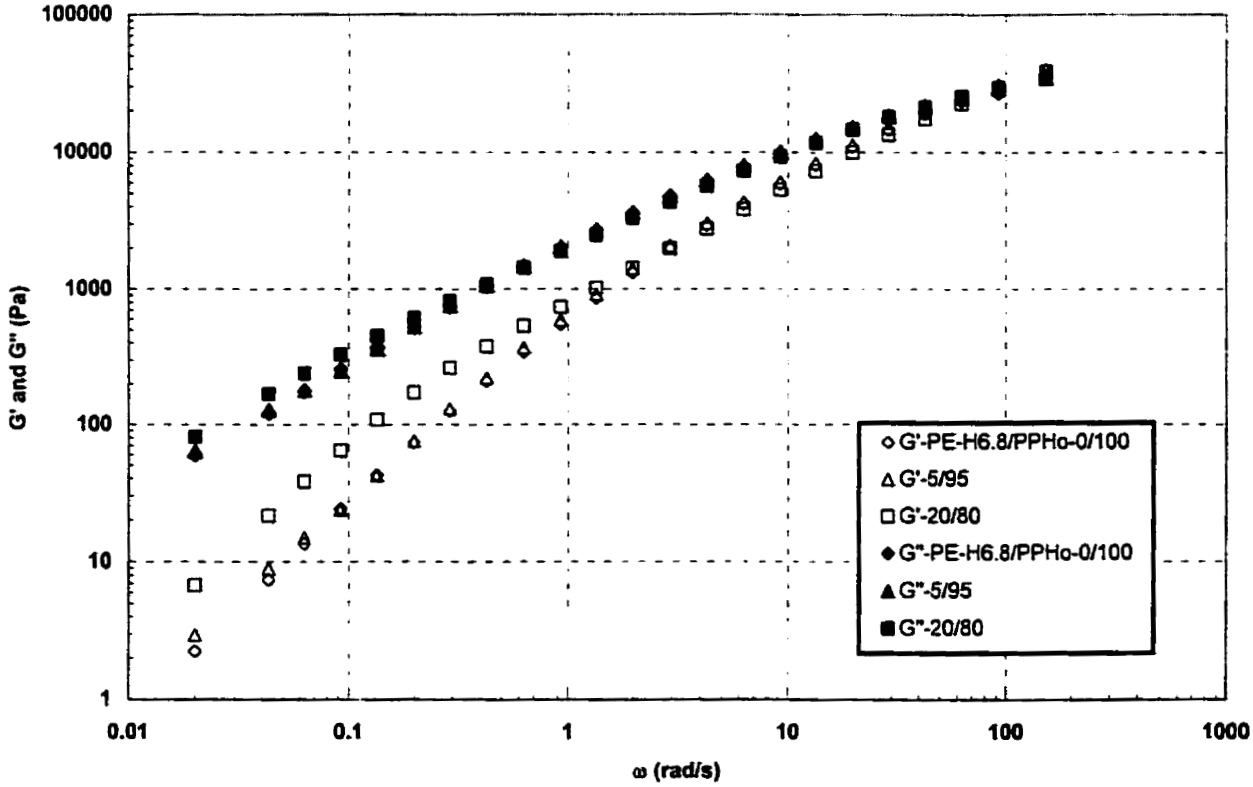

Storage and Loss Moduli for PE-H6.8/PPHo blends at 190°C

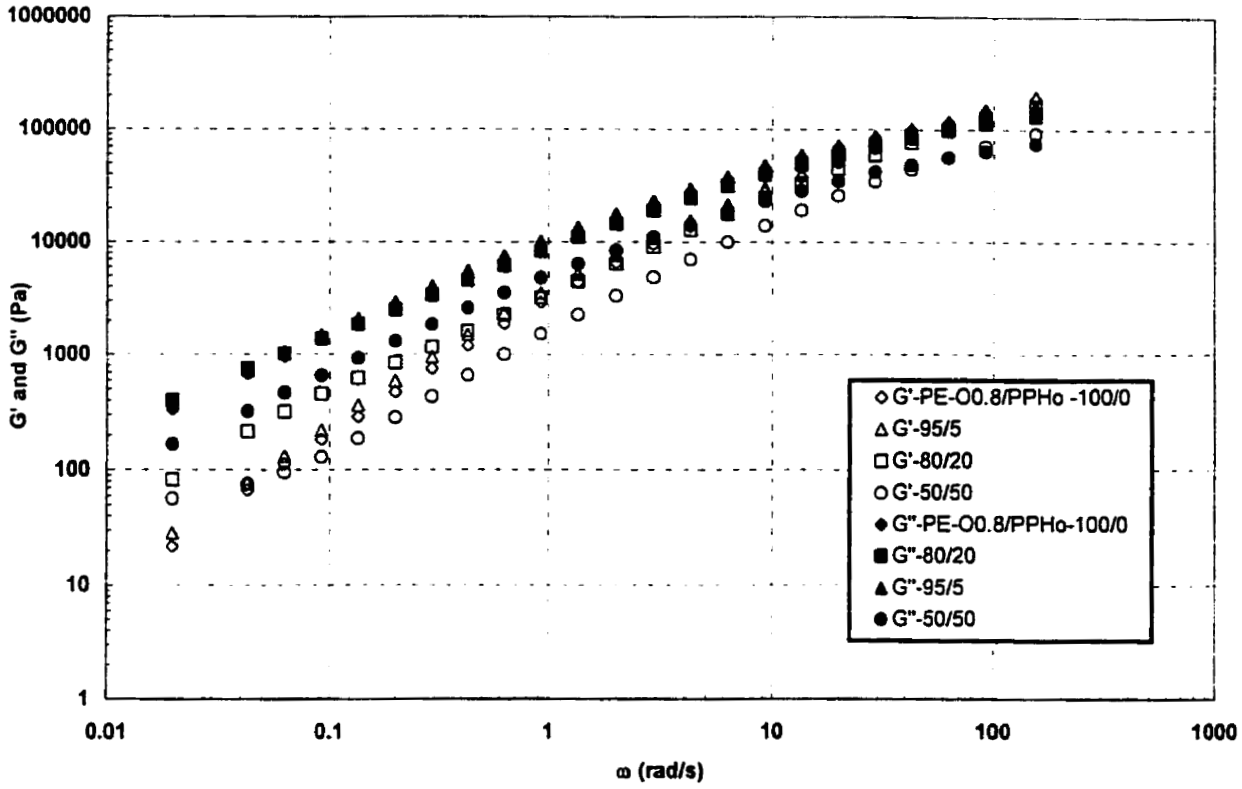

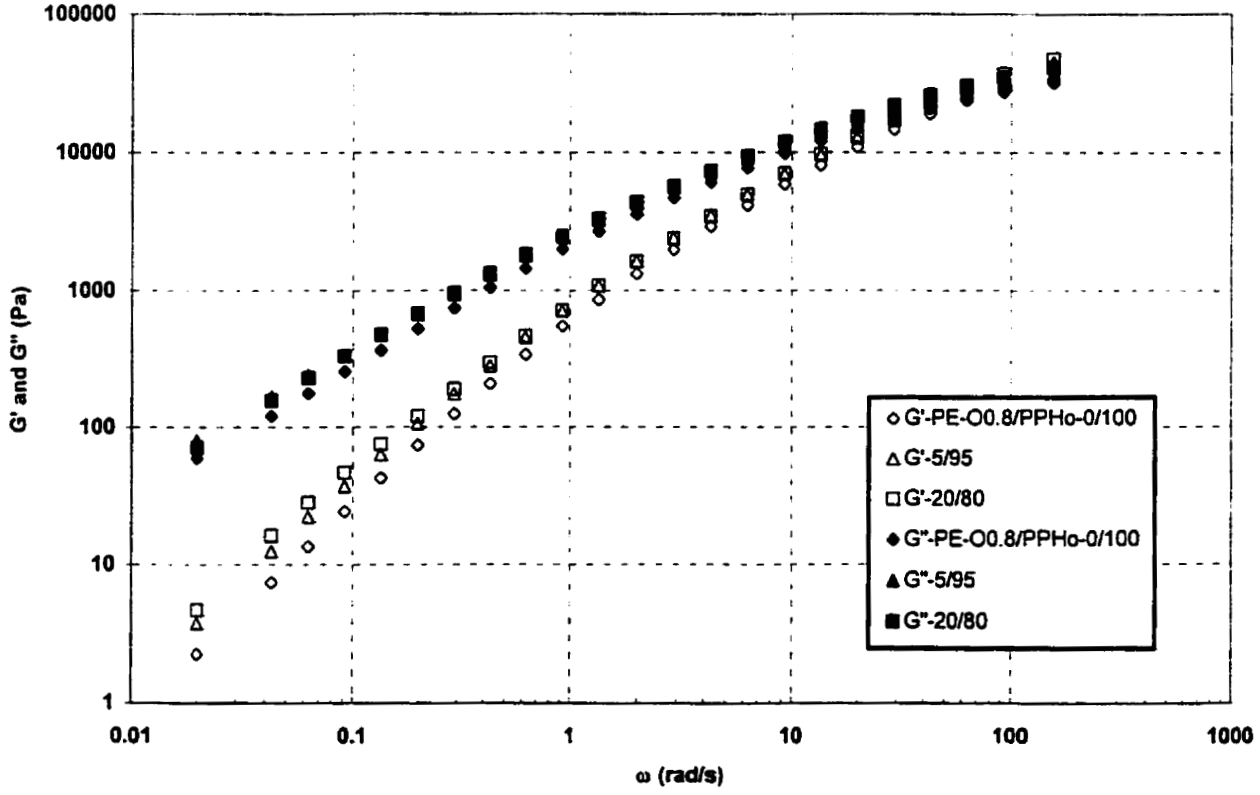

Storage and Loss Moduli of PE-O0.8/PPHo blends at 190°C

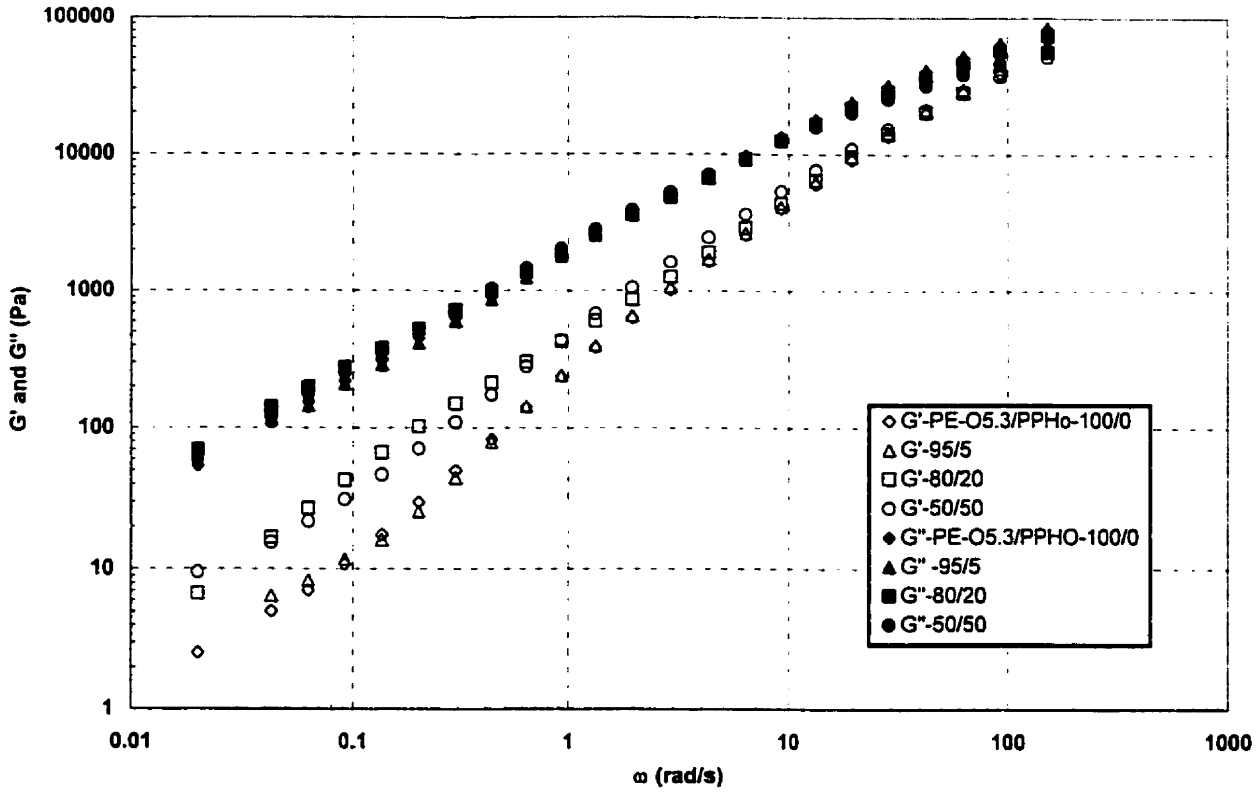

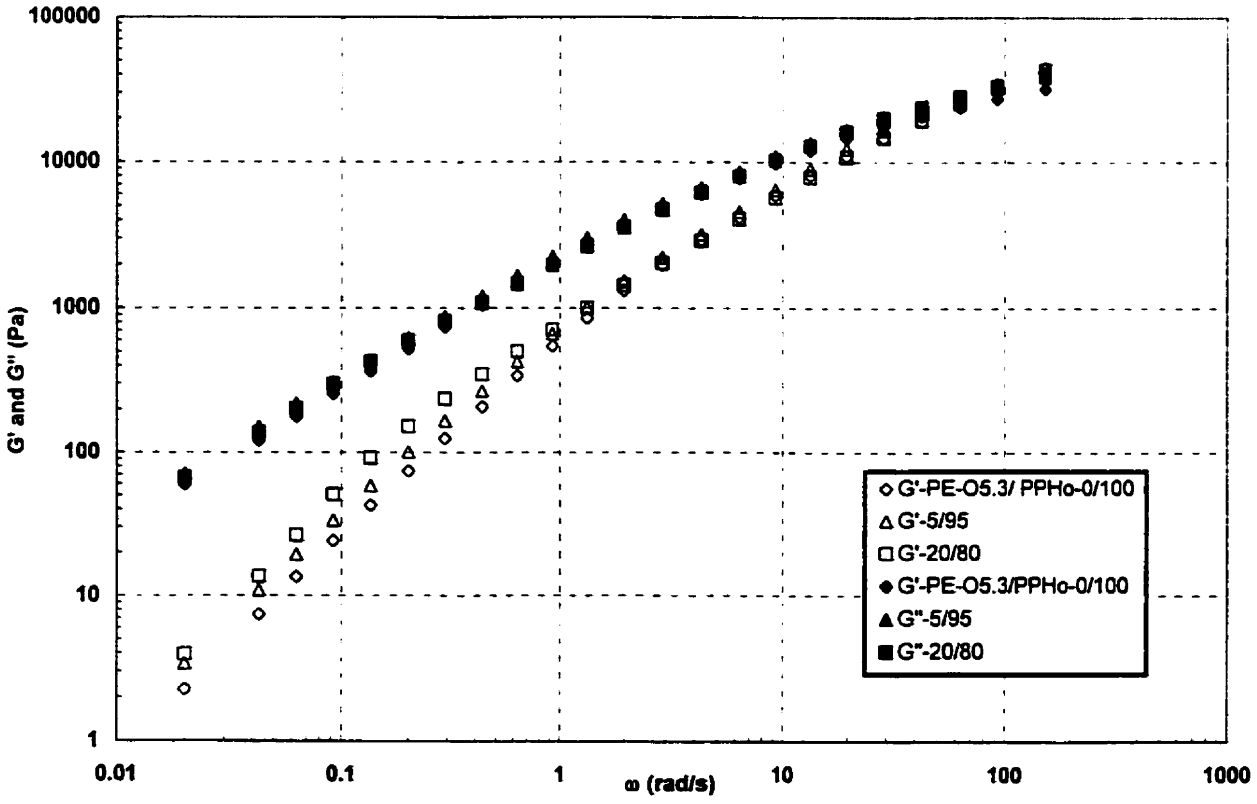

Storage and Loss Moduli for PE-O5.3/PPHo blends at 190°C

APPENDIX – F

Tan δ curves as a function of frequency for LLDPE/PPHo blends

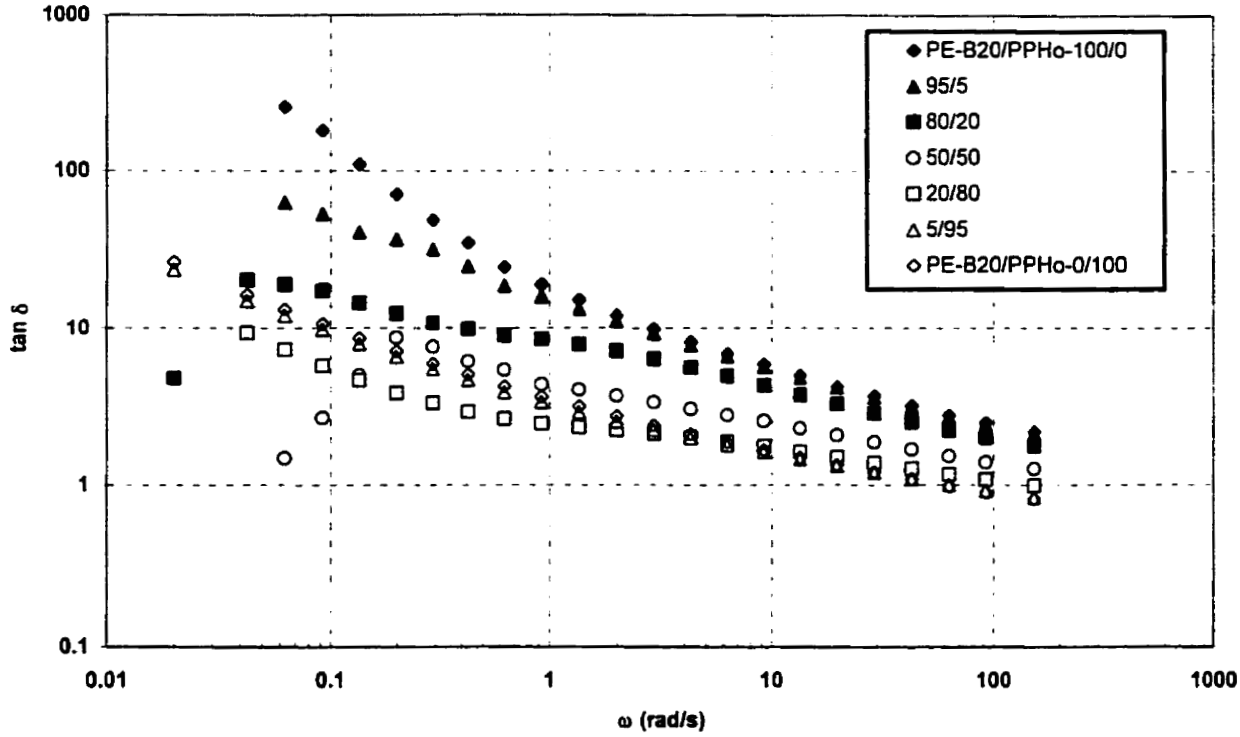

Tan δ as a function of frequency for PE-B20/PPHo blends at 190°C

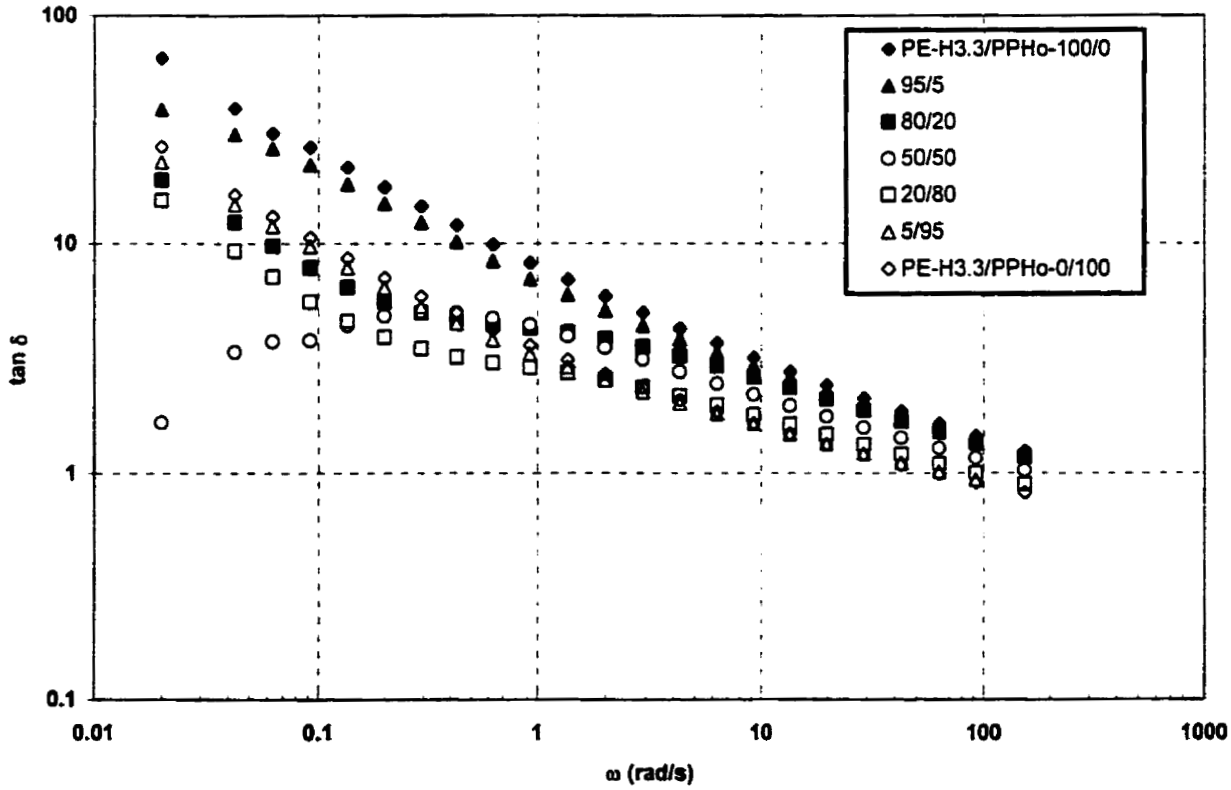

Tan δ as a function of frequency for PE-H3.3/PPHo blends at 190°C

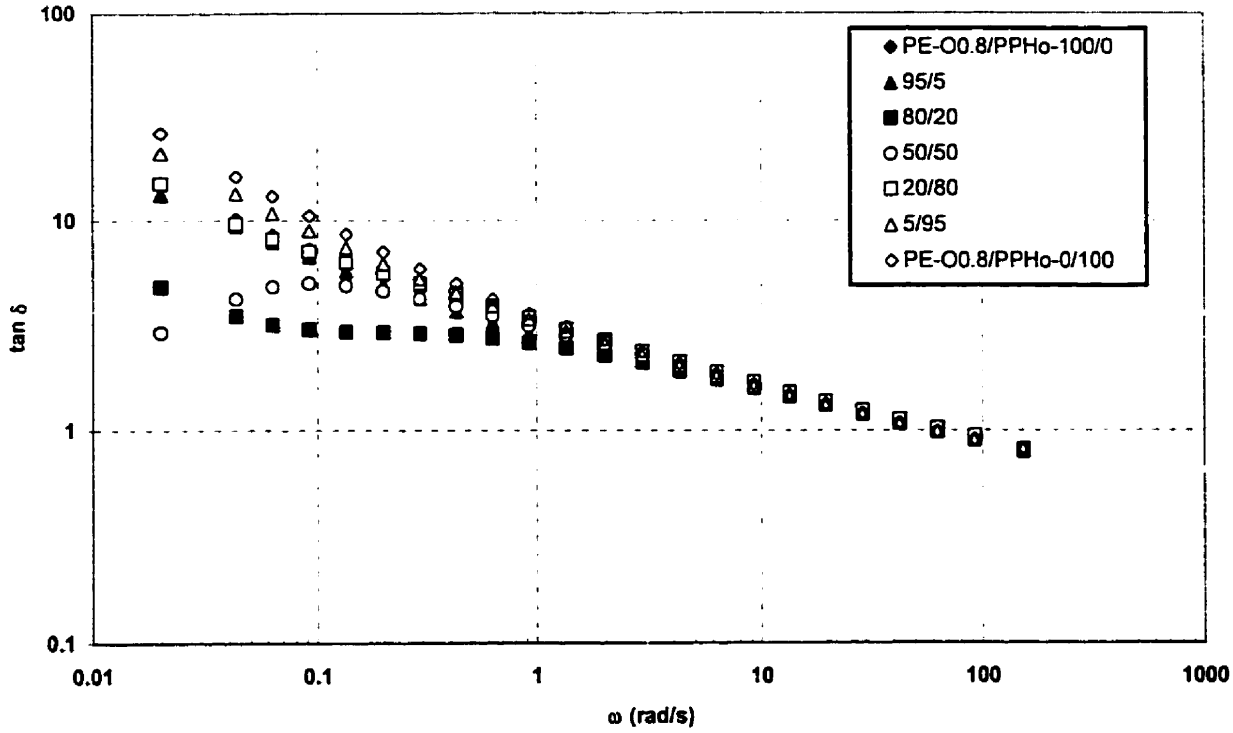

Tan δ as a function of frequency for PE-O0.8/PPHo blends at 190°C

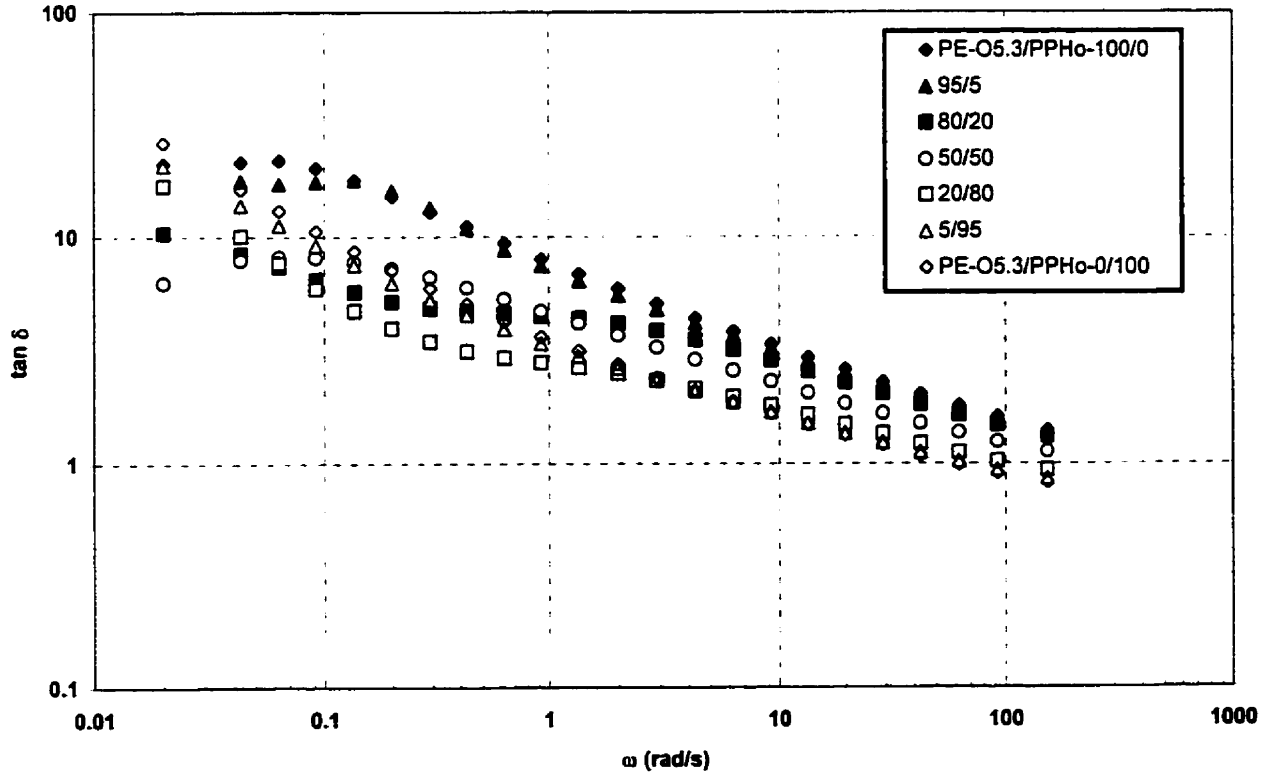

Tan δ as a function of frequency for PE-O5.3/PPHo blends at 190°C